
PEG TRANSFER WORKFLOW RECOGNITION CHALLENGE REPORT: DOES MULTI-MODAL DATA IMPROVE RECOGNITION?

Arnaud Huaulmé Univ Rennes INSERM, LTSI - UMR 1099 F35000, Rennes, France arnaud.huaulme@univ-rennes1.fr	Kanako Harada Department of Mechanical Engineering the University of Tokyo Tokyo 113-8656, Japan	Quang-Minh Nguyen Univ Rennes INSERM, LTSI - UMR 1099 F35000, Rennes, France
Bogyu Park VisionAI hutom Seoul, Republic of Korea	Seungbum Hong VisionAI hutom Seoul, Republic of Korea	Min-Kook Choi VisionAI hutom Seoul, Republic of Korea
Yunshuang Li Zhejiang University Hangzhou, China	Yonghao Long Department of Computer Science and Engineering, The Chinese University of Hong Kong, Hong Kong	Michael Peven Johns Hopkins University Baltimore, USA
Qi Dou Department of Computer Science and Engineering, The Chinese University of Hong Kong, Hong Kong	Satyadwyoom Kumar Netaji Subhas University of Technology Delhi, India	
Seenivasan Lalithkumar National University of Singapore Singapore, Singapore	Ren Hongliang National University of Singapore Singapore, Singapore The Chinese University of Hong Kong Hong Kong, Hong Kong	
Hiroki Matsuzaki National Cancer Center Japan East Hospital Tokyo 104-0045, Japan	Yuto Ishikawa National Cancer Center Japan East Hospital Tokyo 104-0045, Japan	
Yuriko Harai National Cancer Center Japan East Hospital Tokyo 104-0045, Japan	Satoshi Kondo Muroran Institute of Technology Hokkaido, Japan	
Mamoru Mitsuishi Department of Mechanical Engineering the University of Tokyo Tokyo 113-8656, Japan	Pierre Jannin Univ Rennes INSERM, LTSI - UMR 1099 F35000, Rennes, France pierre.jannin@univ-rennes1.fr	

February 14, 2022

ABSTRACT

Background and Objective: Context-aware computer-assisted surgical systems require real time automatic and accurate surgical workflow recognition. Since several years, video has been the most common modality used to develop such methods. With the democratization of robotic-assisted surgery and segmentation method, new modalities are now accessible, such as kinematics. Some previous works used these new modalities as input of their models, but the added value of these modalities is rarely studied. This paper presents the design and results of the "PEg TRAnsfer Workflow recognition" (PETRAW) challenge whose objective was to develop surgical workflow recognition methods based on one or several modalities in order to study their added value.

Methods: The PETRAW challenge provided a data set of 150 peg transfer sequences performed on a virtual simulator. This data set was composed of videos, kinematics, semantic segmentation, and workflow annotations which described the sequences at three different granularity levels: phase, step, and activity. Five tasks were proposed to the participants: three of them were related to the recognition of all granularities with one of the available modalities, while the others addressed the recognition with a combination of modalities. Average application-dependent balanced accuracy (AD-Accuracy) was used as evaluation metric to take unbalanced classes into account and because it is more clinically relevant than a frame-by-frame score.

Results: Seven teams participated in at least one task and four of them in all tasks. Best results are obtained with the use of the video and the kinematics data with an AD-Accuracy between 93% and 90% for the four teams who participated in all tasks.

Conclusion: The improvement between video/kinematic-based methods and the uni-modality ones was significant for all of the teams. However, the difference in testing execution time between the video/kinematic-based and the kinematic-based methods has to be taken into consideration. Is it relevant to spend 20 to 200 times more computing time for less than 3% of improvement? The PETRAW data set is publicly available at www.synapse.org/PETRAW to encourage further research in surgical workflow recognition.

Keywords Surgical Process Model · Workflow recognition · Multi-modality · OR of the future

1 Introduction

In order to bring computer-assisted surgery (CAS) system inside the operating room, it is essential to have a complete and explicit understanding of surgical procedures. Surgical process model (SPM), defined as a "simplified pattern of a surgical process that reflects a predefined subset of interest of the surgical process in a formal or semi-formal representation" [1], can bring this understanding. SPM methodology consists of decomposing a surgical procedure at different levels of granularity: phases, steps, activities, surges, and dexemes [2, 3]. A dexeme is the lowest granularity level, it is a numerical representation of the motion. A surge represents a surgical motion with explicit semantic meaning (e.g., pull). An activity describes a physical action (namely action verbs, e.g., cut) performed on a specific target (e.g., the pouch of Douglas) by a specific surgical instrument (e.g., a scalpel). A step is the succession of activities performed to achieve a surgical objective (e.g., resect the pouch of Douglas). Finally, a phase corresponds to a main period of the intervention (e.g., resection) and is a succession of steps. SPM methodology is used for learning and expertise assessment [4, 5], robotic assistance [6], operating room optimization and management [7, 8], decision support [9], and quality supervision [10].

The major limitation of SPM related state of the art publications [3, 4, 5, 7, 9, 10] is the manual acquisition of the SPMs by human observers. This solution is observer-dependent, time-consuming, and subject to errors [11]. Due to this limitation, the proposed solutions can not be directly used to bring context-awareness CAS applications inside the operating room. To overcome this limitation, automatic workflow recognition methods have been developed for each granularity level: phases [8, 12, 13], steps [14, 15], and activities [6, 16].

Different modalities could be used for workflow recognition. For robotic-assisted surgeries and virtual reality training sessions, video and kinematic data are easily available. However, even if these modalities are available, most of state of the art methods focused on one of them only. Majority of methods are video-based only [17, 18], or kinematic-based only [3, 19]. Only few studies using both modalities to perform the workflow recognition [20, 21, 22]. Except Long et.al. [21], these methods did not compare their multi-modal results to the ones of a uni-modal version of their models.

Segmentation of the surgical scene is very important for surgical understanding and is an active area of research. For example, in 5 editions of EndoVis MICCAI Challenge (2015 to 2020), 6 of the 19 proposed sub-challenges were dedicated on this topic. However, to the best of our knowledge, semantic segmentation was rarely used as a dedicated modality for surgical workflow recognition.

The “PEg TRAnsfer Workflow recognition by different modalities” (PETRAW) sub-challenge, part of Endovis, provides a unique data set for automatic recognition of surgical workflow. The data set contains video, kinematic, and segmentation data for 150 peg transfer training sequences. The participants were challenged to develop model(s) to recognize phases, steps, and activities with one or several available modalities.

2 Methods: Reporting of Challenge Design

This section describes the challenge design through an explanation of the organization, the mission, the data set, and the assessment method of the challenge.

2.1 Challenge organization

The PETRAW challenge was a one-time event organized as part of EndoVis during MICCAI2021 online. Four people were involved in the organization: Arnaud Huaulm  and Pierre Jannin from the University of Rennes (France), Kanako Harada, and Mamoru Mishuishi from the University of Tokyo (Japan). All challenge information was made available to the participants through the Synapse platform: www.synapse.org/PETRAW.

Participation in the challenge was conditioned by the following policies: Participants had to submit a fully automatic method using one or several modalities able to recognize, on the same model, phases, steps, and activities. Only data provided by the organizers and publicly available data sets, including pre-trained networks, are authorized for the training. The publicly available data sets only covered data that were available to everyone when the PETRAW data set was released. The results of all participating teams were announced publicly on the challenge day. Challenge organizers and people from the organizing institutions could participate but were not eligible for the competition. Participating teams were encouraged (but not required) to provide their code as open access.

To have a valid submission, the participating teams had to provide the following elements: the method’s outputs, a write-up, a Docker image allowing the organizers to verify the outputs provided, and a pre-recorded talk to limit technical issues during the challenge day (online event). The submission of multiple results and Docker images are allowed, but only the last submission was officially used for challenge results. No leader-board or evaluation results were provided before the end of the challenge.

The challenge schedule was as follows: Video, kinematic and workflow annotation of the training data set was released on 2021 June 1st, segmentation was released on 2021 June 9th. Submissions were accepted until 2021 September 12th (23:59 PST). The results were announced on 2021 October 1st during the online MICCAI2021. Some teams obtained unexpected results (i.e. inferior to 50% of workflow recognition rate), which made the analysis of the results not relevant. So, each team was allowed to provide a new submission before 2021 October 31st. Teams who have made a new submission were identified in the section 3.2. The test data set and organizers’ evaluation scripts were released with this paper at www.synapse.org/PETRAW

2.2 Mission of the challenge

The PETRAW challenge objective was to study the impact of each modality and their combinations on automatic workflow recognition. To achieve this goal, participants were challenged to recognize, in a unique model, all levels of granularity of the surgical workflow (i.e. phases, steps, and action verb) on five different tasks based on available modalities. Three tasks are the development of uni-modality-based models (i.e. video-based model, kinematic-based model, or semantic segmentation-based model). These models will be used as baselines to be compared to the two others tasks, which were the development of multi-modality-based models (i.e. video + kinematic based model or video + kinematic + semantic segmentation-based model). Not all multi-modality configurations were studied to limit the number of tasks. In the case of models using semantic segmentation information, and to reflect the fact that clinically this modality is only available through computation, the participants were challenged to use the output of a segmentation method as input for PETRAW.

2.3 Challenge data set

The challenge data set was composed of 150 sequences of peg transfer training sessions. The objective of the peg transfer session is to transfer 6 blocks from the left to the right and back. Each block must be extracted from a peg with one hand, transferred to the other hand, and inserted in a peg at the other side of the board.

All cases were acquired by a non-medical expert on the LTSI Laboratory from the University of Rennes. The data set was divided into a training data set composed of 90 cases and a test data set composed of 60 cases. A case was

composed of kinematic data, a video, semantic segmentation of each frame, and workflow annotation. Only the training data set was provided to the participants.

2.3.1 Data acquisition

The challenge data were acquired on a virtual reality simulator (figure 1) developed at the Department of Mechanical Engineering at the University of Tokyo [23] and is composed of: a core laptop (i7-700HQ, 16Go RAM, GTX 1070), a 3D rendering setup (3D screen (24 inches, 144Hz) and 3D glasses) and two haptic user interfaces (3D system TouchTM).



Figure 1: The virtual reality simulator used to data acquisition.

The data acquisition was divided into sessions of 5 cases. A minimum of 5 hours of resting time was observed between two sessions to limit the fatigue of the subject. This choice was made to have the same level of expertise for all cases. Moreover, the COVID-19 crisis does not allow us to recruit multiple participants with enough availability to have a comparable number of cases by subjects. To limit the impact of immediate learning or fatigue inside a single session, 3 cases of each session were randomly chosen for training and the 2 others for testing.

The kinematic and scene information were synchronously acquired at 30 Hz during the simulation of the task. Scene information is data used to generate the 2D video and semantic segmentation after the session at a resolution of 1920x1080 pixels.

Kinematic data represent the position, rotation quaternion, forceps aperture angle, Linear velocity (obtained from simulation, not derived from position), and Angular velocity (obtained from simulation, not derived from orientation) for left and right instruments. Position and linear velocity are in centimeters, angle, and angular velocity in degrees.

Six classes composed the semantic segmentation (figure 2): background (black, hexadecimal code :#000000), base (white, #FFFFFF), left instrument (red, #FF0000), right instrument (green, #00FF00), pegs (blue, #0000FF) and blocks (Magenta, #FF00FF).

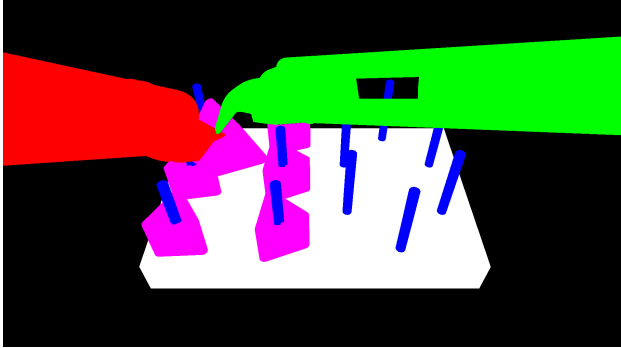


Figure 2: One segmentation mask with the six classes: background(black), base(white), left instrument(red), right instrument(green), pegs(blue) and blocks(Magenta).

Workflow annotation was automatically computed thanks to scene information by ASURA method [11]. To describe the workflow, two phases, twelve steps and six action verbs, two targets, and one surgical instrument were identified (Table 1). Each phase corresponds to one transferring direction. Each step (six by phase) corresponds to the transfer of one block in one direction (e.g.“Block1 L2R” corresponds to the transfer of the first block from the left to the right). For the activities, we differentiated two targets: “block” and “other block”. The “block” corresponds to the one which is currently transferred. “Other block” is an additional target used to differentiate when the user accidentally interacts with another block.

Table 1: Peg-transfer vocabulary.

Phases	Steps	Activities		
		Verb	Target	Tool
Transfer Left To Right (L2R)	Block 1 L2R	Catch	Block	Grasper
	Block 2 L2R	Drop	Other block	
	Block 3 L2R	Extract		
	Block 4 L2R	Hold		
	Block 5 L2R	Insert		
	Block 6 L2R	Touch		
Transfer Right To Left (R2L)	Block 1 R2L			
	Block 2 R2L			
	Block 3 R2L			
	Block 4 R2L			
	Block 5 R2L			
	Block 6 R2L			

One limitation of the method presented on [11] was the inability to differentiate correctly the action verbs “catch” and “touch”. Since the publication, the information provided by the VR simulator has been enhanced to be able to make this difference. Moreover, each workflow annotation was manually reviewed to ensure the annotation quality.

2.3.2 Data pre-processing

A workflow annotation is a task description where each element was characterized by the beginning and the end expressed in milliseconds. We modified it to provide a discrete sequence synchronized at 30Hz with the kinematic, video, and segmentation data. Due to the lack of variability of target and tool, we decided to not include these ones in the workflow description. Furthermore, when no phase, step, or activity occurred, the term “Idle” was added. For each timestamp, we provided the following information: timestamp_number, phase_value, step_value, verb_Left_Hand, verb_Right_Hand.

2.3.3 Ground truth uncertainties

The main source of uncertainty related to ground truth is on the segmentation masks. Due to the transformation of 3D meshes in 2D images, some pixels have a wrong class attribution, especially on boundaries between the right



Figure 3: Zoom of 219x123 pixels on figure 2 to highlighted segmentation errors. Here we could identify right instrument/block (green/magenta) and left/right instruments (red/green) errors where pixels are labelled as background (black). On this zoom, only 51 are miss-segmented.

instrument/peg, left instrument/peg, left instrument/block, and left/right instruments. (figure 3). We estimated this error to be less than 0.5% of pixels.

Another source of uncertainty is workflow annotations. Although the ASURA method is consistent (i.e. same result provided for two identical situations) and a manual check has been performed to limit uncertainties, some components can be not well recognized. We have identified two uncertainties. First on sequence 130 from the training data-set, the block on step "Block 1 R2L" is inserted in a non-standard way. In this case, the block is released by the operator and is inserted when it falls. So here the insert action is not present. The other case is sequence 79 from the test data-set. Here the operator caught a block before the previous one is fully inserted, so an overlap inferior to 0.5 seconds exists between the steps "Block 5 R2L" and "Block 6 R2L". It was chosen to conserve the true beginning of the second one.

2.3.4 Data sets characteristics

Training and test data sets present similar characteristics. The mean and standard deviation duration is 140.2 ± 18.9 seconds for the training data set and 141.7 ± 18.0 seconds for the test one. Figure 4 presents the distribution of each vocabulary component for each granularity between training data set (sub figures 4a, 4c, 4e, 4g) and the test one (sub figures 4b, 4d, 4f, 4h). Even for underrepresented components the distribution is very close, e.g. the left verb touch represents 0.59% of the training data set and 0.60% of the test on, right verb touch represents respectively 0.62% and 0.48%.

Another important characteristic of the data sets is the high classes unbalance of at least one vocabulary term for each granularity. For phase and steps, the term "Idle" represents less than 4% of the data whereas other terms represent more than 47% and 7.5% respectively. This unbalance is more pronounced for the verbs, the least represented verb is "to touch" which is approximately 0.6% of the dataset, whereas the verb "Idle" corresponds to more than 53%. Detailed distribution values for each granularity for both data sets are available in the supplementary material.

2.4 Assessment method

2.4.1 Metrics

To assess the participant workflow recognition models and take into account the high classes unbalance we decided to use the balanced version of the accuracy, precision, recall, and F1. In practice, a clinical application does not need to be precise at a frame resolution. Dergachyova et al. [24], proposed a re-estimation of the classic scores, called application-dependent scores, to take into account an acceptable delay d . When a predicted transition occurs inside a transition window ($2d$) centered on the ground truth transition, all frames between the two transitions are considered correct if it is the same type of transition, e.g. transition for verb "catch" or verb "extract". So we used the balanced application-dependent accuracy (following called AD-Accuracy) with and the acceptable delay fixed at 250 ms.

To assess the participant segmentation models we used the mean Intersection-Over-Union (IoU) over all classes, also known as the Mean Jaccard Index over all classes. The IoU is the area of overlap between the predicted segmentation($Pred$) and the ground truth (GT) divided by the area of union between the $Pred$ and the GT . In our cases it is a multi-class segmentation problem, so the Mean IoU of the image is calculated by taking the IoU of each class and averaging over classes:

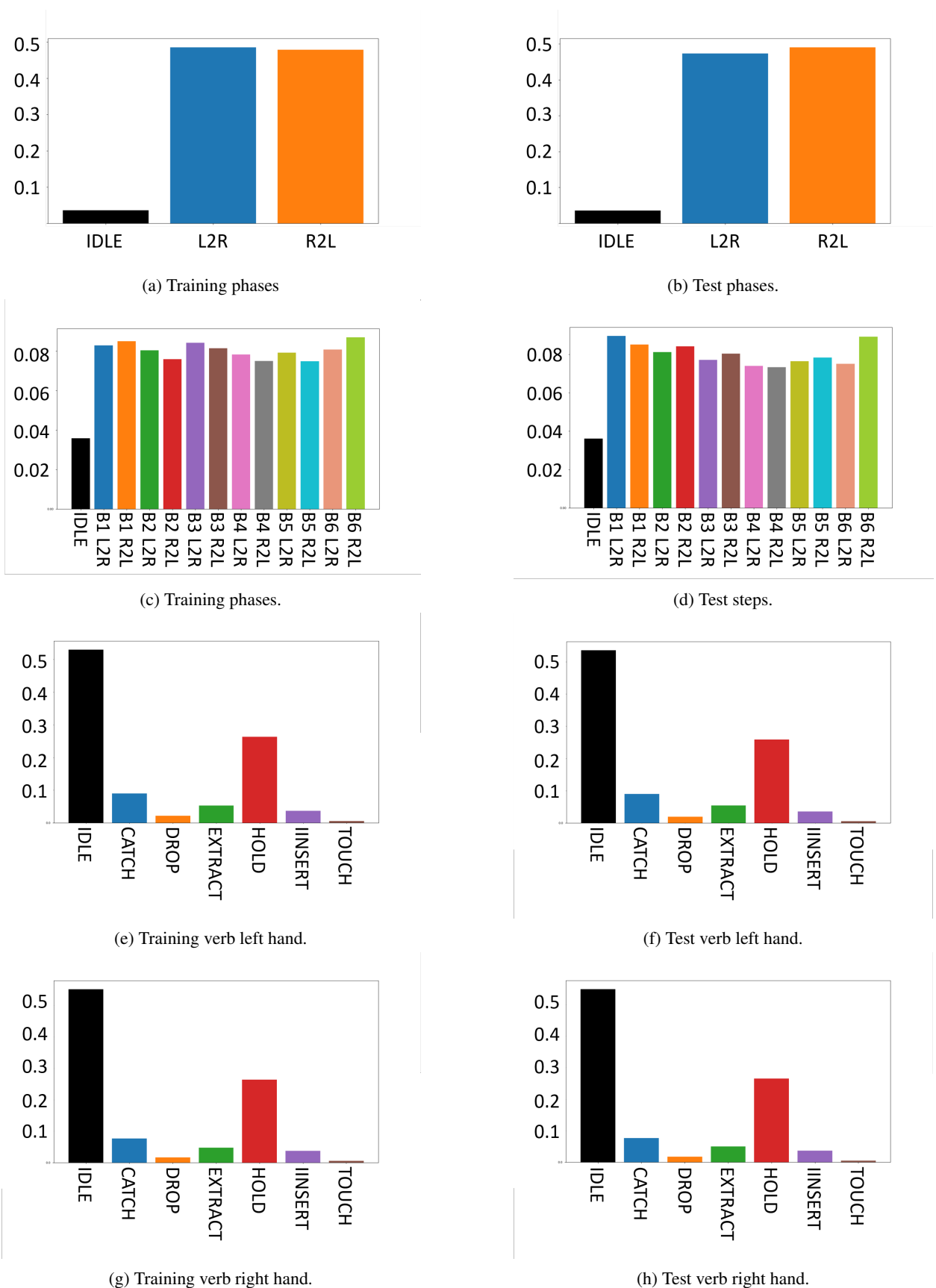


Figure 4: Distribution of each term of each granularity level on training and test data sets. For a and b 'L2R' mean Transfer left to right and 'R2L' mean Transfer right to left. For c and d 'B1 L2R' mean Block 1 L2R, 'B2 L2R' mean Block 2 L2R.

$$\begin{aligned}
MeanIoU_{frame} &= \frac{1}{6} \sum_{class} IoU_{class} \\
&= \frac{1}{6} \sum_{class} \frac{|GT \cap Pred|_{class}}{|GT \cup Pred|_{class}} \\
&= \frac{1}{6} \sum_{class} \frac{TP_{class}}{TP_{class} + FP_{class} + FN_{class}},
\end{aligned} \tag{1}$$

where TP is the number of True Positives, FP the number of False Positives, and FN the number of False Negatives for each class.

2.4.2 Ranking method

The ranking was only done for the workflow recognition models. The metric computed for the segmentation was used for information purposes.

A mean metric-based aggregation method computed on the AD-Accuracy was used for the ranking. For each participant, we aggregated the metric values over all test cases and aggregated overall metrics to obtain a final score for the ranking. We used a metric-based aggregation according to the conclusion of [25], who reported this type of aggregation as one of the most robust.

All tasks consisted of recognizing the phase, the step, the left, and right verbs, so the ranking score for algorithm a_i was computed as follows:

$$s(a_i) = \frac{s_{phase}(a_i) + s_{step}(a_i) + s_{verb_left}(a_i) + s_{verb_right}(a_i)}{4} \tag{2}$$

with,

$$s_{phase}(a_i) = \frac{\sum_{t=0}^T phase_balance_accuracy_case_t}{T} \tag{3}$$

The same equation as 3 was used for s_{step} , s_{verb_left} and s_{verb_right} .

In the case of missing results, we considered results as good as a total random recognition. For example, for a 3-class problem, the missing result would be set to 1/3, and for a 12-class problem, it would be set to 1/12. In practice, we have not encountered this case.

The ranking stability was assessed by testing different ranking methods. The different methods were meanThenRank, medianThenRank, rankThenMean, rankThenMedian, and testBased. MeanThenRank is the method chosen for the ranking. MedianThenRank differs from the previous by taking the median instead of the mean in eq 3. For rankThenMean and rankThenMedian, first, the results of each sequence are ranked between participants, then the final results are the mean or median of all ranks. The testBased method is based on bootstrapping. If the ranking was not stable according to the method chosen, a tie between the different teams was pronounced.

The ranking computation and analysis were performed with the ChallengeR package provided by [26].

2.4.3 Online recognition compatibility

To be online compatible, the proposed methods must satisfy two conditions: to spend less time between two predictions than the duration between the two samples and to be causal, i.e. do not use future samples to predict the current one.

We have not studied the computation time, because it could not be assessed for all teams. Indeed, teams provided a unique docker for all tasks, and some teams did not write the output file on the flow.

To check the causality proposed method, we have mimicked the online availability of the frames. We have recorded one additional sequence of 10 seconds corresponding to the transfer of the first block from the left to the right. This sequence was split into 300 sequences, each one having the information of the next frame in addition to all the information of the previous sequence. Thus, the first sequence only contains the information of the first frame, the second one contains the information of the two first frames, etc. All models were run to predict the workflows and we compared the sequence provided by the last prediction of the split sequences to the prediction of the complete sequence. A model was considered causal only if the results were the same.

For computation time and environmental responsibility reasons, it was chosen not to perform this test on a whole sequence or test data set. Indeed, this would have corresponded to test more than 4 250 split sequences by test sequence or more than 255 000 split sequences for the whole test data set.

3 Results: Reporting of the Challenge Outcomes

3.1 Challenge submission

On September 12th 2021, we had 29 individual participants registered for the PETRAW challenge. Of these participants, 17 were members of one of the six competing teams. In addition, the organizers have also submitted results as a non-competing team to provide a baseline. As explained on section 2.1, some teams obtained unexpected results. Three teams have resubmitted for at least one task.

3.2 Information on participating teams and corresponding methods

In this section, we present each team, the methods they used, and which tasks they participated in. Competing teams are present in alphabetical order and not in consideration of their ranking.

3.2.1 Hutom

The Hutom team was composed of Bogyu Park, Seungbum Hong, and Minkook Choi from VisionAI hutom. They participated in all proposed tasks. They resubmitted docker for all tasks except the kinematic-based recognition task.

Before training a preprocessing step has been done. To conserve temporal information, data were split into clips of 8 frames. Kinematic data were normalized by applying standardization to raw input without data augmentation. Video data were resized at 256 x 256 pixels then random cropping (224 x 224 pixels) and normalization were performed. The cropping was done to preserve spatial information for each frame for one clip. Segmentation data were resized at 512 x 512 pixels.

Similar baseline architecture was used for tasks using the same modality. The segmentation data were computed from the video thanks to a DeepLabV3+ architecture [27]. The workflow recognition was done through a 3D ResNet network [28] for video modality. For segmentation modality a SlowFast50 network [29] was used for segmentation-based recognition and a 3D ResNet network for video/kinematic/segmentation based recognition. Kinematic data were pass on a Bi-LSTM network [30]. For multi-modality recognition tasks, they used a convolutional feature fusion layer to efficiently perform the fusion of the feature output of each modality. They obtained embedding features with individual modality inputs from each model trained accordingly. And then, embedding features by modality were compared with other modalities to learn the different representations for each modality. They used the stop gradient-based SimSiam [31] for the comparison of representations between embedding features. At the same time, embedding features by modality were stacked into one block as a chunk and fused into one embedding through convolution operation. The approach assumed that feature elements by modality in the same column have similar temporal information in similar positions. For all networks, Adam optimizer and initial learning rate of $1e^{-3}$ were used, with a combination of Equalization loss v2 [32] and Normsoftmax Loss [33] as long-tail recognition for resolving data imbalance.

3.2.2 JHU-CIRL

The JHU-CIRL team was composed of Michael Peven and Gregory D. Hager from Johns Hopkins University. They participated in the kinematic-based workflow recognition task.

An under-sampling of the kinematic data was performed to reduce the size of the time dimension to prevent vanishing gradient issues during the training. For the test, the same under-sampling was made. JHU-CIRL did not make other preprocessing considering that the addition of velocity data in addition to positional data was sufficient for the recognition.

A unidirectional LSTM network [34] was used to recognize the four components of the workflow. The model was trained using traditional cross-entropy classification loss and the Adam optimizer. Special attention has been paid to the selection of the following hyperparameters: sampling rate, learning rate, LSTM hidden dimension size, and the number of layers in the LSTM. A 5-fold cross-validation was made to get results from each of these hyperparameters. The best set of hyperparameters was selected for the final training: 15Hz of sampling rate, $1e^{-3}$ for learning rate, 256 LSTM Hidden dimension, and 2 LSTM layers.

3.2.3 MedAIR

The MedAIR team was composed of Yunshuang Li, Yonghao Long, and Qi Dou from Zhejiang University and the Chinese University of Hong Kong. They participated in three tasks: video-based, kinematic-based, and video/kinematic-based recognition. They resubmitted docker for the video-based recognition task.

The MedAIR team resized videos at 224 x 224 pixels and then augmented the data thank to a random horizontal flip and a random rotation of 5°. For kinematics, a linear layer was used to get 2048 dimensions from the 28 dimensions to enrich the information.

For uni-modality recognition (video-based and kinematic-based tasks), MedAIR use a Trans-SVNet model [35]. Firstly, two different CNNs were trained to extract spatial features, one for step and another for left end right verbs. Then, three multi-stage TCN were trained to get temporal features for step and hand verbs. Finally, three transformer layers were used to combine spatial and temporal features to get the final output for the three labels. Phases were not directly predicted by the networks but identified based on the predicted step. A stochastic gradient descent (SGD) optimizer was used with a cross-entropy loss and a learning rate at 5e⁻⁴.

For multi-modality recognition (video/kinematic-based task), MedAIR used a multi-modal relational graph network (MRG-Net) [21]. As for uni-modality recognition, 2 CNNs were used to get features of each frame in the video for step and hand verbs. Then the step labels were obtained using the original MRG-Net structure, which was the result of the fully connected layer with the output of three nodes in the graph. As for the hand verbs label, MedAIR just used the output of k_t^l and k_t^r with fully connected layers respectively to obtain the final label prediction for left verb labels and right verb labels. Phases were identified based on the predicted step. An Adam optimizer was used with a cross-entropy loss and a learning rate at 1e⁻⁴.

3.2.4 MMLAB

The MMLAB team was composed of Satyadwyoom Kumar, Lalithkumar Seenivasan, Hongliang Ren from the Netaji Subhas University of Technology, National University of Singapore, and the Chinese University of Hong Kong. They participated in the video/kinematic-based recognition task.

MMLAB team proposed a multi-task learning model to perform the recognition. First, each video frame was resized at 224 x 224 pixels. A ResNet 50 [36] pre-trained on ImageNet was used to extract visual features for each video frame. These features were passed with the frame-specific kinematic data through four label-specific networks (one by component). Each label-specific network was composed of two LSTMs [37], one by modality, to capture the temporal features. The sequential length was set to 5, allowing the model to infer based on the current and past 4 temporal information. The resultant temporal features were then passed through a single linear layer for recognition. Each label-specific network was trained independently with cross-entropy loss, Adam optimizer, and a learning rate of 1e⁻³ for phase and step recognition, and 1e⁻² for hand verbs.

3.2.5 NCC NEXT

The NCC NEXT team was composed of Hiroki Matsuzaki, Yuto Ishikawa, Kazuyuki Hayashi, Yuriko Harai, and Nobuyoshi Takeshita from National Cancer Center Japan East Hospital. They participated in all proposed tasks. They resubmitted docker for all tasks except the kinematic-based recognition task.

Initial video frames were resized at a resolution of 512 x 256 pixels for video-based workflow recognition and 480 x 270 pixels for segmentation-based workflow recognition. A normalization was also done. No preprocessing was done for kinematic data.

For video-based workflow recognition Xception networks [38] pre-trained on ImageNet, one by component, were used. The Radam optimizer [39] was used with different learning rates with a batch size of 4, 1e⁻³ for phase and step, and 1e⁻⁴ with a cosine decay scheduler for hand verbs. The cross-entropy loss was used.

For Kinematic-based workflow recognition, NCC NEXT used LightGBM [40]. As for the previous task, the training and the tuning of hyperparameters were done separately for each component. The hyperparameters were the learning rate, minimum data in leaf, number of iterations, and number of leaves(Table 2. The optimizer was the gradient boosting and the loss was the mean absolute error (MAE).

Parameters	Phase	Step	Verb_Left	Verb_Right
Learning rate	0.1	0.05	0.05	0.05
min_data_in leaf	9	9	3	9
num_iteration	200	100	100	50
num_leaves	11	31	11	11

Table 2: Hyperparameters for the kinematic based model developed by NCC NEXT

The segmentation was performed by a Deeplabv3+ architecture [27] with an Xception backbone pre-trained on PascalVOC [41]. With the predicted segmentation, a multi-output classification model, based on EfficientNetB7 [42], was trained with Radam optimizer, cross-entropy loss function, a learning rate of 0.0001 with a cosine decay scheduler, and a batch size of 16.

For multi-modality workflow recognition tasks, NCC NEXT combined the method of the three previous tasks with the highest accuracy for each component. For video/kinematic-based workflow recognition, they used the video-based architecture for phase and step recognition and kinematic-based architecture for hand verbs recognition. For video/kinematic/segmentation, they used the video-based architecture for phase recognition, the segmentation-based one for step recognition, and the kinematic-based one for hand verbs recognition.

3.2.6 SK

The SK team was composed of Satoshi Kondo from Muroran Institute of Technology. The team participated in all proposed tasks.

For the preprocessing, SK team have resized the image to 640 x 353 pixels and then performed augmentation. They used shift, with a maximum shift size of 10% of the image size, scaling (0.9 to 1.1 times), rotation (-5 to 5 degrees), color jitter (-0.9 to 1.1 times for brightness, contrast, saturation, and hue), and Gaussian blur (max value of the sigma is 1.0). Finally, the images were normalized. Kinematic data were normalized in each dimension.

For video-based workflow recognition a 18-layer ResNet [36], pre-trained on ImageNet, was used. The final fully-connected layer of ResNet was omitted and a 512-dimensional feature vector was fed into three fully-connected layers to obtain step and hand verbs. Each fully-connected layer was constituted of two layers with ReLU and Dropout after the first layers. An adam optimizer, with a learning rate changes with cosine annealing with an initial value of $7.2e^{-4}$, and a batch size of 96, was used. Initial learning rates for each task were optimized with Optuna library [43]. The loss function used was the cross-entropy loss, with weights for each class depending on classes frequency for hand verbs. Phases were not directly predicted from the image but identify based on the predicted step.

An LSTM [37] with 28 hidden layers was used for the kinematic-based workflow recognition task. The output of the LSTM was fed into three fully connected layers as for the previous task. The same optimizer and loss function were used. The initial learning rate was $1.5e^{-3}$ under a batch size of 6 and the number of data in a sequence was 30.

The image segmentation was done thanks to U-Net [44] with a ResNet18 for its encoder with the summation of cross-entropy loss and dice loss. The same model as for the video-based workflow recognition task was used for the segmentation-based one. Both models were trained separately with Adam optimizer and an initial learning rate of $2.4e^{-5}$ with a batch size of 32 for segmentation, and a learning rate of $1e^{-4}$ with a batch size of 6 for recognition.

For the video/kinematic-based task and video/kinematic/segmentation-based task, the dedicated modality networks previously trained were assembled to make the recognition. Since the SK team used the network parameters trained for the previous task, they did not train any network for these tasks.

3.2.7 MediCIS: non-competing

The MediCIS team was the non-competing team due to the presence of challenge organizers on it. This team was composed of Quang-Minh Nguyen and Arnaud Huault from Rennes University. The team participated in all proposed tasks.

As preprocessing, video, and segmentation data, frames have been resized at 256 x 512 pixels. Additionally, to train the segmentation model, the data were down-sampled to 6 Hz. The kinematic data were z-normalized.

For video-based workflow recognition, MediCIS team used a hierarchical RestNet50 [36] pre-trained on ImageNet to extract spacial features. Then a Multi-Stage Temporal Convolutional Network called MS-TCN++ [45], with two stages, trained from scratch was used.

For kinematic-based workflow recognition, data were directly used as features for a two stages MS-TCN++.

The segmentation model used was a U-Net [46] network trained from scratch with the ADAM optimizer, a cross-entropy loss, a learning rate of $1e^{-4}$, and a batch size of 10. As for the video-based task, the recognition was done thanks to a hierarchical ResNet50 followed by a two-stage MS-TCN++.

For video/kinematic-based and video/kinematic/segmentation-based tasks, uni-modality spacial features extracted thanks to a hierarchical ResNet50 for video and segmentation, were concatenated. Then a two-stage MS-TCN++ was trained.

All workflow recognition models were trained with the Adam optimizer, a cross-entropy loss a learning rate of $1e^{-4}$, and a batch size of 2. For hierarchical ResNet50, an emphasis on the training for granularities harder to recognize was made thanks to the following weights on the loss: 1 for phases, 2 for steps, and 5 for each hand's verb. The number of dilated convolutional layers in MS-TCN++ was set to 10 except for the first layer where it was set to 11. The number of feature maps for each layer was set to 64.

3.3 Workflow recognition results

All results were computed on organizer hardware via the provided Docker images. This section only presents the results used for the ranking (balanced application-dependent accuracy noted AD-Acc). Other results such as application-depend scores by sequence and task of each participating team are available on supplementary material and on the files tab of www.synapse.org/PETRAW.

3.3.1 Task 1: video-based workflow recognition

Task 1 consists of recognizing phases, steps, and hand verbs using video only. Table 3 summarizes the algorithms used by the 5 participating teams.

Team	Hutom *	MedAIR *	NCC Next *	SK	MediCIS
Preprocessing	X	X	X	X	X
Augmentation	X	X		X	
Model	3DResNet	Trans-SVNet	Xception	ResNet18	ResNet50 & MS-TCN++
Optimizer	Adam	SGD	Radam	Adam	Adam
Loss	Equalization v2 & Normsoftmax	cross-entropy	cross-entropy	cross-entropy	cross-entropy
Learning Rate	$1e^{-3}$	$5e^{-4}$	$1e^{-3}$ & $1e^{-4}$	$7.2e^{-4}$	$1e^{-4}$
Causal					X

Table 3: Summary of algorithms used for task 1. Resubmitted models are highlighted with a start.

Figure 5 presents the results of all models for each test sequence. For all sequences, we identified a slight performance decreasing from 95.1% to 82.2% of average AD-Accuracy, except for sequences 79 and 54 that have a performance gap to 77.7% and 72.9% respectively. However, we noticed that for all the test cases, one model had an AD-Accuracy lower than the other ones.

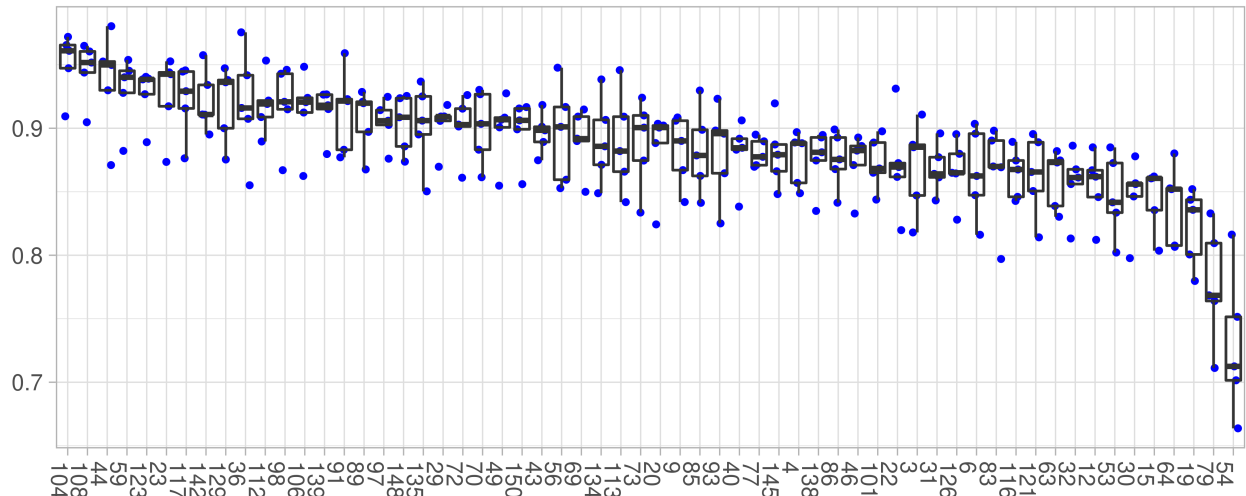


Figure 5: Task 1 recognition AD-Accuracy for each sequence. Each dot represents the AD-Accuracy for one model.

Figure 6 presents the average AD-Accuracy for each model. Two teams, SK and Hutom, obtained results superior to 90%. Two other, MediCiS and NCC NEXT obtained results superior to 87% percent, and MedAIR obtained results around 84%.

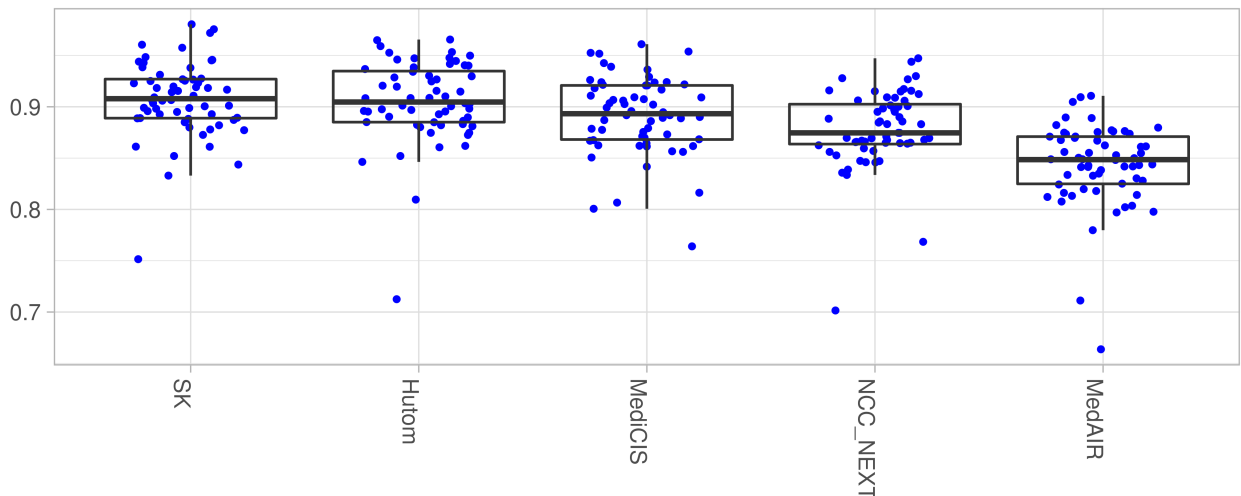


Figure 6: Average task 1 recognition AD-Accuracy for each model. Each dot represents the AD-Accuracy for one sequence.

Figure 7 presents the different rankings according to the chosen method. Except for the rankThenMedian and the testBased method between SK and HutomS teams, the ranking is consistent.

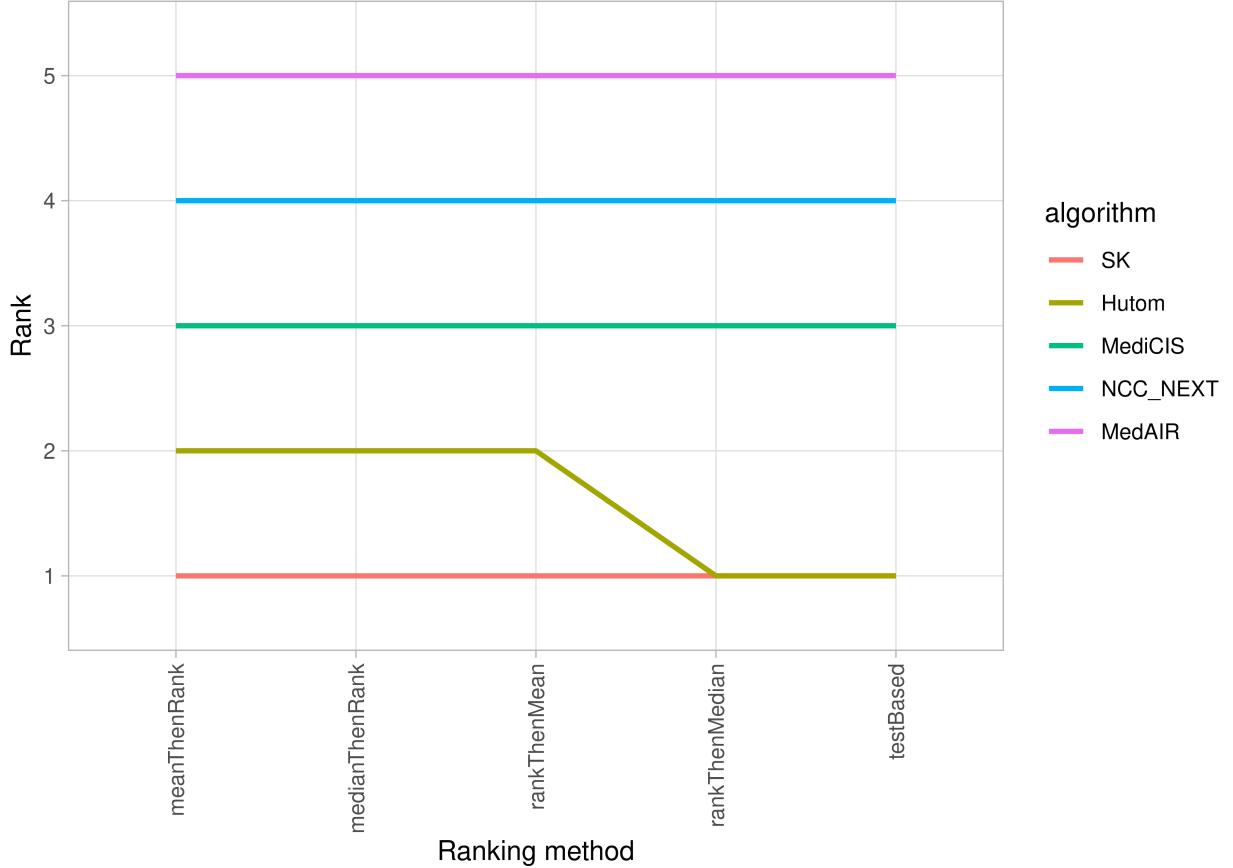


Figure 7: Task 1 recognition ranking stability through different ranking methods. The rank 1 correspond to the best method.

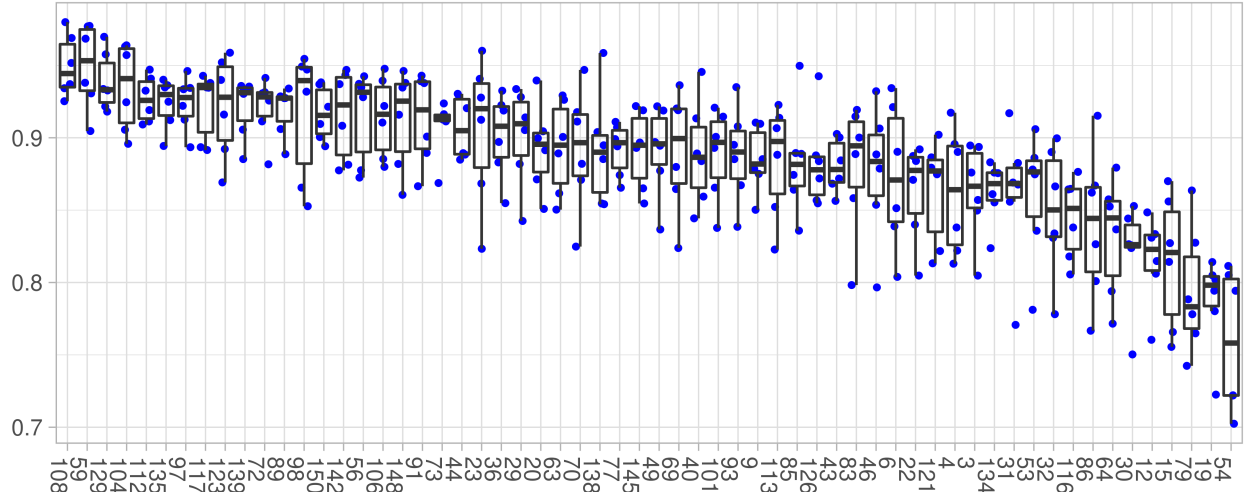
3.3.2 Task 2: Kinematic-based workflow recognition

Task 2 consists of recognizing phases, steps, and hand verbs using kinematic data only. Table 4 summarizes the method used by the 6 participating teams.

Team	Hutom	JHU-CIRL	MedAIR	NCC Next	SK	MediCIS
Preprocessing	X	X	X	X	X	X
Augmentation						
Model	Bi-LSTM	Uni-LSTM	Trans-SVNet	LightGBM	LSTM	MS-TCN++
Optimizer	Adam	Adam	SGD	Gradient Boosting	Adam	Adam
Loss	Equalization v2 & Normsoftmax	cross-entropy	cross-entropy	MAE	cross-entropy	cross-entropy
Learning Rate	1e ⁻³	1e ⁻³	5e ⁻⁴	1e ⁻¹ & 5e ⁻²	1.5e ⁻³	1e ⁻⁴
Causal		X		X	X	

Table 4: Summary of models used for task 2

As for the previous task, the results performances by sequence slightly decrease (figure 8). Best performances were superior to 90% for all teams. Three sequences have average results inferior to 80%, on these sequences we found again sequences 79 and 54. In contrast to task 1, the majority of the sequences did not have outliers.



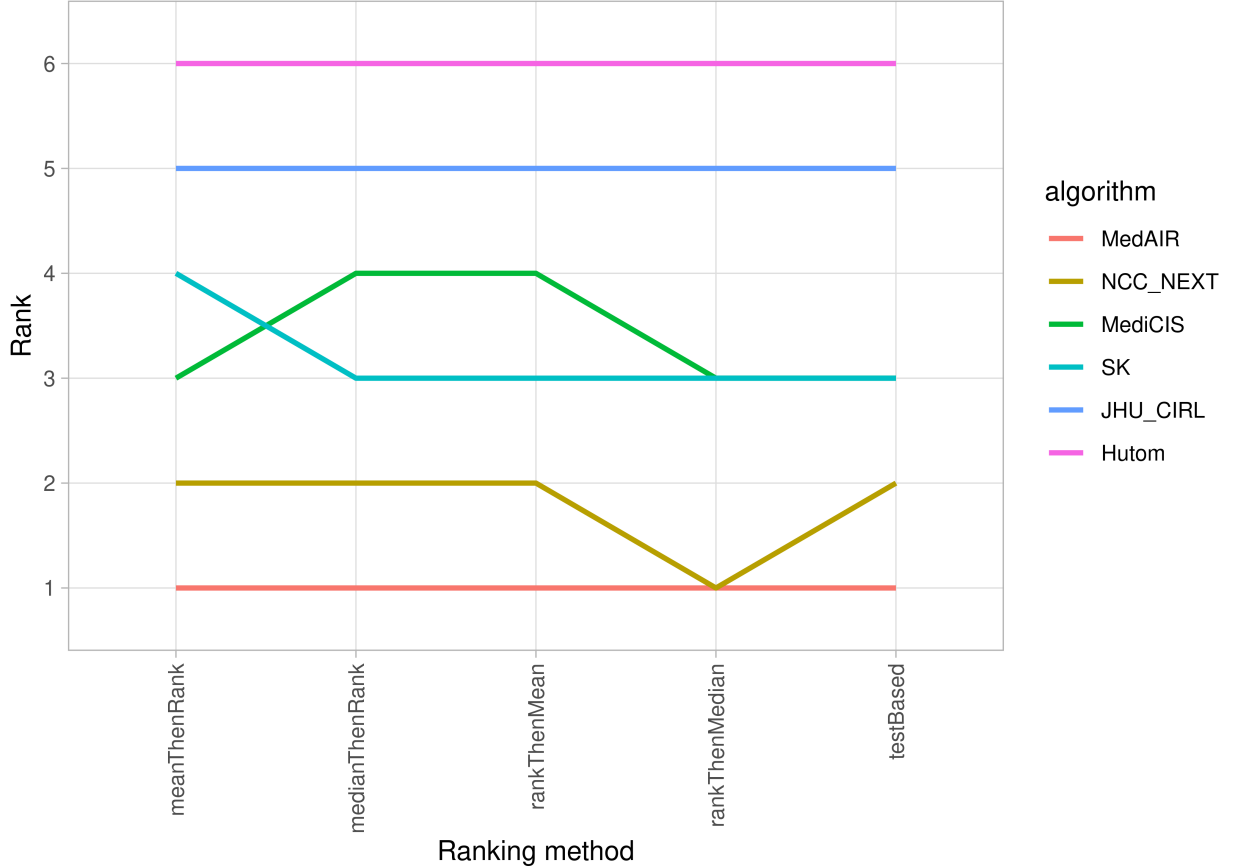


Figure 10: Task 2 recognition ranking stability through different ranking methods.

3.3.3 Task 3: Segmentation-based workflow recognition

Task 3 consists of recognizing phases, steps, and hand verbs using kinematic data only. First, we will focus on the result of the segmentation models provided by the participants, then on the workflow recognition models.

Segmentation models

Table 5 summarizes the method used by the 4 participating teams to perform the segmentation.

Team	Hutom *	NCC Next *	SK	MediCIS
Preprocessing	X	X	X	X
Augmentation	X		X	
Model	DeepLabV3+	DeepLabV3+	U-Net	U-Net
Optimizer	Adam	Radam	Adam	Adam
Loss	Equalization v2 & Normsoftmax	cross-entropy	cross-entropy	cross-entropy
Learning Rate	1e ⁻³	1e ⁻⁴	2.4e ⁻⁵	1e ⁻⁴

Table 5: Summary of segmentation models of task 3. Resubmit models are highlighted with a start.

Table 6 presents the Intersection-over-Union (IoU) for each class for each sequence independently. For all classes (Macro), the IoU varied between 93,9% and 91,1%. Pegs were the less recognized structure with an IoU between 83,9% and 82,3%. We haven't identified specific sequences with lower performances.

Table 7 presents the results of each team for all classes (Macro) and each class independently. NCC Next, SK and MediCIS obtained closed macro results with 96,9%, 96,4%, and 94,0% respectively. Hutom team obtained 85,0%,

principally due to the low IoU for pegs (63.3%). Figure 11 presents the ground truth and the segmentation result of each team for one frame.

	Mean	Median	Max	Min
Background	98.8	98.9	98.9	98.7
Base	96.1	96.2	96.3	95.6
Pegs	83.2	83.1	83.9	82.3
Blocks	91.7	91.7	92.5	90.8
Left tool	94.9	95.3	97.6	87.3
Right tool	94.0	94.5	96.9	88.9
Macro	93.1	93.2	94.0	91.1

Table 6: Mean Intersection-Over-Union over all classes for each sequence independently

	Hutom *	NCC Next *	SK	MediCIS
Background	97.7	99.5	99.2	98.9
Base	91.4	98.4	98.4	96.1
Pegs	63.3	92.1	92.0	85.3
Blocks	82.8	96.0	96.0	92.2
Left tool	89.3	98.1	96.1	96.0
Right tool	85.5	97.8	96.7	95.8
Macro	85.0	96.9	96.4	94.0

Table 7: Mean Intersection-Over-Union over all classes for each team. Resubmitted models are highlighted with a star and best results in bold.

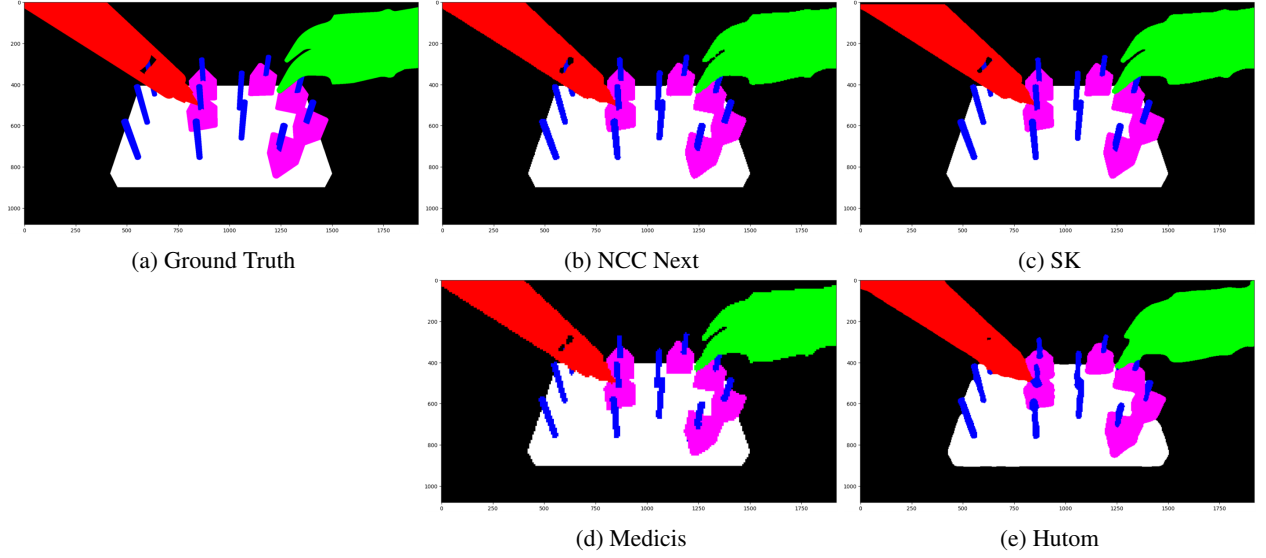


Figure 11: Ground truth (a) and segmentation results to each team (b to e) for one frame.

Workflow models

Table 8 summarizes the method used by the 4 participating teams to perform the workflow recognition.

Figure 12 presents the results by sequence. We identified a slight performance decreasing from 87.5% to 76.6%. The same two sequences as previously have very low results, 79 and 54, with respective performances of 67.4% and 65.5%. Moreover, for all test cases, one model has results lower than 70%.

Team	Hutom *	NCC Next *	SK	MediCIS
Preprocessing	X	X	X	X
Augmentation	X		X	
Model W	SlowFast50	EfficientNetB7	ResNet18	ResNet50 & MS-TCN++
Optimizer	Adam	Radam	Adam	Adam
Loss	Equalization v2 & Normsoftmax	cross-entropy	cross-entropy	cross-entropy
Learning Rate	1e ⁻³	1e ⁻⁴	1e ⁻⁴	1e ⁻⁴
Causal				X

Table 8: Summary of models used for task 3 for the workflow recognition. Resubmitted models are highlighted with a start.

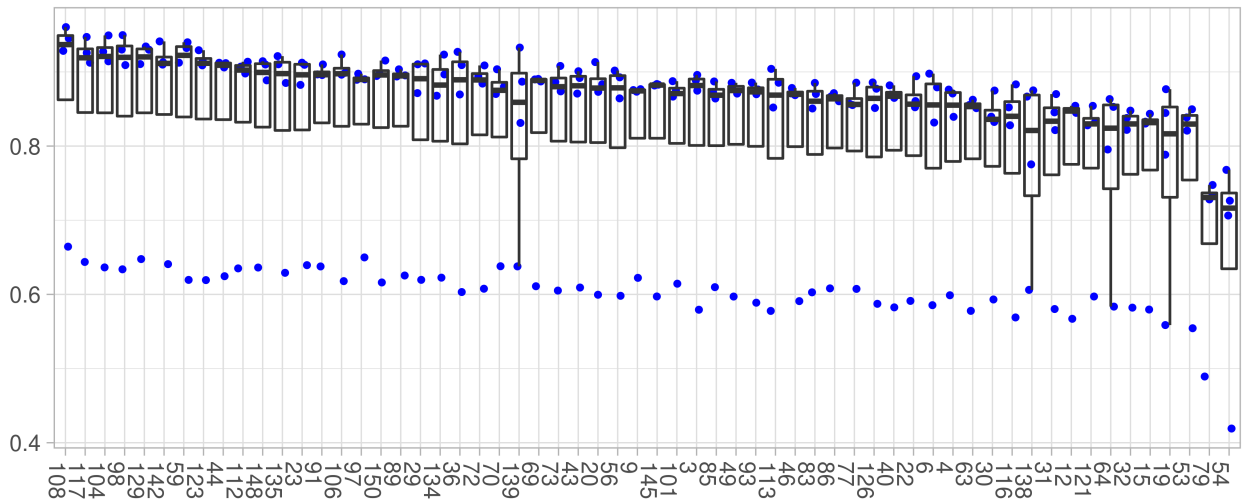


Figure 12: Task 3 recognition AD-Accuracy for each sequence. Each dot represents the AD-Accuracy for one model.

Three teams have results between 88.5% and 87.2%, the last one is Hutom with an average AD-Accuracy of 60.3% (figure 12).

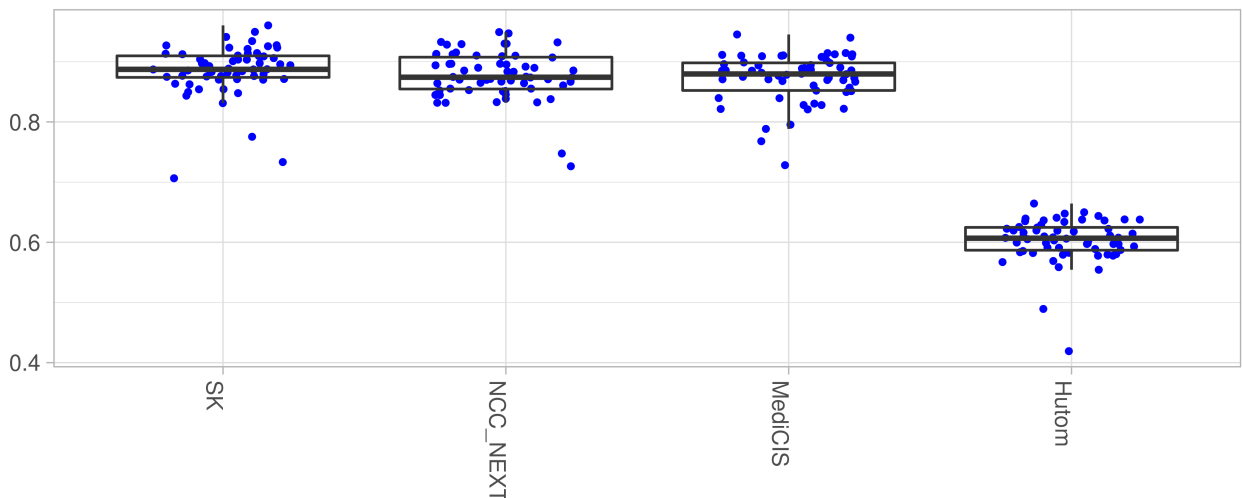


Figure 13: Average task 3 recognition AD-Accuracy for each model. Each dot represents the AD-Accuracy for one sequence.

The choice of method did not influence the ranking, except for between the second and the third teams: NCC NEXT and MediCIS (figure 14).

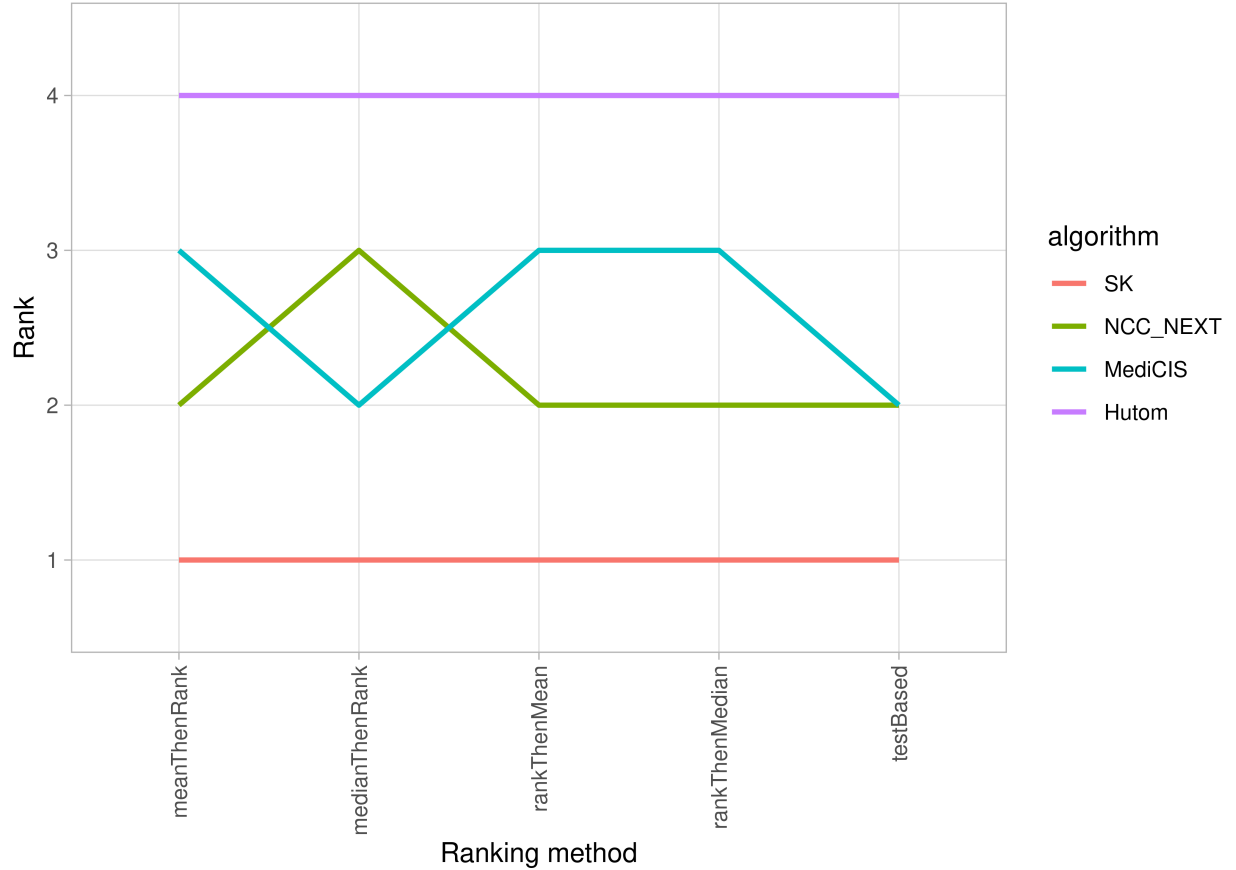


Figure 14: Task 3 recognition ranking stability through different ranking methods.

3.3.4 Task 4: video/kinematic-based workflow recognition

Task 4 consists of recognizing phases, steps, and hand verbs using kinematic data only. Table 9 summarizes the method used by the 6 participating teams.

Team	Hutom *	MedAIR	MMLAB	NCC NEXT *	SK	MediCIS
Preprocessing	X	X	X	X	X	X
Augmentation	X	X			X	
Model	3D ResNet & Bi-LSTM	MRG-Net & CNN	ResNet50 & LSTM	Xception & LightGBM	ResNet18 & LSTM	ResNet50 & MS-TCN++
Optimizer	Adam	Adam	Adam	Radam & Gradient Boosting	Adam	Adam
Loss	Equalization v2 & Normsoftmax	cross-entropy	cross-entropy	cross-entropy & MAE	cross-entropy	cross-entropy
Learning Rate	1e ⁻³	1e ⁻⁴	1e ⁻³ & 1e ⁻²	1e ⁻¹ & 5e ⁻² & 1e ⁻³ & 1e ⁻⁴	7.2e ⁻⁴ & 1.5e ⁻³	1e ⁻⁴
Causal			X			

Table 9: Summary of models used for task 4. Resubmitted models are highlighted with a start.

For task 4, we observe the same characteristics as the previous tasks (figure 15). A slight performance decreased from 95.1% to 83.1% for the majority of the sequence, and a decreasing of performance for sequences 79 and 54 with an AD-Accuracy of 81.2% and 76.5%. However, for this task, there are a few outliers.

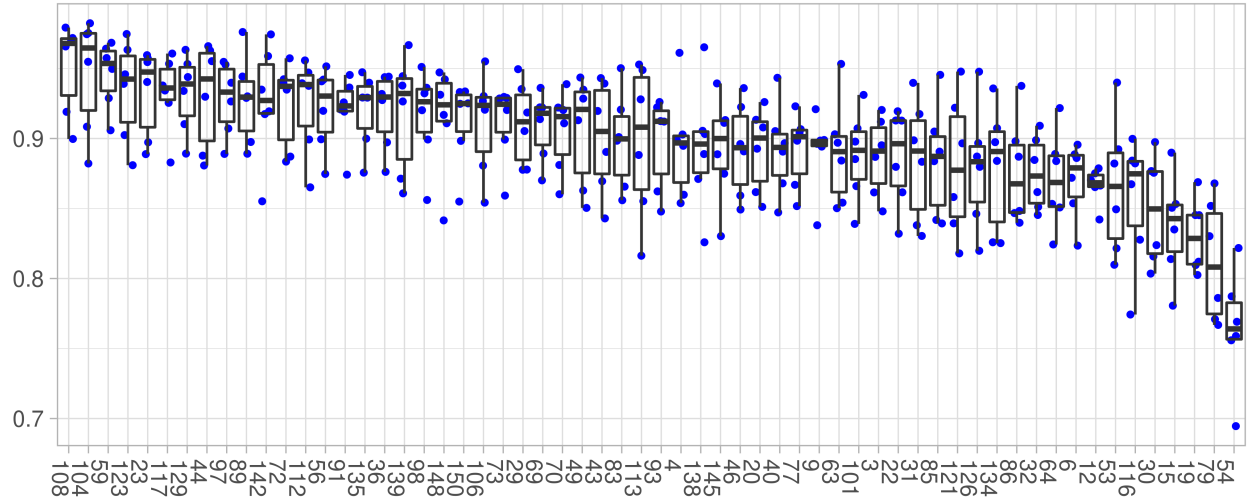


Figure 15: Task 4 recognition AD-Accuracy for each sequence. Each dot represents the AD-Accuracy for one model.

Figure 16 presents the result by team. NCC NEXT had the best results, with an average AD-Accuracy of 93.1%. The three following teams had very similar results between 91.6% and 90.2%. The two last teams had results superior to 84.5%.

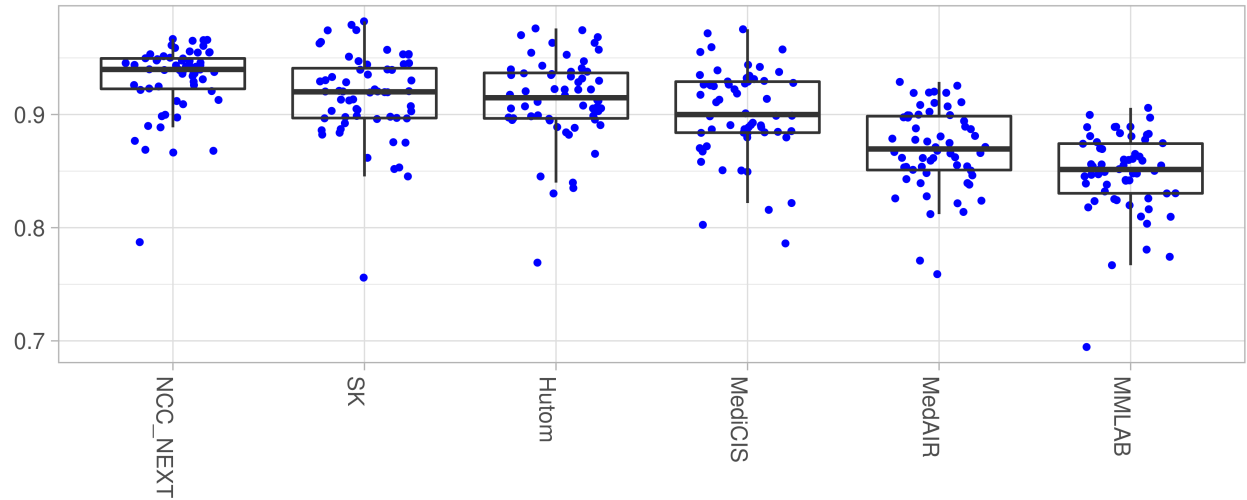


Figure 16: Average task 4 recognition AD-Accuracy for each model. Each dot represents the AD-Accuracy for one sequence.

Even if the results were closed between the second and the fourth team, the ranking is not influenced by the ranking method chosen (figure 17).

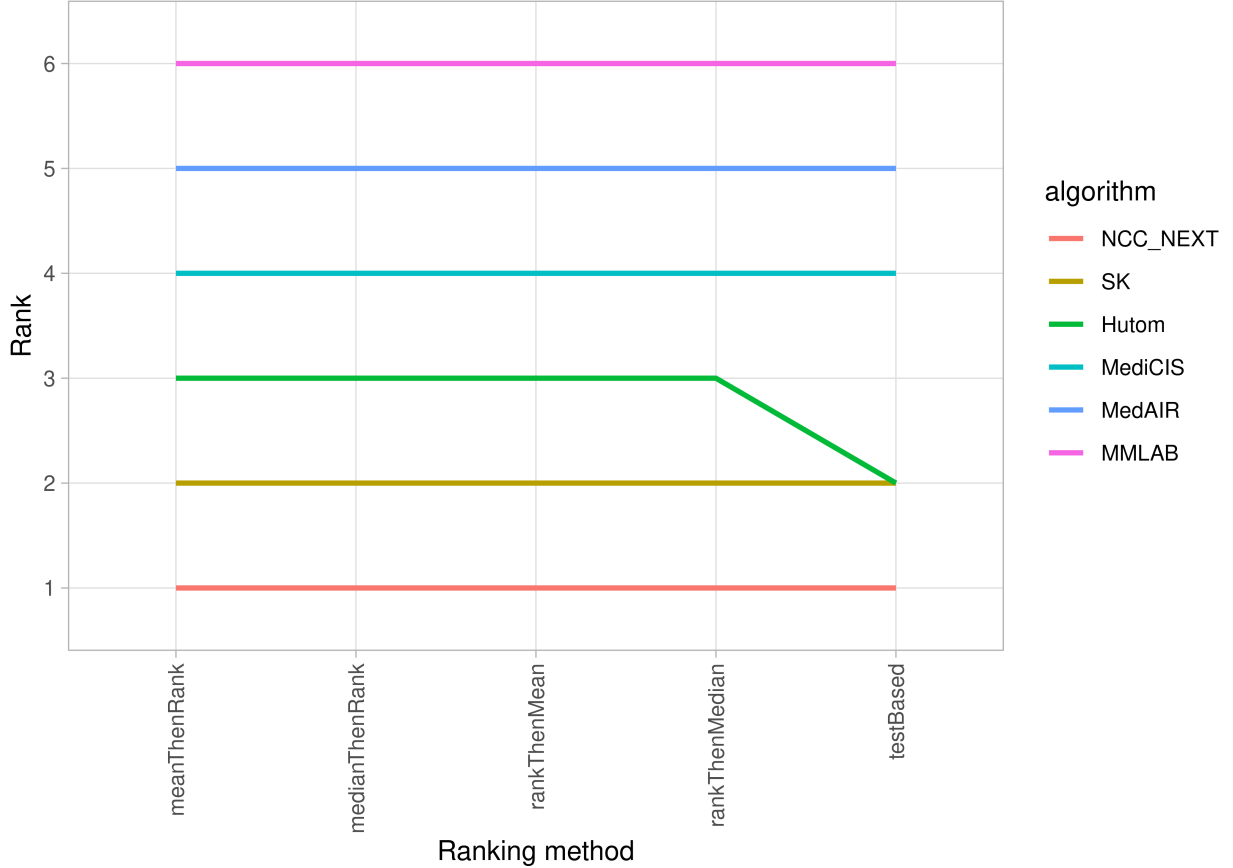


Figure 17: Task 4 recognition ranking stability through different ranking methods.

3.3.5 Task 5: video/kinematic/segmentation-based workflow recognition

Task 5 consists of recognizing phases, steps, and hand verbs using kinematic data only. Table 10 summarizes the recognition method used by the 4 participating teams. The models to create the segmentation were the same as the one described in table 5.

Team	Hutom *	NCC NEXT *	SK	MediCIS
Preprocessing	X	X	X	X
Augmentation	X		X	
Model	3D ResNet & Bi-LSTM	Xception, EfficientNetB7 & LightGBM	ResNet18 & LSTM	ResNet50 & MS-TCN++
Optimizer	Adam	Radam & Gradient Boosting	Adam	Adam
Loss	Equalization v2 & Normsoftmax	cross-entropy & MAE	cross-entropy	cross-entropy
Learning Rate	1e ⁻³	1e ⁻¹ , 5e ⁻² , 1e ⁻³ & 1e ⁻⁴	7.2e ⁻⁴ , 1.5e ⁻³ & 1e ⁻⁴	1e ⁻⁴
Causal				

Table 10: Summary of models used for task 5. Resubmitted models are highlighted with a start.

As for the previous tasks, the results by sequence (figure 18) showed a slight decrease of performance between 97.2% and 85.9%. Sequences 79 and 54 have again the lowest performances with an important decrease, respectively 80.8% and 78.0%.

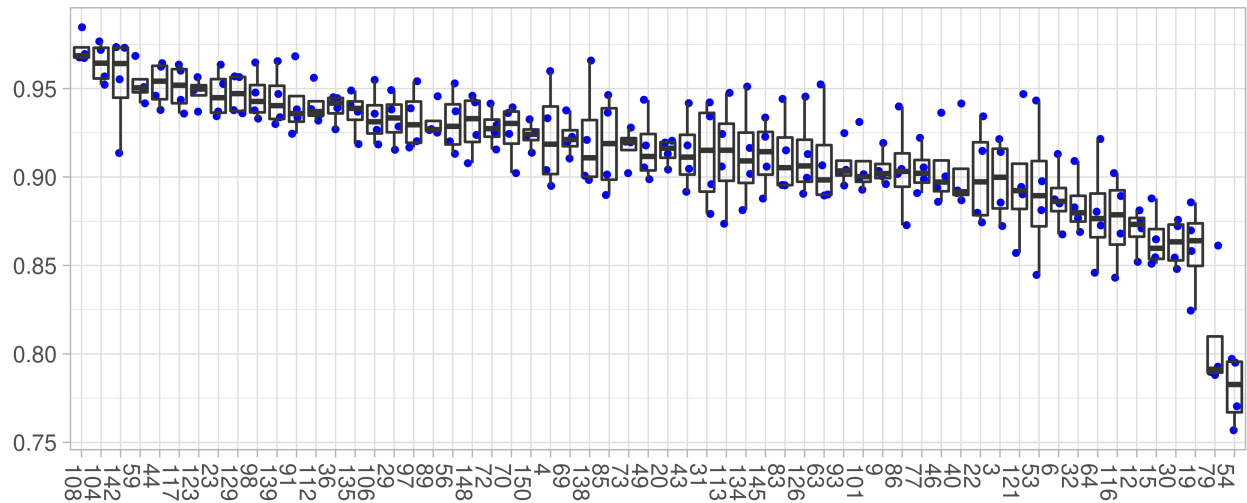


Figure 18: Task 5 recognition AD-Accuracy for each sequence. Each dot represents the AD-Accuracy for one model.

All team had results between 93.1% and 89.8% (figure 16). SK and Hutom had very close results with 91.4 and 91.3 respectively. However, the ranking method chosen did not influence the final rank (figure 17).

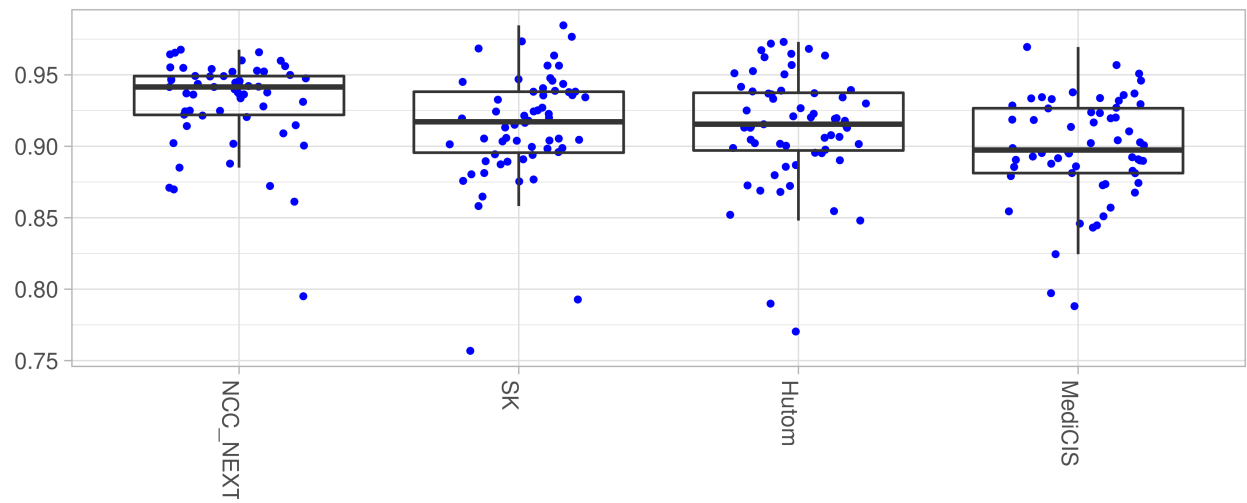


Figure 19: Average task 5 recognition AD-Accuracy for each model. Each dot represents the AD-Accuracy for one sequence.

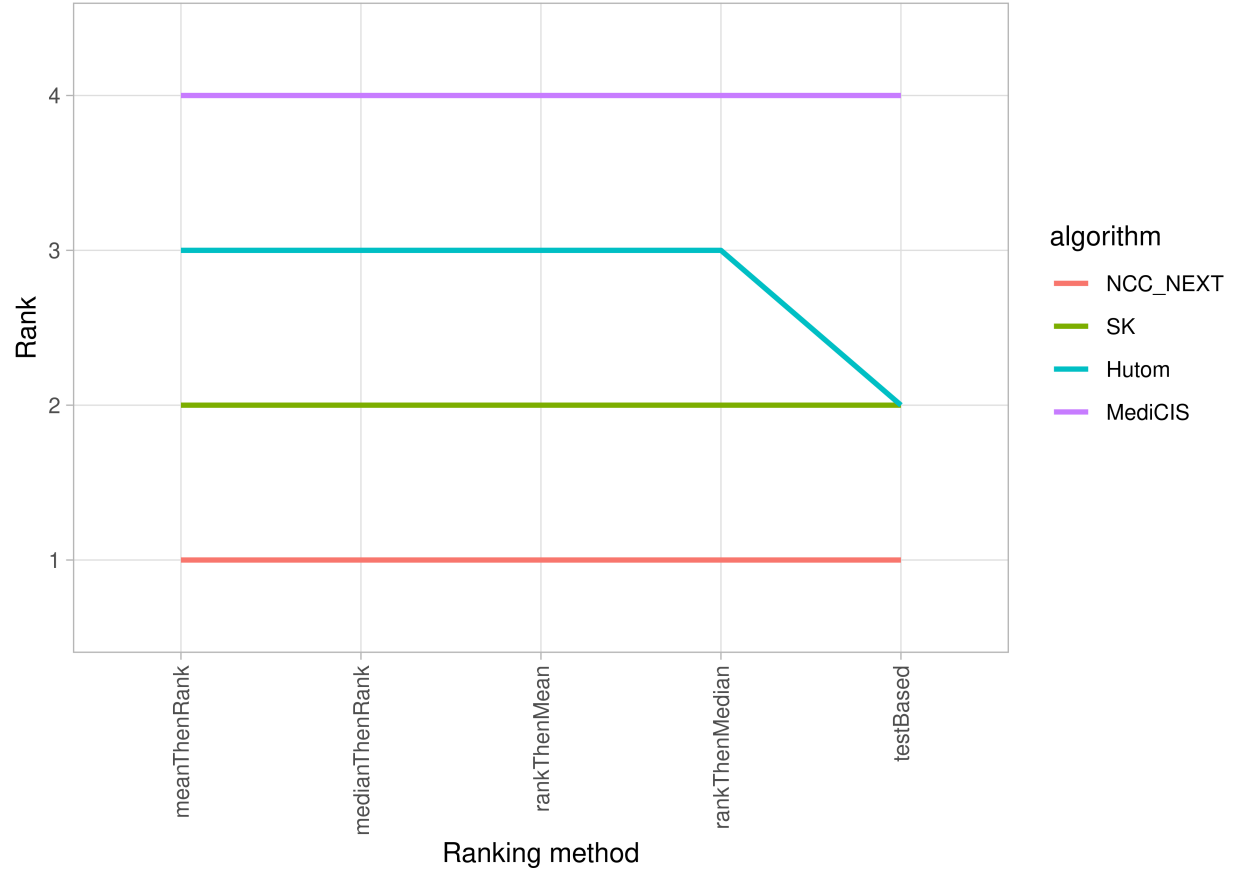


Figure 20: Task 5 recognition ranking stability through different ranking methods.

3.3.6 Workflow recognition results summary

Table 11 summarizes the results of each team on all tasks. All best methods obtained results superior to 90% except for task 3.

Team	Task 1	Task 2	Task 3	Task 4	Task 5
Hutom	90.51 *	84.31	60.28 *	91.33 *	91.27 *
JHU-CIRL		86.45			
MedAIR	84.31 *	90.72		86.98	
MMLAB				84.80	
NCC NEXT	87.77 *	90.32	87.71 *	93.09 *	93.09 *
SK	90.77	89.66	88.51	91.61	91.37
MediCIS	89.15	89.71	87.22	90.18	89.81

Table 11: Average AD-Accuracy of each team for all tasks. Best results are highlighted in bold for each task. Resubmitted models are highlighted with a star.

4 Discussion

To provide automatic context-aware computer-assisted surgical systems an accurate surgical workflow recognition method is mandatory. The proposed methods obtained good results but were not perfect, even if the PETRAW dataset present several limitations. The peg transfer task is easier than a real operation because the environment is simpler, the objects are clearly identified, the field of view is always the same, and the lighting is constant. Furthermore, all sequences have been performed by the same operator, so the variability on the PETRAW dataset is limited.

By analyzing individual sequence recognition, we observe, for all tasks, a slight decrease in performances except for two sequences, 54 and 79, with had very low results compared to the other ones whatever the modality used. We have analyzed these two sequences in details to understand the specificity of these sequences. In sequence 54, there are 2 droppings of the block during the transfer between the two hands, forcing the operator to catch again the block and one block got stuck on the peg, forcing the operator to touch the block. Sequence 79, is one of sequence identified as containing uncertainty (see section 2.3.3), however, the steps overlapping of 0.5 seconds did not explain the low performance because it was partially compensated by the delay of 0.25 seconds used to compute the AD-Accuracy. A block got also stuck on a peg in this sequence. The main variation was in the order in which the blocks were caught, which did not correspond to the one of the majority of the sequences. These deviations from the most common workflow would explain the low performances.

For task 1, video-based recognition, the models based on ResNet have the best results, and it is even the simplest model that ranked first. For task 2, kinematic-based recognition, the LSTM based methods present the lowest results. For task 3, the two segmentation models, DeepLabV3 and U-Net, present similar IoU results and the differences are probably due to differences in training characteristics. For the workflow recognition, EfficientNetB7 and ResNet models present similar results. For tasks 4 and 5, the strategy used by the NCC NEXT team, consisting of using for each workflow component (phase, step, and verbs) the modality which provided the best results on uni-modality tasks, provided the best result.

For the segmentation-based recognition task (task 3), the quality of the segmentation seems to have an influence, up to a certain threshold, on the workflow recognition. The three teams with more than 94.0% of macro IoU obtained closed recognition results (between 88.5% and 87.2%), but the ranking is inverted between the two first teams. On the other side, the last team obtains an IoU of 85%, but the workflow recognition rate drops drastically with only 60.3%. Further works are required to confirm that the quality of the segmentation influences the workflow recognition up to a certain threshold. Because here, the combinations of segmentation and workflow recognition models are different.

For tasks 1 to 4, at least one team submit a causal model. Causal models generally have lower performance than acausal ones. Surprisingly, except for task 4, the causal models obtained performance closed to the best model. For example on task 2, the best model obtained an AD-Accuracy of 90.7%, the causal model of NCC NEXT obtained 90.3%, and 89.7% for the SK one. Obviously, it is not possible to conclude that causal models obtained similar results that acausal ones. Because, first during the challenge we don't have the two versions of a similar model and secondly due to the data simplicity. But the result of causal models are promising to develop applications such as the implementation of an automatic report after training sessions on a virtual simulator.

Among the seven participating teams, four teams (Hutom, NCC Next, SK, and MediCIS) have participated in multi-modality tasks (4 and 5) with a combination of the same or similar models used for uni-modality tasks, allowing a fair study of the impact of each modality and their combinations on automatic workflow recognition. For all cases, the recognition was improved with the use of several modalities, however, the addition of the segmentation modality to the two others decreased the performance. To check if these performance modifications were significant we used a Wilcoxon test. Table 12 indicates when the performances modification were significant with a p-value inferior to 0.05. The improvement from uni-modality to multi-modality models was always significant except between task 2 and task 5 for MediCIS team. The degradation due to the addition of segmentation modality to the video/kinematic-based models was only significant for MediCIS team. So it seems more pertinent to choose the combination of video and kinematic data to have better results than others modality combinations.

Team	Hutom	NCC NEXT	SK	MediCIS
T1 <> T4	X	X	X	X
T2 <> T4	X	X	X	X
T1 <> T5	X	X	X	X
T2 <> T5	X	X	X	
T3 <> T5	X	X	X	X
T4 <> T5				X

Table 12: Significant performance modification between uni-modality and multi-modality tasks. T1 <> T4 is the significant test between task 1 and task 4. An "X" means that the performance variation is significant (p-value <0.05).

However, performances are not the only important point when we develop automatic recognition models. It is also important to take into account the environmental aspect [47]. To answer this question we have examined the execution time to compute the result of the sixty test sequences (table 13). These durations are an interpolation assuming that the results of each task have been computed independently, not the real computation time. For example, the Hutom team used the results for tasks 1 to 3 to provide results of tasks 4 and 5. For NCC Next team, the duration cannot

be determined because the results were locally written at the end of the docker execution. Execution time was very different between teams, with less time for SK except for task 2. The best execution time performances were obtained for task 2 with 3 min for SK and less than 1 minute for Hutom and MediCIS teams. Even if the results of task 4 are better, it is more time-consuming than task 2, with 53, 57, and 2 hundred minutes for SK, Hutom, and MediCIS respectively. It is important to ask ourselves if it makes sense to spend 20 to 200 times more computing time for less than a 3% improvement. The training time should be also taken into account, because it is much more time consuming [48, 49]. However, we did not have access to this information. Another aspect to take into account is data storage. Videos can require a lot of storage space, especially for long surgeries. Whereas, kinematic data are less voluminous.

Team	Hutom	NCC NEXT	SK	MediCIS
Task 1	56 min	CBD	50 min	202 min
Task 2	< 1 min	CBD	3 min	< 1 min
Task 3	13 550 min	CBD	145 min	725 min
Task 4	57 min	CBD	53 min	203 min
Task 5	13 600 min	CBD	175 min	928 min

Table 13: Execution time to compute results of the 60 test sequences.CBD: Cannot Be Determined

Future works will focus on compensating the limitations of the current dataset by including peg transfer sequence performed by several operators in different systems. But also tests on more realistic data are necessary to validate the fact that kinematic data brings the best performance in recognition rate and it is the most environmentally responsible modality.

Acknowledgements

Authors thanks the IRT b<>com for the provision of the software “Surgery Workflow Toolbox [annotate]”, used for this work.

References

- [1] P. Jannin, M. Raimbault, X. Morandi, and B. Gibaud. Modeling surgical procedures for multimodal image-guided neurosurgery. In *Lecture Notes in Computer Science (including subseries Lecture Notes in Artificial Intelligence and Lecture Notes in Bioinformatics)*, volume 2208, pages 565–572. Springer Verlag, 10 2001.
- [2] Florent Lalys and Pierre Jannin. Surgical process modelling: a review. *International Journal of Computer Assisted Radiology and Surgery*, 9(3):495–511, 11 2013.
- [3] F Despinoy, D Bouget, G Forestier, C Penet, N Zemiti, P Poignet, and P Jannin. Unsupervised trajectory segmentation for surgical gesture recognition in robotic training. *IEEE Transactions on Biomedical Engineering*, 63(6):1280–1291, 8 2015.
- [4] Arnaud Huaulmé, Kanako Harada, Germain Forestier, Mamoru Mitsuishi, and Pierre Jannin. Sequential surgical signatures in micro-suturing task. *International Journal of Computer Assisted Radiology and Surgery*, 13(9):1419–1428, 5 2018.
- [5] Germain Forestier, Laurent Riffaud, François Petitjean, Pierre Louis Henaux, and Pierre Jannin. Surgical skills: Can learning curves be computed from recordings of surgical activities? *International Journal of Computer Assisted Radiology and Surgery*, 13(5):629–636, 5 2018.
- [6] S.-Y. Ko, J Kim, W.-J. Lee, and D.-S. Kwon. Surgery task model for intelligent interaction between surgeon and laparoscopic assistant robot. *International Journal of Assistive Robotics and Mechatronics*, 8(1):38–46, 10 2007.
- [7] Warren S. Sandberg, Bethany Daily, Marie Egan, James E. Stahl, Julian M. Goldman, Richard A. Wiklund, and David Rattner. Deliberate Perioperative Systems Design Improves Operating Room Throughput:. *Anesthesiology*, 103(2):406–418, 10 2005.
- [8] Beenish Bhatia, Tim Oates, Yan Xiao, and Peter Hu. Real-time identification of operating room state from video. In *Proceedings of the National Conference on Artificial Intelligence*, volume 2, pages 1761–1766, 10 2007.
- [9] Gwenole Quellec, Mathieu Lamard, Beatrice Cochener, and Guy Cazuguel. Real-Time Task Recognition in Cataract Surgery Videos Using Adaptive Spatiotemporal Polynomials. *IEEE Transactions on Medical Imaging*, 34(4):877–887, 4 2015.

- [10] Arnaud Huaultmé, Pierre Jannin, Fabian Reche, Jean-Luc Faucheron, Alexandre Moreau-Gaudry, and Sandrine Voros. Offline identification of surgical deviations in laparoscopic rectopexy. *Artificial Intelligence in Medicine*, 104:1–26, 9 2019.
- [11] A Huaultmé, F Despinoy, S A Heredia Perez, K Harada, M Mitsuishi, and P Jannin. Automatic annotation of surgical activities using virtual reality environments. *International Journal of Computer Assisted Radiology and Surgery*, 14(10):1663–1671, 7 2019.
- [12] Nicolas Padoy, Tobias Blum, S.-A. Seyed Ahmad S.-A. Seyed Ahmad Ahmadi, Hubertus Feussner, Marie Odile M.-O. Marie Odile M.-O. Berger, and Nassir Navab. Statistical modeling and recognition of surgical workflow. *Medical Image Analysis*, 16(3):632–641, 1 2010.
- [13] Andru P. Twinanda, Sherif Shehata, Didier Mutter, Jacques Marescaux, Michel De Mathelin, and Nicolas Padoy. EndoNet: A Deep Architecture for Recognition Tasks on Laparoscopic Videos. *IEEE Transactions on Medical Imaging*, 36(1):86–97, 2 2016.
- [14] L Bouarfa, P P Jonker, and J Dankelman. Discovery of high-level tasks in the operating room. *Journal of Biomedical Informatics*, 44(3):455–462, 10 2011.
- [15] A James, D Vieira, B Lo, A Darzi, and G.-Z. Yang. Eye-Gaze Driven Surgical Workflow Segmentation. *Medical Image Computing and Computer-Assisted Intervention MICCAI 2007*, pages 110–117, 11 2007.
- [16] Florent Lalys, David Bouget, Laurent Riffaud, and Pierre Jannin. Automatic knowledge-based recognition of low-level tasks in ophthalmological procedures. *International Journal of Computer Assisted Radiology and Surgery*, 8(1):39–49, 4 2012.
- [17] Duygu Sarikaya and Pierre Jannin. Surgical Gesture Recognition with Optical Flow only. *arXiv*, 4 2019.
- [18] Isabel Funke, Sebastian Bodenstedt, Florian Oehme, Felix von Bechtolsheim, Jürgen Weitz, and Stefanie Speidel. Using 3D Convolutional Neural Networks to Learn Spatiotemporal Features for Automatic Surgical Gesture Recognition in Video. In *Lecture Notes in Computer Science (including subseries Lecture Notes in Artificial Intelligence and Lecture Notes in Bioinformatics)*, volume 11768 LNCS, pages 467–475, 2019.
- [19] Robert DiPietro and Gregory D. Hager. Automated Surgical Activity Recognition with One Labeled Sequence, 10 2019.
- [20] Arnaud Huaultmé, Duygu Sarikaya, Kévin Le Mut, Fabien Despinoy, Yonghao Long, Qi Dou, Chin-Boon Chng, Wenjun Lin, Satoshi Kondo, Laura Bravo-Sánchez, Pablo Arbeláez, Wolfgang Reiter, Manoru Mitsuishi, Kanako Harada, and Pierre Jannin. Micro-surgical anastomose workflow recognition challenge report. *Computer Methods and Programs in Biomedicine*, 212:106452, 11 2021.
- [21] Yong-Hao Long, Jie-Ying Wu, Bo Lu, Yue-Ming Jin, Mathias Unberath, Yun-Hui Liu, Pheng-Ann Heng, and Qi Dou. Relational Graph Learning on Visual and Kinematics Embeddings for Accurate Gesture Recognition in Robotic Surgery. *arXiv*, 2020.
- [22] Yidan Qin, Max Allan, Yisong Yue, Joel W. Burdick, and Mahdi Azizian. Learning Invariant Representation of Tasks for Robust Surgical State Estimation. *arXiv*, 2 2021.
- [23] S.A Heredia Perez, Kanako Harada, and Mamoru Mitsuishi. Haptic Assistance for Robotic Surgical Simulation. *27th Annual Congress of Japan Society of Computer Aided Surgery*, 20(4):232–233, 11 2018.
- [24] O Dergachyova, D Bouget, A Huaultmé, X Morandi, and P Jannin. Automatic data-driven real-time segmentation and recognition of surgical workflow. *International Journal of Computer Assisted Radiology and Surgery*, 10 2016.
- [25] Lena Maier-Hein, Matthias Eisenmann, Annika Reinke, Sinan Onogur, Marko Stankovic, Patrick Scholz, Tal Arbel, Hrvoje Bogunovic, Andrew P Bradley, Aaron Carass, Carolin Feldmann, Alejandro F Frangi, Peter M Full, Bram van Ginneken, Allan Hanbury, Katrin Honauer, Michal Kozubek, Bennett A Landman, Keno März, Oskar Maier, Klaus Maier-Hein, Bjoern H Menze, Henning Müller, Peter F Neher, Wiro Niessen, Nasir Rajpoot, Gregory C Sharp, Korsuk Sirinukunwattana, Stefanie Speidel, Christian Stock, Danail Stoyanov, Abdel Aziz Taha, Fons van der Sommen, Ching-Wei Wang, Marc-André Weber, Guoyan Zheng, Pierre Jannin, and Annette Kopp-Schneider. Why rankings of biomedical image analysis competitions should be interpreted with care. *Nature Communications*, 9(1):5217, 12 2018.
- [26] Manuel Wiesenfarth, Annika Reinke, Bennett A. Landman, Matthias Eisenmann, Laura Aguilera Saiz, M. Jorge Cardoso, Lena Maier-Hein, and Annette Kopp-Schneider. Methods and open-source toolkit for analyzing and visualizing challenge results. *Scientific Reports*, 11(1):2369, 12 2021.
- [27] Liang Chieh Chen, Yukun Zhu, George Papandreou, Florian Schroff, and Hartwig Adam. Encoder-decoder with atrous separable convolution for semantic image segmentation. In *Lecture Notes in Computer Science (including*

- subseries Lecture Notes in Artificial Intelligence and Lecture Notes in Bioinformatics), volume 11211 LNCS, pages 833–851, 2018.*
- [28] Kensho Hara, Hirokatsu Kataoka, and Yutaka Satoh. Can Spatiotemporal 3D CNNs Retrace the History of 2D CNNs and ImageNet? In *Proceedings of the IEEE Computer Society Conference on Computer Vision and Pattern Recognition*, pages 6546–6555, 2018.
 - [29] Mike Schuster and Kuldip K Paliwal. Bidirectional Recurrent Neural Networks. *IEEE TRANSACTIONS ON SIGNAL PROCESSING*, 45(11), 1997.
 - [30] Christoph Feichtenhofer, Haoqi Fan, Jitendra Malik, and Kaiming He. Slowfast networks for video recognition. In *Proceedings of the IEEE International Conference on Computer Vision*, volume 2019-Octob, pages 6201–6210, 2019.
 - [31] Xinlei Chen and Kaiming He. Exploring Simple Siamese Representation Learning. 2020.
 - [32] Jingru Tan, Xin Lu, Gang Zhang, Changqing Yin, and Quanquan Li. Equalization Loss v2: A New Gradient Balance Approach for Long-tailed Object Detection. 12 2020.
 - [33] Andrew Zhai and Hao Yu Wu. Classification is a Strong Baseline for Deep Metric Learning. *30th British Machine Vision Conference 2019, BMVC 2019*, 11 2018.
 - [34] Robert Dipietro, Colin Lea, Anand Malpani, Narges Ahmadi, S. Swaroop Vedula, Gyu-sung I. Lee, Mija R Lee, and Gregory D Hager. Recognizing surgical activities with recurrent neural networks. In *Lecture Notes in Computer Science (including subseries Lecture Notes in Artificial Intelligence and Lecture Notes in Bioinformatics)*, volume 9900 LNCS, pages 551–558, 2016.
 - [35] Xiaojie Gao, Yueming Jin, Yonghao Long, Qi Dou, and Pheng Ann Heng. Trans-SVNet: Accurate Phase Recognition from Surgical Videos via Hybrid Embedding Aggregation Transformer. *Lecture Notes in Computer Science (including subseries Lecture Notes in Artificial Intelligence and Lecture Notes in Bioinformatics)*, 12904 LNCS:593–603, 3 2021.
 - [36] Kaiming He, Xiangyu Zhang, Shaoqing Ren, and Jian Sun. Deep residual learning for image recognition. In *Proceedings of the IEEE Computer Society Conference on Computer Vision and Pattern Recognition*, volume 2016-Decem, pages 770–778, 2016.
 - [37] Sepp Hochreiter and Jürgen Schmidhuber. Long Short-Term Memory. *Neural Computation*, 9(8):1735–1780, 11 1997.
 - [38] François Chollet. Xception: Deep Learning with Depthwise Separable Convolutions. *Proceedings - 30th IEEE Conference on Computer Vision and Pattern Recognition, CVPR 2017*, 2017-January:1800–1807, 10 2016.
 - [39] Liyuan Liu, Haoming Jiang, Pengcheng He, Weizhu Chen, Xiaodong Liu, Jianfeng Gao, and Jiawei Han. On the Variance of the Adaptive Learning Rate and Beyond. 8 2019.
 - [40] Guolin Ke, Qi Meng, Thomas Finley, Taifeng Wang, Wei Chen, Weidong Ma, Qiwei Ye, and Tie-Yan Liu. LightGBM: A Highly Efficient Gradient Boosting Decision Tree. *Advances in Neural Information Processing Systems*, 30, 2017.
 - [41] Mark Everingham, Luc Van Gool, Christopher K.I. Williams, John Winn, and Andrew Zisserman. The Pascal Visual Object Classes (VOC) Challenge. *International Journal of Computer Vision* 2009 88(2), 88(2):303–338, 9 2009.
 - [42] Mingxing Tan and Quoc V. Le. EfficientNet: Rethinking Model Scaling for Convolutional Neural Networks. *36th International Conference on Machine Learning, ICML 2019*, 2019-June:10691–10700, 5 2019.
 - [43] Takuya Akiba, Shotaro Sano, Toshihiko Yanase, Takeru Ohta, and Masanori Koyama. Optuna: A Next-generation Hyperparameter Optimization Framework. *Proceedings of the ACM SIGKDD International Conference on Knowledge Discovery and Data Mining*, pages 2623–2631, 7 2019.
 - [44] Olaf Ronneberger, Philipp Fischer, and Thomas Brox. U-Net: Convolutional Networks for Biomedical Image Segmentation. *Lecture Notes in Computer Science (including subseries Lecture Notes in Artificial Intelligence and Lecture Notes in Bioinformatics)*, 9351:234–241, 2015.
 - [45] Shijie Li, Yazan Abu Farha, Yun Liu, Ming-Ming Cheng, and Juergen Gall. MS-TCN++: Multi-Stage Temporal Convolutional Network for Action Segmentation. *Proceedings of the IEEE Computer Society Conference on Computer Vision and Pattern Recognition*, 2019-June:3570–3579, 6 2020.
 - [46] Karen Simonyan and Andrew Zisserman. Very Deep Convolutional Networks for Large-Scale Image Recognition. *3rd International Conference on Learning Representations, ICLR 2015 - Conference Track Proceedings*, 9 2014.
 - [47] Pierre Jannin. Towards responsible research in digital technology for health care. 9 2021.

- [48] David Patterson, Joseph Gonzalez, Quoc Le, Chen Liang, Lluis-Miquel Munguia, Daniel Rothchild, David So, Maud Texier, and Jeff Dean. Carbon Emissions and Large Neural Network Training.
- [49] Emma Strubell, Ananya Ganesh, and Andrew McCallum. Energy and Policy Considerations for Deep Learning in NLP. 2019.

Supplementary material

A. Authors' contributions

A. Huaulmé was the challenge coordinator, the primary contact with the participant teams, and a member of the MediCIS team. He acquired the dataset, collected, computed, and analyzed the results, and wrote the paper. K. Harada and M. Mitsuishi were members of the challenge organizers and supervised the development of the peg transfer simulator. P. Jannin was the challenge supervisor. Q-M. Nguyen was a member of the MediCIS team. B. Park, S. Hong, and M-K Choi were members of the Hutom team. M. Peven was a member of the JHU-CIRL team. Y. Li, Y. Long, and Q. Dou were members of the MedAIR team. S. Kumar, S. Lalithkumar, and R. Hongliang were members of the MMLAB Team. H. Matsizaki, Y. Ishikawa and Y. Harai were members of NCC Next team. S. Kondo was a member of the SK team. All co-authors participated in the proofreading of the parts concerning their work.

B. Data sets characteristics

The following tables present the numerical value of the vocabulary term distribution in the training and test data set.

Phase	Training	Test
Transfer Left to Right (L2R)	48.54 %	47.35%
Transfer Right to Left (R2L)	47.87 %	49.05%
Idle	3.59 %	3.60 %

Table 14: Phase distribution in training and test data sets

Step	Training	Test
Block 1 L2R	8.29 %	8.96 %
Block 1 R2L	8.50 %	8.51 %
Block 2 L2R	8.03 %	8.12 %
Block 2 R2L	7.58 %	8.41 %
Block 3 L2R	8.42 %	7.72 %
Block 3 R2L	8.14 %	8.04 %
Block 4 L2R	7.82 %	7.40 %
Block 4 R2L	7.49 %	7.34 %
Block 5 L2R	7.91 %	7.65 %
Block 5 R2L	7.48 %	7.83 %
Block 6 L2R	8.07 %	7.51 %
Block 6 R2L	8.69 %	8.92 %
Idle	3.59 %	3.60 %

Table 15: Step distribution in training and test data sets

Verb Left	Training	Test
Catch	8.97 %	8.99 %
Drop	2.15 %	1.91 %
Extract	5.32 %	5.43 %
Hold	26.33 %	25.90 %
Insert	3.66 %	3.61 %
Touch	0.59 %	0.60 %
Idle	52.98 %	53.56 %

Table 16: Verb Left distribution in training and test data sets

Verb Right	Training	Test
Catch	7.65 %	7.64 %
Drop	1.68 %	1.76 %
Extract	4.75 %	5.01 %
Hold	26.42 %	26.53 %
Insert	3.75 %	3.66 %
Touch	0.62 %	0.48 %
Idle	55.14 %	54.91 %

Table 17: Verb Right distribution in training and test data sets

B. Detailed results for each team

The results for each team by sequence and task are presented on the following pages. Eight balanced scores were computed, the frame-by-frame and application-dependent version of the accuracy, precision, recall, and F1. To limit the number of results, we only present here the ones for all granularities, as used during the challenge. The results for each granularity independently are available at <https://www.synapse.org/PETRAW> on the files section.

B.1 Hutom

Table 18: Results of team Hutom for task1 recognition.

Sequence	Frame-by-Frame				Application-Dependant			
	Accuracy	Precision	recall	F1	Accuracy	Precision	recall	F1
003	85.80	95.45	94.88	94.95	88.51	96.53	95.95	96.03
004	86.28	96.39	96.40	96.30	89.69	97.38	97.35	97.29
006	86.23	96.45	96.34	96.34	90.35	97.34	97.28	97.25
009	89.03	96.08	95.93	95.91	90.85	96.95	96.81	96.78
012	83.62	94.13	93.92	93.87	86.19	94.86	94.71	94.64
015	83.17	93.48	92.64	92.84	86.05	94.18	93.52	93.64
019	83.01	93.36	93.09	93.00	85.20	94.25	94.06	93.90
020	87.17	95.38	95.25	95.18	90.05	96.39	96.27	96.20
022	83.70	93.85	93.16	93.19	87.26	95.04	94.36	94.39
023	92.63	97.03	96.87	96.91	95.27	98.08	97.99	98.00
029	87.20	95.10	94.69	94.77	90.58	96.33	96.00	96.04
030	82.44	92.67	92.11	92.10	84.63	93.61	93.14	93.09
031	86.74	96.13	96.04	96.05	89.60	97.25	97.21	97.19
032	85.47	95.27	94.97	94.95	88.63	96.41	96.24	96.20
036	91.66	96.13	95.86	95.91	94.17	97.23	97.00	97.02
040	86.02	95.45	94.76	94.90	88.31	96.32	95.77	95.84
043	87.72	95.75	95.90	95.70	90.12	96.89	97.08	96.89
044	89.83	96.98	96.80	96.78	94.98	98.52	98.37	98.39
046	85.81	94.48	93.96	93.95	88.24	95.74	95.18	95.18
049	88.03	95.30	94.47	94.49	90.84	96.45	95.68	95.68
053	84.86	93.50	93.33	93.21	88.50	94.64	94.48	94.42
054	68.61	81.64	80.25	79.53	71.25	82.85	81.28	80.61
056	91.97	96.34	95.88	96.01	94.77	97.21	96.83	96.93
059	90.01	94.97	94.35	94.39	94.02	96.06	95.50	95.51
063	84.30	93.39	93.16	92.97	87.46	94.76	94.48	94.32
064	85.75	92.52	92.86	92.55	88.02	93.47	93.86	93.53
069	87.95	94.29	93.95	93.91	91.48	95.65	95.41	95.32
070	88.65	96.08	95.77	95.83	93.02	97.45	97.13	97.20
072	87.21	95.08	94.70	94.71	90.29	96.32	96.06	96.03
073	88.33	94.65	94.15	94.12	91.01	95.70	95.21	95.19
077	86.86	96.81	96.91	96.82	88.97	97.91	98.01	97.92
079	77.33	87.19	87.05	86.28	80.95	88.54	88.32	87.58
083	85.42	93.27	93.38	93.19	89.03	94.70	94.76	94.58
085	89.54	96.74	96.57	96.60	92.97	97.81	97.69	97.69

Table 18: Results of team Hutom for task1 recognition. (continued)

Sequence	Frame-by-Frame				Application-Dependant			
	Accuracy	Precision	recall	F1	Accuracy	Precision	recall	F1
086	87.05	96.87	97.02	96.91	89.27	98.04	98.22	98.10
089	89.55	97.10	96.68	96.84	92.86	98.02	97.66	97.79
091	90.96	96.27	96.16	96.17	95.91	97.72	97.65	97.66
093	86.88	95.94	95.86	95.78	89.82	97.30	97.22	97.13
097	88.68	96.68	96.75	96.69	92.48	98.25	98.32	98.26
098	92.08	97.70	97.69	97.66	94.60	98.89	98.92	98.88
101	85.33	95.51	95.38	95.29	89.76	96.70	96.58	96.50
104	92.58	97.16	96.95	97.01	96.55	98.58	98.39	98.46
106	89.04	96.88	96.71	96.72	92.06	98.04	97.86	97.88
108	93.60	97.73	97.54	97.61	96.49	98.68	98.56	98.60
112	91.47	97.37	97.07	97.18	95.33	98.45	98.30	98.35
113	86.19	95.16	94.79	94.81	88.20	96.05	95.84	95.81
116	84.78	93.46	93.73	93.29	87.46	94.61	94.80	94.45
117	91.06	97.14	97.09	96.99	94.47	98.47	98.45	98.35
121	86.63	96.79	96.48	96.53	89.54	97.75	97.51	97.53
123	90.79	96.25	95.91	96.01	94.05	97.44	97.18	97.25
126	86.33	96.12	96.06	96.05	89.53	97.17	97.15	97.13
129	90.34	96.17	96.05	96.04	94.72	97.55	97.39	97.40
134	88.82	97.32	97.12	97.08	93.84	98.52	98.30	98.27
135	90.48	96.97	96.98	96.94	93.68	98.28	98.36	98.29
138	85.22	95.26	94.99	95.00	88.11	96.27	96.06	96.07
139	89.94	97.02	96.96	96.89	92.67	98.35	98.32	98.26
142	90.58	97.21	97.24	97.21	93.41	98.49	98.56	98.52
145	89.44	95.58	95.41	95.27	91.96	96.70	96.53	96.37
148	88.39	95.10	95.01	94.96	90.87	96.28	96.24	96.18
150	89.15	95.30	94.58	94.45	91.56	96.39	95.77	95.62
Mean	87.40	95.29	95.04	94.99	90.51	96.43	96.22	96.16

Table 19: Results of team Hutom for task2 recognition.

Sequence	Frame-by-Frame				Application-Dependant			
	Accuracy	Precision	recall	F1	Accuracy	Precision	recall	F1
003	78.64	88.98	88.27	88.02	80.48	89.89	89.24	88.97
004	80.43	91.61	90.34	90.30	82.20	92.40	91.16	91.11
006	78.53	90.03	88.81	88.79	80.39	91.08	89.98	89.95
009	83.24	90.82	89.79	89.78	85.02	91.98	91.01	90.97
012	74.15	83.17	82.82	82.72	76.04	83.93	83.68	83.52
015	73.37	83.97	83.05	82.92	75.55	84.64	83.91	83.71
019	70.92	80.46	79.25	78.37	72.25	81.16	80.00	79.09
020	82.68	91.97	91.49	91.44	85.08	92.90	92.53	92.44
022	78.26	86.39	86.21	85.67	80.48	87.45	87.24	86.72
023	84.75	91.43	91.29	91.19	86.84	92.41	92.35	92.24
029	82.41	89.36	88.11	88.13	84.25	90.33	89.34	89.26
030	72.78	82.23	81.01	80.33	75.03	83.01	81.89	81.16
031	75.09	83.15	81.75	81.65	77.07	84.07	82.85	82.69
032	81.18	90.69	90.60	90.48	83.09	91.79	91.80	91.62
036	85.98	91.17	90.25	90.30	88.30	92.34	91.58	91.55
040	82.37	89.68	88.51	88.59	84.43	90.60	89.68	89.67
043	83.36	91.04	90.55	90.43	85.64	92.28	91.81	91.66
044	86.21	91.70	91.34	91.33	88.49	92.76	92.53	92.48
046	77.57	85.37	85.11	84.90	79.66	86.51	86.27	86.05
049	81.97	90.57	90.25	90.11	83.67	91.44	91.22	91.04
053	76.25	86.85	86.58	86.43	78.11	87.65	87.43	87.24

Table 19: Results of team Hutom for task2 recognition. (continued)

Sequence	Frame-by-Frame				Application-Dependant			
	Accuracy	Precision	recall	F1	Accuracy	Precision	recall	F1
054	67.58	75.91	75.13	75.05	70.24	77.03	76.36	76.25
056	84.63	91.52	90.33	90.52	87.25	92.51	91.56	91.66
059	87.63	91.00	90.41	90.50	90.46	91.99	91.56	91.59
063	82.87	90.83	89.90	89.70	85.04	91.98	91.17	90.93
064	76.79	84.83	83.47	83.13	79.40	85.96	84.68	84.28
069	79.76	87.05	86.31	86.15	82.38	88.18	87.58	87.37
070	79.87	89.44	88.09	88.21	82.48	90.55	89.34	89.37
072	85.45	92.56	91.37	91.59	88.17	93.88	92.91	93.02
073	83.99	92.20	91.03	91.13	86.87	93.29	92.17	92.25
077	84.48	93.96	93.59	93.57	86.55	95.12	94.93	94.86
079	71.27	82.20	82.21	82.08	74.24	83.62	83.58	83.49
083	77.87	85.92	85.03	84.82	79.82	86.90	86.09	85.83
085	81.93	92.72	91.89	91.55	83.58	93.63	92.93	92.55
086	77.57	91.73	91.32	91.12	80.10	93.10	92.78	92.52
089	88.28	94.39	93.71	93.67	90.60	95.46	94.90	94.83
091	85.59	93.84	93.46	93.38	88.95	95.35	94.98	94.92
093	84.63	93.64	93.28	93.20	86.72	94.88	94.51	94.38
097	88.89	94.29	93.75	93.77	91.25	95.45	95.03	95.01
098	82.73	92.70	91.91	91.81	85.27	93.79	93.06	92.95
101	81.75	91.56	91.00	91.00	83.77	92.50	92.16	92.08
104	88.04	91.84	90.61	90.77	90.55	92.94	91.78	91.92
106	86.36	92.51	91.91	91.98	87.99	93.37	92.94	92.97
108	91.38	94.12	93.27	93.47	93.70	95.18	94.51	94.64
112	87.44	94.54	93.78	93.92	91.13	95.67	95.07	95.14
113	80.19	90.55	89.88	90.04	82.28	91.40	90.85	90.95
116	77.92	88.35	87.30	86.99	80.56	89.65	88.54	88.24
117	86.58	93.49	93.12	93.08	89.35	94.62	94.36	94.28
121	78.40	89.21	88.84	88.79	81.33	90.24	89.94	89.85
123	86.41	91.09	90.22	90.35	89.22	92.12	91.29	91.39
126	82.36	92.89	91.67	91.84	85.47	93.88	92.92	92.99
129	88.90	93.03	92.32	92.43	92.16	94.20	93.53	93.61
134	79.39	90.22	89.39	89.50	82.37	91.57	90.78	90.88
135	88.27	94.99	94.80	94.79	91.22	96.14	96.05	96.00
138	83.51	93.20	92.62	92.64	85.46	94.27	93.83	93.78
139	87.47	93.88	93.74	93.72	90.56	95.38	95.36	95.32
142	84.95	93.31	92.77	92.80	87.75	94.49	94.02	94.02
145	83.62	92.98	92.99	92.78	86.51	94.23	94.31	94.06
148	84.00	91.61	90.12	90.26	86.06	92.81	91.40	91.51
150	86.11	91.87	91.40	91.19	89.42	92.94	92.58	92.34
Mean	81.92	90.11	89.39	89.32	84.31	91.18	90.56	90.45

Table 20: Results of team Hutom for task3 recognition.

Sequence	Frame-by-Frame				Application-Dependant			
	Accuracy	Precision	recall	F1	Accuracy	Precision	recall	F1
003	55.95	84.67	84.49	81.66	57.93	85.10	84.96	82.20
004	57.98	87.05	86.56	83.61	59.88	87.49	87.04	84.14
006	56.44	86.43	86.45	84.18	58.55	86.97	87.06	84.97
009	60.72	83.95	85.74	83.04	62.23	84.61	86.35	83.79
012	54.60	85.06	84.68	82.23	56.71	85.49	85.10	82.67
015	54.90	85.01	83.94	81.81	57.96	85.67	84.42	82.38
019	54.71	83.61	83.15	81.09	55.86	84.00	83.53	81.56
020	58.28	83.46	85.31	82.05	59.95	83.98	85.81	82.65

Table 20: Results of team Hutom for task3 recognition. (continued)

Sequence	Frame-by-Frame				Application-Dependant			
	Accuracy	Precision	recall	F1	Accuracy	Precision	recall	F1
022	57.48	83.15	84.29	81.26	59.12	83.63	84.89	81.92
023	61.12	86.70	85.80	83.35	63.94	87.24	86.45	84.05
029	59.96	86.24	86.54	84.20	61.96	86.93	87.08	84.88
030	58.02	85.19	85.62	82.78	59.31	85.59	86.09	83.31
031	56.84	86.33	86.07	83.64	58.03	86.70	86.53	84.12
032	56.68	83.76	85.47	82.55	58.21	84.79	86.06	83.31
036	58.97	85.23	86.44	83.97	60.32	86.34	86.99	84.54
040	56.94	86.60	87.39	84.92	58.25	86.94	87.86	85.45
043	58.79	86.06	87.10	84.62	60.92	86.89	88.00	85.61
044	59.90	85.59	87.01	84.56	62.45	86.35	87.86	85.58
046	56.78	86.92	86.38	83.76	59.09	87.54	87.08	84.61
049	57.44	85.82	86.51	83.36	59.71	86.61	87.31	84.36
053	54.23	82.17	82.32	79.36	55.44	82.42	82.64	79.66
054	40.67	71.71	71.60	68.31	41.91	72.19	71.98	68.78
056	57.08	84.77	84.41	81.23	59.81	85.49	84.97	81.88
059	59.17	84.81	85.52	83.19	61.96	85.36	85.98	83.66
063	56.33	86.60	85.67	82.58	57.78	87.09	86.14	83.06
064	55.68	85.82	84.63	82.12	58.35	86.33	85.25	82.84
069	58.59	86.05	85.78	82.87	61.10	86.52	86.31	83.49
070	61.13	86.86	88.28	85.72	63.80	88.00	89.15	86.84
072	58.42	85.82	84.94	82.34	60.77	86.66	85.60	83.12
073	58.61	84.91	84.65	82.53	60.51	85.66	85.37	83.39
077	58.40	86.68	87.64	84.85	60.74	87.25	88.30	85.72
079	47.43	77.42	78.48	73.77	48.93	78.08	78.95	74.48
083	58.41	85.53	85.99	83.11	60.28	86.25	86.64	83.82
085	57.63	88.45	87.42	84.62	60.98	89.10	88.26	85.78
086	58.43	86.67	86.43	84.08	60.81	87.51	87.16	84.97
089	60.54	88.46	88.41	85.90	62.55	88.95	88.92	86.56
091	60.72	86.14	87.07	84.58	63.77	87.12	87.97	85.70
093	56.37	84.55	84.27	81.47	58.88	85.54	85.27	82.66
097	62.27	87.49	89.04	86.58	64.99	88.38	89.93	87.73
098	61.72	85.43	86.19	83.07	63.38	85.87	86.80	83.86
101	58.92	86.54	87.71	84.98	61.44	87.39	88.42	85.81
104	61.27	86.14	86.57	82.70	63.64	86.86	87.29	83.62
106	59.54	86.19	87.39	84.64	61.79	87.04	88.16	85.59
108	62.73	88.64	88.65	86.48	66.44	89.56	89.52	87.43
112	61.41	86.50	87.52	84.83	63.51	87.42	88.25	85.70
113	55.20	85.87	85.74	83.16	57.77	86.45	86.26	83.80
116	55.59	85.72	86.05	82.46	56.89	86.18	86.49	83.03
117	61.55	86.84	87.86	84.93	64.37	87.64	88.69	85.94
121	57.97	86.69	87.50	84.19	59.71	87.29	87.88	84.60
123	60.31	86.66	87.28	84.66	61.93	87.35	87.81	85.27
126	56.99	85.67	86.60	84.01	58.73	86.25	87.11	84.60
129	61.56	88.09	86.76	83.86	64.76	88.68	87.36	84.61
134	60.25	89.46	89.37	86.67	62.26	90.19	90.14	87.74
135	61.18	85.92	87.43	84.52	62.91	86.57	88.06	85.29
138	58.41	86.10	87.37	84.75	60.61	87.18	88.37	86.00
139	61.72	87.63	88.62	85.83	63.78	88.73	89.47	86.88
142	61.43	87.14	88.05	85.03	64.08	88.00	88.93	86.11
145	57.17	83.94	85.39	82.31	59.72	84.85	86.15	83.22
148	61.35	85.44	87.09	84.05	63.62	86.23	87.90	85.00
150	59.44	85.98	86.38	83.54	61.61	86.70	87.09	84.46
Mean	58.14	85.57	85.98	83.21	60.28	86.25	86.62	83.98

Table 21: Results of team Hutom for task4 recognition.

Sequence	Frame-by-Frame				Application-Dependant			
	Accuracy	Precision	recall	F1	Accuracy	Precision	recall	F1
003	87.10	95.70	95.19	95.28	89.51	96.60	96.09	96.19
004	88.12	96.89	96.51	96.60	89.48	97.56	97.20	97.28
006	87.89	97.71	97.40	97.50	89.56	98.46	98.22	98.28
009	88.08	95.60	95.29	95.28	89.62	96.45	96.21	96.18
012	84.68	94.27	94.21	94.15	86.53	94.99	95.00	94.92
015	81.36	92.88	92.01	92.12	83.50	93.55	92.83	92.86
019	82.78	93.62	93.06	93.16	84.53	94.41	93.95	94.00
020	89.12	97.05	97.19	97.08	90.79	97.82	98.03	97.90
022	89.42	95.80	95.44	95.45	91.28	96.69	96.36	96.35
023	93.58	97.55	97.36	97.41	95.46	98.31	98.15	98.19
029	88.97	96.41	95.89	96.06	90.53	97.28	96.96	97.06
030	87.03	93.44	92.53	92.63	89.74	94.30	93.49	93.54
031	90.32	95.21	94.66	94.75	91.75	96.16	95.76	95.79
032	88.32	96.87	97.06	96.93	89.88	97.77	98.02	97.86
036	91.39	96.66	96.41	96.49	93.18	97.70	97.59	97.62
040	89.09	96.04	95.53	95.59	90.53	96.84	96.45	96.47
043	90.18	96.85	97.08	96.92	94.31	97.99	98.30	98.11
044	91.58	96.66	96.39	96.44	92.98	97.63	97.52	97.52
046	89.26	94.47	94.14	94.07	92.25	95.60	95.32	95.22
049	91.45	97.16	97.21	97.12	93.48	98.06	98.24	98.11
053	86.44	95.32	94.97	94.97	88.21	96.03	95.75	95.71
054	73.36	83.83	82.81	81.99	76.91	84.55	83.57	82.72
056	92.60	97.02	96.69	96.75	94.08	97.82	97.60	97.62
059	94.27	97.17	96.98	97.02	96.84	98.10	98.00	98.02
063	88.21	95.48	94.84	94.89	90.30	96.38	95.88	95.89
064	86.63	94.17	93.62	93.66	88.89	94.99	94.53	94.54
069	89.55	95.57	95.43	95.41	92.22	96.61	96.48	96.46
070	89.29	95.81	95.16	95.34	92.21	96.84	96.30	96.44
072	93.75	96.68	96.31	96.38	95.73	97.44	97.23	97.24
073	91.34	97.34	96.86	96.92	92.86	97.99	97.54	97.60
077	89.34	97.77	97.64	97.67	90.66	98.49	98.41	98.42
079	80.91	89.45	89.17	88.86	83.03	90.51	90.17	89.89
083	86.97	93.89	93.57	93.61	89.84	94.96	94.73	94.72
085	86.94	97.24	97.36	97.28	89.06	98.05	98.24	98.13
086	82.27	96.08	95.99	95.70	83.98	96.77	96.75	96.45
089	94.59	98.00	97.78	97.86	97.61	98.95	98.83	98.86
091	91.05	97.99	98.01	97.98	93.64	98.95	98.97	98.94
093	89.14	97.06	97.10	97.01	91.21	97.97	98.06	97.96
097	93.65	98.09	97.82	97.87	95.28	98.93	98.78	98.79
098	87.98	96.77	96.68	96.50	89.93	97.59	97.54	97.34
101	88.91	97.31	97.28	97.25	90.72	98.29	98.35	98.29
104	95.07	97.46	97.32	97.34	97.45	98.42	98.35	98.36
106	90.35	96.62	96.36	96.41	92.05	97.47	97.31	97.32
108	94.97	97.91	97.68	97.73	97.01	98.63	98.49	98.52
112	92.35	98.00	97.79	97.86	94.71	99.02	98.92	98.95
113	87.27	96.07	95.48	95.62	88.82	96.96	96.51	96.60
116	86.19	94.33	94.04	93.87	88.42	95.44	95.20	95.02
117	92.48	97.66	97.78	97.66	93.78	98.41	98.64	98.49
121	88.71	96.98	96.78	96.84	92.20	97.94	97.85	97.87
123	93.93	97.31	96.80	96.97	96.33	98.17	97.75	97.89
126	87.49	97.09	96.90	96.93	89.67	97.93	97.89	97.87
129	93.59	97.23	96.92	97.04	96.33	98.19	97.96	98.05
134	90.71	97.28	97.29	97.25	93.58	98.23	98.30	98.23

Table 21: Results of team Hutom for task4 recognition. (continued)

Sequence	Frame-by-Frame				Application-Dependant			
	Accuracy	Precision	recall	F1	Accuracy	Precision	recall	F1
135	92.01	97.76	97.77	97.72	93.99	98.59	98.69	98.61
138	88.08	96.54	96.20	96.19	90.55	97.56	97.28	97.26
139	92.28	97.76	97.69	97.68	93.78	98.52	98.48	98.47
142	90.75	97.47	97.52	97.47	93.49	98.52	98.62	98.56
145	88.67	96.67	96.59	96.51	91.12	97.75	97.76	97.65
148	90.17	96.70	96.60	96.60	91.68	97.56	97.48	97.47
150	91.09	95.55	95.71	95.52	93.36	96.41	96.66	96.45
Mean	89.22	96.12	95.86	95.85	91.34	97.00	96.83	96.79

Table 22: Results of team Hutom for task5 recognition.

Sequence	Frame-by-Frame				Application-Dependant			
	Accuracy	Precision	recall	F1	Accuracy	Precision	recall	F1
003	85.19	95.08	94.27	94.41	87.23	96.01	95.29	95.41
004	90.82	96.14	95.72	95.81	93.32	97.04	96.66	96.72
006	88.27	96.48	96.11	96.21	91.30	97.32	97.07	97.12
009	90.57	95.97	95.57	95.62	91.92	96.83	96.54	96.54
012	83.17	91.88	90.25	90.53	85.21	92.61	91.17	91.37
015	83.57	92.19	90.19	90.77	85.46	92.71	91.05	91.50
019	85.55	92.64	91.49	91.65	88.57	93.50	92.60	92.64
020	88.56	95.81	95.41	95.47	91.31	96.77	96.47	96.50
022	85.76	93.80	92.36	92.59	87.98	94.80	93.61	93.77
023	92.66	96.79	96.34	96.48	95.26	97.75	97.47	97.55
029	89.17	95.50	94.47	94.78	91.54	96.53	95.75	95.96
030	83.19	92.94	91.74	92.05	84.80	93.59	92.64	92.85
031	90.25	94.95	93.66	93.86	93.42	95.77	94.64	94.78
032	84.74	94.59	93.72	93.90	86.89	95.54	95.00	95.06
036	92.18	95.53	94.61	94.85	93.90	96.44	95.69	95.87
040	87.10	94.73	93.47	93.71	88.69	95.44	94.45	94.60
043	88.26	95.18	94.52	94.55	90.46	96.32	95.88	95.84
044	93.26	97.19	96.86	96.95	96.23	98.47	98.28	98.32
046	86.44	94.16	93.23	93.39	90.04	95.31	94.47	94.61
049	89.72	95.68	94.76	94.99	91.79	96.62	95.94	96.08
053	86.89	93.93	93.29	93.40	89.76	94.97	94.43	94.52
054	74.24	82.57	80.68	80.27	77.04	83.54	81.85	81.37
056	91.40	95.42	94.25	94.54	93.71	96.25	95.33	95.54
059	91.28	95.71	94.82	95.01	94.16	96.52	95.88	95.98
063	87.49	94.37	93.84	93.94	90.66	95.63	95.23	95.28
064	85.78	92.81	92.27	92.22	87.26	93.54	93.23	93.10
069	89.21	94.57	94.12	94.16	91.97	95.60	95.29	95.27
070	90.32	96.09	95.36	95.59	93.94	97.33	96.80	96.94
072	89.52	95.97	95.33	95.46	91.56	96.96	96.55	96.58
073	88.07	94.90	93.75	93.97	90.22	95.77	94.80	94.95
077	88.13	97.13	97.04	97.05	89.88	98.16	98.17	98.14
079	76.84	85.58	85.93	85.08	78.99	86.75	87.23	86.32
083	86.75	93.55	92.60	92.61	89.55	94.70	93.81	93.77
085	91.41	97.15	96.77	96.88	93.64	98.01	97.81	97.85
086	87.80	96.81	96.73	96.70	90.17	97.91	97.96	97.89
089	89.92	96.72	95.59	96.02	92.51	97.52	96.56	96.91
091	92.24	96.37	95.92	96.02	96.82	97.68	97.44	97.47
093	87.39	94.97	94.22	94.30	89.52	96.01	95.47	95.48
097	89.59	96.83	96.67	96.69	92.03	97.97	97.96	97.92
098	93.73	97.66	97.41	97.48	96.47	98.72	98.63	98.65

Table 22: Results of team Hutom for task5 recognition. (continued)

Sequence	Frame-by-Frame				Application-Dependant			
	Accuracy	Precision	recall	F1	Accuracy	Precision	recall	F1
101	87.88	96.16	95.72	95.77	90.16	97.14	96.82	96.83
104	94.23	97.22	97.02	97.09	97.19	98.41	98.30	98.34
106	90.16	96.71	96.25	96.38	92.67	97.76	97.38	97.49
108	94.07	97.40	96.95	97.09	96.72	98.36	98.12	98.19
112	91.57	97.23	96.38	96.58	93.84	98.16	97.60	97.70
113	88.65	95.36	94.06	94.38	90.59	96.12	95.10	95.32
116	85.09	93.73	93.63	93.51	86.80	94.87	94.84	94.70
117	93.51	97.47	97.19	97.25	96.35	98.61	98.44	98.47
121	87.11	96.03	95.48	95.62	89.02	96.92	96.53	96.62
123	92.42	96.54	95.83	96.06	95.04	97.62	97.09	97.26
126	89.12	96.39	95.79	95.98	91.30	97.23	96.97	97.03
129	91.91	96.70	96.42	96.52	95.69	97.99	97.77	97.83
134	91.56	96.93	96.50	96.62	95.11	98.00	97.72	97.78
135	90.96	97.08	96.83	96.86	93.69	98.16	98.08	98.06
138	89.58	95.36	94.76	94.88	92.10	96.49	96.12	96.16
139	90.51	96.95	96.78	96.80	93.00	98.26	98.17	98.15
142	94.45	97.01	96.53	96.67	97.31	98.18	97.87	97.95
145	90.34	96.17	95.66	95.62	92.28	97.17	96.79	96.69
148	88.69	95.01	94.27	94.36	90.78	96.11	95.49	95.55
150	89.07	95.13	93.80	93.80	91.37	96.13	94.95	94.91
Mean	88.79	95.22	94.52	94.63	91.27	96.21	95.69	95.73

B.2 JHU CIRL

Table 23: Results of team JHU_CIRL for task2 recognition.

Sequence	Frame-by-Frame				Application-Dependant			
	Accuracy	Precision	recall	F1	Accuracy	Precision	recall	F1
003	83.56	95.46	95.82	95.60	85.70	96.35	96.67	96.47
004	81.71	94.33	94.42	94.31	83.80	95.18	95.19	95.09
006	82.33	96.04	96.05	95.97	85.14	97.16	97.11	97.05
009	85.46	95.33	95.41	95.18	87.85	96.25	96.28	96.09
012	80.88	93.19	93.25	93.08	83.10	93.88	93.96	93.77
015	74.66	88.49	85.84	85.31	76.58	89.03	86.44	85.91
019	79.44	93.38	93.97	93.41	81.41	94.28	94.72	94.22
020	83.88	95.84	96.35	96.03	87.13	96.90	97.36	97.06
022	81.42	94.10	94.18	93.90	84.00	95.14	95.11	94.91
023	79.06	89.89	90.38	89.83	82.33	91.03	91.41	90.93
029	83.86	94.61	94.63	94.48	88.19	95.92	95.87	95.79
030	80.13	92.99	93.45	93.16	82.38	93.81	94.23	93.95
031	82.34	94.28	93.81	93.80	85.58	95.49	95.02	95.02
032	80.67	94.15	94.55	94.23	83.39	95.39	95.74	95.46
036	82.64	91.98	90.73	90.62	85.48	93.32	91.95	91.84
040	82.82	93.93	93.42	93.44	85.94	95.04	94.58	94.56
043	83.62	94.23	94.52	94.25	86.83	95.44	95.70	95.48
044	85.65	95.41	95.53	95.38	88.84	96.78	96.84	96.74
046	82.15	93.52	93.95	93.54	85.37	94.66	95.04	94.70
049	85.27	95.29	95.64	95.39	87.72	96.49	96.84	96.60
053	80.99	94.42	94.85	94.43	83.58	95.47	95.80	95.47
054	78.56	92.30	91.47	90.95	81.14	93.33	92.46	91.97
056	84.48	95.72	95.54	95.50	87.76	96.73	96.52	96.48
059	90.24	97.07	96.94	96.92	93.80	98.22	98.08	98.07
063	84.07	94.87	95.21	94.85	86.16	95.81	96.14	95.82

Table 23: Results of team JHU_CIRL for task2 recognition. (continued)

Sequence	Frame-by-Frame				Application-Dependant			
	Accuracy	Precision	recall	F1	Accuracy	Precision	recall	F1
064	73.99	86.61	83.26	82.66	77.16	87.67	84.25	83.72
069	83.39	93.24	93.55	93.25	86.46	94.53	94.78	94.51
070	84.05	94.40	94.36	94.19	87.09	95.52	95.40	95.29
072	88.05	96.36	96.42	96.38	91.13	97.65	97.69	97.64
073	87.45	96.03	95.86	95.83	91.13	97.29	97.09	97.10
077	84.52	96.04	96.20	96.04	87.42	97.42	97.47	97.33
079	76.26	90.86	88.39	86.75	78.84	92.08	89.49	87.93
083	84.28	93.70	93.97	93.68	88.87	95.25	95.41	95.21
085	82.74	95.71	96.05	95.77	86.41	96.89	97.16	96.93
086	82.76	94.98	95.21	95.04	86.21	96.40	96.58	96.44
089	85.44	95.26	95.29	95.11	88.87	96.27	96.25	96.11
091	85.97	96.42	96.66	96.46	90.08	97.93	97.99	97.91
093	81.59	94.99	95.40	95.06	83.85	96.13	96.47	96.17
097	85.52	95.28	95.42	95.24	89.35	96.80	96.78	96.65
098	83.33	95.41	95.42	95.17	86.55	96.67	96.57	96.39
101	83.61	95.87	96.24	96.00	86.55	97.04	97.33	97.14
104	86.11	94.87	95.00	94.74	89.58	96.29	96.32	96.19
106	85.79	95.19	95.03	95.07	88.53	96.21	96.05	96.08
108	89.58	96.67	96.32	96.40	92.52	97.78	97.47	97.53
112	87.89	96.82	96.69	96.71	90.92	97.89	97.87	97.84
113	82.14	95.01	94.82	94.75	85.22	95.90	95.75	95.69
116	81.30	93.06	91.67	91.36	83.80	94.38	92.75	92.54
117	87.19	96.01	96.06	95.92	89.15	96.83	96.87	96.73
121	79.59	94.48	94.06	94.12	82.17	95.49	95.11	95.14
123	88.93	95.92	95.52	95.58	91.60	96.96	96.60	96.67
126	82.35	95.38	95.28	95.25	85.68	96.55	96.49	96.43
129	87.98	95.32	95.23	95.18	91.81	96.69	96.50	96.51
134	81.23	94.57	94.55	94.41	85.53	96.10	96.02	95.92
135	86.11	96.12	96.25	96.14	89.43	97.35	97.43	97.36
138	82.59	94.99	94.93	94.75	85.41	96.08	96.04	95.89
139	85.56	95.25	95.58	95.25	88.52	96.69	96.90	96.64
142	84.46	95.20	95.25	95.15	88.14	96.64	96.63	96.56
145	82.39	94.62	95.20	94.80	85.46	95.87	96.38	96.04
148	85.49	94.49	94.45	94.25	88.19	95.78	95.65	95.53
150	86.13	95.19	95.58	95.24	90.05	96.51	96.84	96.56
Mean	83.43	94.52	94.42	94.19	86.45	95.68	95.52	95.33

B.3 MedAIR

Table 24: Results of team MedAIR for task1 recognition.

Sequence	Frame-by-Frame				Application-Dependant			
	Accuracy	Precision	recall	F1	Accuracy	Precision	recall	F1
003	79.26	93.65	93.38	92.86	81.80	94.45	94.15	93.69
004	82.85	96.31	96.23	95.90	84.89	96.98	96.93	96.64
006	79.67	95.28	95.30	94.84	81.61	96.08	96.02	95.62
009	82.09	94.36	94.07	93.53	84.19	95.14	94.87	94.39
012	78.92	94.45	94.03	93.70	81.21	95.17	94.67	94.39
015	77.64	92.95	92.97	92.54	80.36	93.47	93.52	93.09
019	76.80	92.73	92.69	92.00	77.98	93.25	93.21	92.56
020	79.74	93.80	93.81	93.12	82.43	94.54	94.51	93.90
022	79.92	94.70	94.39	93.81	81.98	95.50	95.23	94.69
023	85.04	95.38	95.25	94.66	87.35	96.15	96.07	95.53

Table 24: Results of team MedAIR for task1 recognition. (continued)

Sequence	Frame-by-Frame				Application-Dependant			
	Accuracy	Precision	recall	F1	Accuracy	Precision	recall	F1
029	83.64	95.13	94.79	94.12	86.97	96.08	95.72	95.11
030	77.89	93.35	92.67	92.19	79.77	94.11	93.44	93.03
031	81.92	95.53	95.72	95.21	84.32	96.56	96.67	96.25
032	79.19	93.76	93.07	92.42	81.32	94.66	94.03	93.37
036	83.69	95.00	95.02	94.62	85.51	95.80	95.77	95.47
040	81.00	94.83	94.65	94.26	83.83	95.73	95.48	95.17
043	85.06	95.61	95.52	95.21	87.48	96.60	96.51	96.29
044	84.19	95.45	95.35	94.90	87.10	96.68	96.60	96.24
046	80.81	93.85	93.94	93.31	83.28	94.76	94.73	94.23
049	82.77	95.54	95.82	95.39	85.48	96.62	96.87	96.51
053	78.09	92.50	92.91	92.11	80.22	93.44	93.70	93.01
054	64.34	82.15	79.81	78.42	66.37	83.02	80.59	79.27
056	81.59	94.66	94.48	93.96	85.28	95.43	95.22	94.80
059	85.23	94.89	94.29	94.11	88.22	95.73	95.12	95.00
063	80.16	93.51	93.86	93.31	83.03	94.62	94.92	94.44
064	78.24	92.38	92.82	92.13	80.77	93.24	93.61	93.01
069	81.83	92.93	92.81	92.22	85.00	93.77	93.67	93.14
070	82.81	95.17	95.16	94.59	86.14	96.12	96.11	95.64
072	83.49	95.91	95.57	95.18	86.11	96.77	96.48	96.15
073	80.58	93.16	92.35	91.98	83.36	94.08	93.21	92.90
077	84.36	96.47	96.38	96.10	87.09	97.39	97.31	97.10
079	69.02	83.24	84.52	82.76	71.12	84.25	85.42	83.79
083	77.39	92.57	92.91	92.07	79.70	93.43	93.71	92.96
085	80.72	94.99	95.05	94.55	84.13	95.88	95.91	95.52
086	81.22	95.21	95.40	94.81	84.14	96.27	96.36	95.88
089	82.67	95.39	95.06	94.71	86.76	96.24	95.88	95.60
091	83.41	95.52	95.38	94.95	87.71	96.81	96.66	96.32
093	80.22	94.14	94.13	93.48	82.51	95.04	95.08	94.45
097	84.04	95.81	95.67	95.27	87.61	96.82	96.69	96.37
098	83.83	95.90	95.69	95.26	86.70	96.86	96.62	96.26
101	81.38	95.08	95.05	94.81	84.38	96.02	96.02	95.79
104	88.29	95.79	95.52	95.10	90.94	96.73	96.50	96.13
106	84.24	95.88	95.54	95.34	86.24	96.65	96.35	96.16
108	87.02	97.02	96.88	96.67	90.47	97.81	97.70	97.52
112	86.48	96.55	96.17	96.04	88.96	97.43	97.09	96.98
113	81.67	95.93	95.76	95.60	84.18	96.80	96.76	96.61
116	81.73	93.48	93.88	93.34	84.28	94.45	94.78	94.33
117	83.64	95.47	95.44	94.97	87.63	96.58	96.50	96.04
121	80.06	95.19	94.87	94.42	81.41	95.72	95.45	94.98
123	86.18	95.94	95.38	94.86	88.90	96.88	96.28	95.80
126	79.79	95.32	94.91	94.66	82.80	96.34	95.97	95.72
129	85.12	95.37	95.16	94.79	87.54	96.30	96.09	95.77
134	81.05	95.66	95.60	95.15	84.89	96.80	96.77	96.43
135	82.32	95.94	95.80	95.33	85.03	96.93	96.76	96.37
138	81.12	94.50	94.51	94.23	83.49	95.47	95.44	95.22
139	84.93	95.68	95.58	95.27	87.97	96.86	96.80	96.60
142	86.87	95.95	95.78	95.43	91.07	97.29	97.02	96.78
145	81.69	94.82	95.15	94.69	84.82	95.86	96.23	95.84
148	85.36	94.76	94.85	94.51	87.37	95.66	95.69	95.43
150	82.28	93.58	93.85	93.30	85.60	94.83	95.02	94.55
Mean	81.61	94.43	94.31	93.82	84.31	95.35	95.21	94.78

Table 25: Results of team MedAIR for task2 recognition.

Sequence	Frame-by-Frame				Application-Dependant			
	Accuracy	Precision	recall	F1	Accuracy	Precision	recall	F1
003	88.30	96.98	96.96	96.93	89.47	97.67	97.75	97.68
004	88.73	97.35	97.08	97.14	89.56	97.92	97.79	97.80
006	90.80	97.50	97.42	97.41	92.12	98.25	98.26	98.22
009	89.91	96.56	96.20	96.22	90.97	97.24	97.00	96.99
012	81.56	91.89	90.56	90.43	83.34	92.41	91.13	90.98
015	85.33	94.77	93.27	93.57	87.00	95.38	94.01	94.23
019	79.11	89.97	87.65	87.57	80.20	90.58	88.34	88.20
020	92.39	97.30	96.80	96.96	93.96	98.00	97.66	97.77
022	87.20	95.61	95.10	95.21	89.20	96.36	96.00	96.04
023	94.46	96.92	96.19	96.36	96.01	97.69	97.08	97.20
029	91.25	94.76	93.77	93.88	92.81	95.47	94.68	94.72
030	83.92	90.38	88.82	88.81	85.28	91.07	89.61	89.56
031	86.05	93.51	91.70	91.68	86.91	94.05	92.50	92.41
032	84.41	94.39	93.77	93.88	86.64	95.21	94.75	94.81
036	91.42	95.95	94.89	95.05	93.25	96.82	95.96	96.06
040	87.30	94.14	92.83	93.07	88.39	94.68	93.59	93.75
043	88.64	96.11	95.50	95.62	90.02	96.93	96.56	96.60
044	91.88	97.20	96.80	96.93	93.03	98.12	97.88	97.97
046	91.55	96.35	96.52	96.34	93.21	97.02	97.26	97.06
049	89.94	96.79	96.31	96.42	91.88	97.78	97.50	97.53
053	85.92	96.56	95.65	95.80	87.48	97.29	96.45	96.58
054	70.97	80.35	78.92	79.18	72.21	81.05	79.81	80.01
056	92.31	97.14	96.10	96.39	93.72	97.75	97.04	97.22
059	96.12	98.38	97.83	98.02	97.69	99.11	98.83	98.93
063	90.64	96.21	95.62	95.64	92.62	97.27	96.59	96.60
064	84.66	91.51	88.02	87.49	85.74	92.06	88.72	88.10
069	91.96	96.85	96.53	96.62	93.63	97.66	97.45	97.50
070	89.81	95.93	95.06	95.30	91.77	96.62	95.91	96.07
072	91.31	97.69	96.88	97.18	92.57	98.17	97.65	97.83
073	91.05	96.56	95.63	95.72	92.37	97.19	96.36	96.41
077	88.57	97.76	97.61	97.65	89.91	98.48	98.41	98.43
079	76.59	87.63	85.90	85.84	77.81	88.34	86.69	86.61
083	88.33	94.13	93.54	93.56	90.01	95.08	94.61	94.57
085	87.19	96.02	95.60	95.48	88.89	96.70	96.49	96.29
086	81.30	95.73	95.44	94.99	82.65	96.54	96.40	95.91
089	92.26	97.95	97.66	97.78	93.40	98.53	98.29	98.39
091	92.86	97.77	97.56	97.61	94.29	98.64	98.59	98.59
093	86.86	96.17	95.73	95.77	88.52	96.97	96.74	96.70
097	93.09	97.94	97.50	97.66	94.61	98.80	98.50	98.61
098	93.20	98.03	97.92	97.93	94.92	98.83	98.81	98.80
101	88.04	96.87	96.69	96.69	90.06	97.82	97.58	97.55
104	94.63	97.46	97.16	97.23	96.30	98.28	98.03	98.08
106	92.27	97.50	96.91	97.12	93.94	98.10	97.64	97.81
108	96.29	98.09	97.44	97.66	97.99	98.75	98.35	98.47
112	93.16	98.23	97.86	97.98	94.71	98.90	98.73	98.79
113	89.35	97.47	96.70	96.92	91.38	98.09	97.57	97.72
116	86.08	94.23	91.68	92.03	87.64	94.81	92.43	92.71
117	91.80	97.24	96.96	96.96	93.48	98.07	97.95	97.90
121	87.26	96.97	96.35	96.51	88.64	97.49	97.01	97.12
123	93.67	96.79	96.05	96.28	95.21	97.38	96.78	96.96
126	86.71	97.01	96.35	96.58	88.78	97.90	97.44	97.60
129	94.84	97.38	96.61	96.92	96.97	98.20	97.53	97.80
134	86.53	96.62	95.84	96.07	88.31	97.37	96.85	96.98

Table 25: Results of team MedAIR for task2 recognition. (continued)

Sequence	Frame-by-Frame				Application-Dependant			
	Accuracy	Precision	recall	F1	Accuracy	Precision	recall	F1
135	92.40	97.41	96.99	97.08	93.63	98.08	97.93	97.93
138	89.20	96.91	96.07	96.28	90.39	97.62	97.07	97.19
139	92.53	97.27	97.07	97.11	93.58	98.02	97.94	97.94
142	93.35	97.65	97.15	97.29	94.69	98.37	98.03	98.12
145	89.89	96.97	96.70	96.75	91.90	97.88	97.86	97.81
148	92.50	96.85	96.49	96.60	93.79	97.62	97.38	97.45
150	91.79	96.34	95.87	95.91	93.83	97.10	96.79	96.76
Mean	89.19	95.87	95.13	95.22	90.72	96.59	96.01	96.04

Table 26: Results of team MedAIR for task4 recognition.

Sequence	Frame-by-Frame				Application-Dependant			
	Accuracy	Precision	recall	F1	Accuracy	Precision	recall	F1
003	83.87	95.44	95.16	95.16	86.15	96.47	96.17	96.19
004	83.56	95.43	95.31	95.28	85.39	96.24	96.10	96.09
006	83.25	96.11	95.80	95.88	85.37	97.08	96.76	96.86
009	87.12	95.37	95.33	95.22	89.42	96.33	96.29	96.21
012	83.75	94.31	93.27	93.59	87.87	94.91	94.03	94.29
015	79.91	93.64	91.74	92.22	81.39	94.14	92.45	92.86
019	79.96	92.62	92.21	92.09	81.20	93.41	92.99	92.84
020	84.58	95.17	95.14	95.02	86.17	96.18	96.23	96.09
022	84.09	94.64	94.33	94.37	86.16	95.67	95.47	95.47
023	87.18	96.02	95.24	95.51	89.73	97.03	96.36	96.61
029	85.78	95.51	94.89	95.08	87.77	96.44	95.90	96.07
030	80.45	93.03	92.40	92.43	82.39	93.75	93.20	93.21
031	82.23	95.75	95.16	95.31	83.80	96.68	96.18	96.32
032	83.55	94.95	94.54	94.71	85.11	95.93	95.61	95.74
036	85.25	95.46	95.36	95.31	87.61	96.69	96.55	96.51
040	84.72	93.99	92.95	93.22	86.80	94.85	93.96	94.17
043	81.79	92.57	92.32	92.25	84.29	93.88	93.66	93.59
044	86.48	95.04	94.68	94.71	88.78	96.22	95.84	95.85
046	83.52	93.12	92.51	92.46	85.93	94.24	93.63	93.56
049	82.40	94.04	93.87	93.77	85.04	95.17	95.04	94.91
053	80.49	94.37	94.91	94.50	82.15	95.41	95.77	95.40
054	74.35	85.02	85.34	83.96	75.89	85.82	86.20	84.80
056	87.97	95.83	95.12	95.21	89.94	96.61	96.00	96.08
059	90.60	96.88	96.19	96.45	92.88	97.74	97.21	97.42
063	83.26	94.32	94.32	94.15	85.42	95.24	95.21	95.06
064	83.16	93.88	93.88	93.73	85.33	94.73	94.84	94.66
069	85.80	93.39	92.63	92.60	88.93	94.54	93.86	93.83
070	85.46	95.17	94.85	94.96	88.11	96.14	95.86	95.96
072	87.02	96.47	96.39	96.38	88.71	97.48	97.48	97.44
073	87.04	95.98	95.64	95.70	89.92	97.21	96.95	96.99
077	84.41	96.08	95.94	95.95	86.69	97.12	96.98	97.00
079	75.57	88.63	88.51	87.62	77.09	89.54	89.45	88.53
083	84.23	94.21	94.28	94.13	86.56	95.30	95.40	95.26
085	81.94	94.92	94.73	94.62	83.93	95.95	95.86	95.72
086	82.52	95.32	95.03	95.02	84.82	96.31	96.07	96.08
089	87.19	96.77	96.26	96.44	89.75	97.84	97.38	97.56
091	87.99	96.28	95.86	95.97	91.92	97.71	97.42	97.49
093	84.16	95.40	95.48	95.36	86.22	96.54	96.73	96.56
097	88.59	96.32	95.69	95.88	90.72	97.56	97.02	97.18
098	88.85	97.01	96.88	96.89	92.02	98.34	98.30	98.30

Table 26: Results of team MedAIR for task4 recognition. (continued)

Sequence	Frame-by-Frame				Application-Dependant			
	Accuracy	Precision	recall	F1	Accuracy	Precision	recall	F1
101	84.09	95.60	95.45	95.45	86.60	96.70	96.70	96.64
104	88.36	95.35	95.01	95.08	90.84	96.54	96.19	96.28
106	86.27	95.41	94.76	94.96	88.06	96.34	95.74	95.92
108	89.12	96.76	96.09	96.36	91.91	97.81	97.32	97.52
112	86.41	96.34	95.90	95.97	89.93	97.44	97.15	97.19
113	83.05	95.64	95.46	95.45	85.52	96.76	96.61	96.58
116	80.97	94.11	93.84	93.77	82.77	94.99	94.69	94.66
117	89.78	96.73	96.49	96.56	92.55	97.94	97.72	97.78
121	81.92	95.01	94.16	94.38	83.94	95.84	95.03	95.22
123	88.79	95.79	95.41	95.48	90.24	96.60	96.25	96.31
126	82.41	95.35	94.51	94.78	84.62	96.44	95.78	95.98
129	88.91	95.10	94.24	94.41	91.03	96.12	95.25	95.39
134	80.83	94.40	93.78	93.90	82.59	95.50	94.86	94.95
135	87.09	96.27	95.91	95.97	89.99	97.48	97.19	97.24
138	85.21	95.51	94.67	94.92	87.11	96.55	95.89	96.06
139	85.26	94.97	94.93	94.86	87.13	96.16	96.11	96.04
142	88.81	96.46	96.05	96.22	91.94	97.75	97.36	97.50
145	85.31	94.95	94.59	94.65	87.48	95.95	95.69	95.69
148	89.20	95.91	95.46	95.60	91.09	96.97	96.58	96.69
150	87.00	94.99	94.42	94.38	89.83	96.17	95.65	95.64
Mean	84.71	94.92	94.52	94.54	86.98	95.94	95.60	95.60

B.4 MMLAB

Table 27: Results of team MMLAB for task4 recognition.

Sequence	Frame-by-Frame				Application-Dependant			
	Accuracy	Precision	recall	F1	Accuracy	Precision	recall	F1
003	82.34	93.42	93.12	92.95	84.80	94.31	93.94	93.84
004	83.66	94.86	94.85	94.73	85.98	95.77	95.72	95.66
006	80.34	94.78	94.66	94.52	82.35	95.62	95.36	95.27
009	81.20	92.87	92.84	92.37	83.80	93.87	93.66	93.29
012	79.78	91.22	90.75	90.63	84.21	91.86	91.41	91.28
015	76.61	90.11	89.88	89.62	78.06	90.74	90.51	90.23
019	78.75	92.23	92.49	92.00	80.96	93.12	93.18	92.77
020	82.75	94.86	95.12	94.87	85.11	95.69	95.87	95.66
022	81.69	93.47	92.96	92.71	83.20	94.16	93.63	93.41
023	86.34	96.46	96.49	96.32	88.88	97.25	97.19	97.07
029	84.61	95.54	95.56	95.39	87.78	96.45	96.42	96.27
030	78.45	90.37	88.48	88.55	80.35	91.08	89.20	89.25
031	81.15	92.48	92.07	91.79	83.04	93.35	92.92	92.70
032	82.56	94.44	94.64	94.29	84.54	95.34	95.42	95.10
036	87.00	95.09	95.02	94.92	89.72	96.26	96.16	96.12
040	82.27	94.09	93.83	93.59	84.72	94.97	94.64	94.44
043	84.41	94.20	94.31	93.92	86.95	95.31	95.41	95.12
044	85.29	95.39	95.54	95.25	88.07	96.58	96.58	96.41
046	82.35	93.35	93.16	92.73	84.93	94.34	94.14	93.82
049	83.30	94.84	94.93	94.53	86.28	95.84	95.99	95.67
053	78.56	93.28	93.59	93.08	80.98	94.22	94.48	94.05
054	66.22	78.13	78.88	77.56	69.46	79.25	79.92	78.67
056	84.94	95.67	95.45	95.45	87.47	96.69	96.45	96.47
059	86.95	94.15	93.64	93.61	90.59	95.08	94.55	94.56
063	81.89	93.35	93.24	92.92	85.02	94.64	94.32	94.08

Table 27: Results of team MMLAB for task4 recognition. (continued)

Sequence	Frame-by-Frame				Application-Dependant			
	Accuracy	Precision	recall	F1	Accuracy	Precision	recall	F1
064	79.92	91.54	90.50	90.38	82.43	92.28	91.26	91.18
069	84.69	94.82	94.69	94.41	87.01	95.69	95.54	95.29
070	83.79	94.34	94.13	94.04	86.02	95.14	94.97	94.88
072	85.99	94.62	94.36	94.29	88.35	95.71	95.44	95.40
073	82.97	93.31	92.85	92.69	85.92	94.34	93.75	93.69
077	82.75	95.42	95.36	95.10	85.17	96.31	96.27	96.08
079	74.22	86.16	87.04	85.83	76.69	87.41	88.16	87.03
083	81.31	91.30	91.02	90.75	85.59	92.52	92.28	92.09
085	80.50	94.69	94.93	94.66	84.18	95.84	96.02	95.82
086	82.09	94.74	95.18	94.80	84.67	95.85	96.14	95.86
089	84.90	95.38	95.08	95.09	88.91	96.35	96.02	96.07
091	84.50	94.28	93.54	93.53	87.42	95.33	94.60	94.64
093	82.14	94.08	94.02	93.76	84.78	95.19	95.03	94.85
097	85.62	94.96	94.86	94.53	88.90	95.89	95.76	95.50
098	83.06	96.25	96.10	95.69	85.61	97.18	96.99	96.67
101	81.65	93.90	93.84	93.64	83.90	94.84	94.74	94.58
104	85.95	94.34	94.45	94.10	88.22	95.41	95.43	95.17
106	83.18	93.33	92.92	92.83	85.42	94.28	93.86	93.81
108	86.34	93.92	93.45	93.43	89.97	94.97	94.51	94.52
112	83.71	94.62	94.50	94.38	86.51	95.62	95.44	95.36
113	79.36	93.14	92.88	92.67	81.63	94.15	93.82	93.66
116	74.67	89.20	87.58	87.28	77.43	90.51	88.60	88.39
117	85.20	94.51	94.46	94.29	88.29	95.60	95.54	95.41
121	78.66	93.68	93.88	93.54	81.80	94.75	94.82	94.57
123	85.34	93.31	92.84	92.68	88.09	94.24	93.75	93.64
126	79.45	94.03	93.96	93.78	81.98	95.00	94.93	94.79
129	86.03	94.04	93.87	93.73	88.92	95.25	94.99	94.90
134	78.09	91.31	91.49	91.16	82.53	92.53	92.61	92.31
135	83.84	93.51	93.41	93.27	87.56	94.80	94.66	94.53
138	79.79	92.25	92.27	92.05	82.59	93.28	93.23	93.06
139	83.54	93.83	93.62	93.26	86.08	95.17	94.83	94.58
142	81.51	93.74	93.48	93.33	85.52	95.11	94.77	94.68
145	79.81	92.58	92.50	92.00	83.03	93.73	93.68	93.23
148	81.91	92.84	92.64	92.28	84.15	93.88	93.58	93.33
150	82.07	92.82	92.74	92.31	85.50	94.02	93.82	93.53
Mean	82.03	93.32	93.17	92.90	84.80	94.33	94.11	93.91

B.5 NCC NEXT

Table 28: Results of team NCC_NEXT for task1 recognition.

Sequence	Frame-by-Frame				Application-Dependant			
	Accuracy	Precision	recall	F1	Accuracy	Precision	recall	F1
003	83.09	94.96	95.05	94.79	84.71	95.80	95.78	95.58
004	83.48	95.80	95.58	95.49	85.70	96.63	96.37	96.29
006	82.50	96.00	95.53	95.66	84.73	97.05	96.63	96.75
009	84.32	94.77	94.72	94.44	86.70	95.88	95.81	95.58
012	82.26	94.48	94.92	94.58	84.58	95.34	95.70	95.42
015	81.77	94.83	94.00	94.16	83.55	95.50	94.68	94.84
019	81.64	93.95	94.19	93.94	83.58	94.75	95.00	94.77
020	85.01	95.89	96.01	95.83	88.84	97.06	97.10	96.98
022	84.91	94.95	94.73	94.66	86.95	95.94	95.69	95.63
023	89.18	96.53	96.65	96.56	91.73	97.53	97.62	97.56

Table 28: Results of team NCC_NEXT for task1 recognition. (continued)

Sequence	Frame-by-Frame				Application-Dependant			
	Accuracy	Precision	recall	F1	Accuracy	Precision	recall	F1
029	87.45	95.33	94.23	94.53	90.92	96.41	95.37	95.64
030	84.33	94.90	94.53	94.47	85.61	95.60	95.34	95.23
031	84.61	95.18	95.00	95.02	86.41	96.06	95.87	95.90
032	84.21	95.06	94.86	94.75	86.77	96.16	95.98	95.88
036	88.70	96.31	96.17	96.17	91.60	97.64	97.55	97.53
040	85.74	95.69	95.52	95.42	88.46	96.59	96.47	96.37
043	87.27	95.75	95.79	95.61	89.84	97.00	97.13	96.93
044	90.07	97.11	96.96	96.94	92.99	98.38	98.27	98.26
046	84.58	94.34	94.53	94.30	87.10	95.47	95.61	95.41
049	86.93	96.23	96.14	96.01	90.07	97.40	97.20	97.06
053	81.47	93.10	90.92	91.42	83.36	93.93	91.71	92.23
054	67.38	82.29	81.19	80.03	70.15	83.44	82.27	81.16
056	83.59	94.76	93.82	93.80	85.95	95.54	94.60	94.59
059	88.51	95.99	95.12	95.28	92.79	97.16	96.33	96.52
063	81.83	93.31	93.71	93.36	83.88	94.40	94.72	94.39
064	82.58	93.49	92.68	92.86	85.27	94.39	93.55	93.73
069	86.38	94.57	94.56	94.26	88.99	95.86	95.81	95.54
070	85.11	95.32	95.42	95.20	88.31	96.52	96.54	96.44
072	87.67	96.10	95.27	95.45	90.14	97.12	96.36	96.52
073	84.71	94.67	94.51	94.39	87.46	95.90	95.66	95.59
077	85.37	96.47	95.89	96.01	86.97	97.47	96.91	97.04
079	75.05	85.81	87.11	86.08	76.84	86.84	88.05	87.07
083	84.15	94.82	95.06	94.82	86.93	96.12	96.23	96.08
085	84.09	95.77	96.02	95.83	86.25	97.02	97.24	97.07
086	83.49	95.41	95.66	95.38	86.78	96.88	96.98	96.78
089	86.37	96.19	96.09	96.04	89.72	97.37	97.22	97.22
091	85.33	95.30	94.94	94.90	88.31	96.60	96.21	96.22
093	83.59	94.44	94.52	94.25	86.46	95.77	95.75	95.56
097	87.48	96.56	96.05	96.14	90.59	97.93	97.44	97.53
098	88.27	96.66	96.58	96.47	91.49	97.71	97.60	97.56
101	84.06	95.78	95.96	95.79	86.50	96.82	97.01	96.84
104	91.32	96.52	96.13	96.13	94.73	97.83	97.52	97.56
106	87.84	96.48	96.39	96.29	91.24	97.72	97.58	97.53
108	91.53	97.23	97.18	97.16	94.39	98.26	98.18	98.18
112	86.66	96.78	96.92	96.74	90.88	98.20	98.22	98.13
113	83.95	96.24	95.83	95.84	86.58	97.24	96.81	96.84
116	82.39	93.12	93.19	92.72	84.60	94.35	94.25	93.88
117	88.29	96.51	96.18	96.15	91.56	97.93	97.61	97.59
121	83.42	96.40	96.18	96.14	86.56	97.51	97.28	97.28
123	89.98	96.67	96.58	96.45	92.68	97.75	97.61	97.54
126	83.73	95.79	95.02	95.25	86.49	96.94	96.24	96.44
129	87.66	95.25	94.70	94.81	90.00	96.28	95.73	95.85
134	84.53	96.38	96.34	96.14	88.58	97.88	97.78	97.70
135	86.64	96.43	96.52	96.38	89.52	97.62	97.65	97.56
138	83.95	95.04	94.77	94.70	87.46	96.50	96.23	96.21
139	87.78	96.45	96.43	96.17	91.51	98.22	98.18	98.02
142	86.30	96.37	96.67	96.45	89.51	97.90	98.09	97.92
145	83.53	94.96	95.55	95.15	86.61	96.38	96.92	96.59
148	86.44	95.47	95.46	95.31	88.57	96.52	96.48	96.38
150	87.25	94.95	95.03	94.87	90.62	96.20	96.32	96.15
Mean	85.03	95.13	94.95	94.83	87.77	96.27	96.07	95.98

Table 29: Results of team NCC_NEXT for task2 recognition.

Sequence	Frame-by-Frame				Application-Dependant			
	Accuracy	Precision	recall	F1	Accuracy	Precision	recall	F1
003	83.79	90.86	87.72	88.17	84.97	91.66	88.77	89.13
004	78.99	84.75	79.57	80.29	81.30	85.28	80.34	80.95
006	82.27	93.73	90.26	90.79	83.88	94.56	91.32	91.77
009	86.10	93.56	91.70	92.20	87.50	94.44	92.98	93.32
012	80.25	88.75	84.36	85.28	81.48	89.17	84.94	85.76
015	83.64	90.83	87.27	88.46	85.60	91.33	88.09	89.15
019	76.84	86.51	81.03	81.56	78.02	87.02	81.74	82.19
020	87.49	92.70	90.22	90.99	89.14	93.42	91.26	91.90
022	85.17	91.44	88.01	88.95	87.09	92.13	89.04	89.85
023	89.74	94.36	91.81	92.60	91.24	95.09	92.76	93.44
029	91.59	94.67	91.91	92.77	93.37	95.29	92.96	93.63
030	81.46	89.45	84.53	85.95	82.64	89.87	85.25	86.54
031	90.50	92.84	89.87	90.78	91.70	93.39	90.66	91.50
032	87.56	93.95	91.34	92.18	89.96	94.71	92.50	93.17
036	90.93	92.71	89.36	90.36	92.25	93.39	90.33	91.22
040	89.80	92.16	89.58	90.40	91.34	92.78	90.60	91.26
043	85.62	88.90	86.29	86.76	87.18	89.66	87.35	87.71
044	87.75	90.12	87.67	87.54	88.94	90.81	88.68	88.43
046	88.63	91.86	89.02	89.63	90.64	92.71	90.15	90.66
049	90.07	93.58	91.29	92.01	92.17	94.61	92.73	93.29
053	88.67	92.58	90.38	90.77	90.59	93.66	91.87	92.17
054	77.78	84.67	81.85	82.28	80.51	85.66	83.20	83.49
056	92.37	95.28	92.70	93.58	94.25	95.91	93.70	94.44
059	90.89	95.04	92.79	93.50	93.07	95.76	93.81	94.40
063	90.75	93.70	90.99	91.55	92.92	94.68	92.40	92.78
064	86.53	91.10	87.20	87.76	87.94	91.61	88.09	88.49
069	89.97	94.11	91.45	92.15	92.02	94.78	92.44	93.02
070	92.15	95.92	94.12	94.70	94.69	96.68	95.18	95.64
072	91.15	95.70	93.55	94.30	93.07	96.50	94.89	95.44
073	87.80	94.13	91.90	92.50	91.43	94.84	93.01	93.44
077	88.45	96.15	94.45	95.10	91.10	97.00	95.60	96.13
079	84.60	89.51	86.66	87.03	86.36	90.50	87.98	88.24
083	89.61	92.59	90.72	91.32	91.47	93.38	91.86	92.32
085	91.40	96.47	94.65	95.29	94.97	97.34	96.00	96.44
086	89.81	93.88	92.35	92.90	91.52	94.63	93.45	93.86
089	90.46	96.15	93.75	94.64	92.86	97.18	95.01	95.82
091	84.39	89.63	86.86	87.34	86.65	90.73	88.50	88.74
093	91.79	96.08	94.12	94.80	93.50	96.91	95.52	95.99
097	89.78	93.66	91.30	91.62	92.20	94.44	92.48	92.66
098	90.75	96.38	95.13	95.58	93.19	97.29	96.42	96.72
101	89.78	94.65	92.53	93.18	91.46	95.44	93.81	94.28
104	90.48	93.89	91.66	92.31	92.45	94.84	92.91	93.47
106	92.88	95.75	93.53	94.36	94.77	96.59	94.73	95.43
108	91.93	94.91	92.67	93.43	93.42	95.66	93.87	94.45
112	91.08	95.56	93.14	94.00	93.25	96.31	94.32	95.00
113	90.22	94.26	91.33	92.31	92.27	95.10	92.62	93.42
116	85.02	90.92	88.10	88.78	86.47	91.79	89.24	89.82
117	92.19	94.77	92.73	93.38	93.78	95.70	93.97	94.50
121	86.20	92.77	89.68	90.19	90.21	93.56	90.70	91.10
123	85.19	88.01	85.26	85.95	86.91	88.61	86.22	86.78
126	90.90	96.12	93.97	94.75	94.25	97.00	95.05	95.73
129	90.44	95.35	92.60	93.73	93.37	96.47	93.95	94.97
134	83.95	92.59	90.22	90.91	86.10	93.53	91.51	92.07

Table 29: Results of team NCC_NEXT for task2 recognition. (continued)

Sequence	Frame-by-Frame				Application-Dependant			
	Accuracy	Precision	recall	F1	Accuracy	Precision	recall	F1
135	91.97	95.96	94.17	94.78	94.01	96.78	95.43	95.86
138	93.45	95.23	92.86	93.67	95.86	96.25	94.30	94.96
139	91.06	93.86	91.84	92.27	93.53	95.15	93.51	93.80
142	92.16	95.80	93.28	94.18	94.33	96.71	94.48	95.26
145	89.73	95.32	93.59	94.15	92.19	96.38	95.17	95.54
148	92.40	95.22	92.47	93.27	94.61	96.22	93.92	94.58
150	88.59	93.83	91.78	92.33	90.95	94.78	93.34	93.65
Mean	88.28	93.09	90.45	91.14	90.32	93.89	91.61	92.16

Table 30: Results of team NCC_NEXT for task3 recognition.

Sequence	Frame-by-Frame				Application-Dependant			
	Accuracy	Precision	recall	F1	Accuracy	Precision	recall	F1
003	84.17	94.95	94.81	94.67	87.47	96.18	96.04	95.91
004	84.80	95.67	95.68	95.62	87.09	96.78	96.78	96.72
006	81.08	94.99	94.60	94.65	83.17	96.13	95.77	95.81
009	83.70	94.50	94.18	94.08	87.33	96.11	95.80	95.69
012	81.11	94.94	94.52	94.66	84.48	95.98	95.51	95.64
015	80.69	93.93	92.84	93.05	83.28	94.66	93.71	93.86
019	82.46	93.87	93.95	93.73	84.47	94.72	94.77	94.56
020	84.73	95.11	94.75	94.65	88.33	96.52	96.18	96.10
022	84.09	94.69	94.35	94.36	86.06	95.70	95.42	95.39
023	87.13	95.39	95.10	95.12	91.24	96.65	96.43	96.44
029	82.83	94.18	93.16	93.39	87.14	95.52	94.56	94.76
030	81.06	92.71	91.60	91.74	83.25	93.67	92.63	92.75
031	82.54	94.56	94.37	94.38	84.55	95.50	95.29	95.33
032	80.99	93.36	92.80	92.84	83.78	94.50	94.00	94.02
036	88.26	95.82	95.56	95.59	90.92	97.13	96.91	96.93
040	83.35	94.23	93.52	93.69	86.50	95.53	94.91	95.03
043	85.84	95.35	95.35	95.17	89.18	96.75	96.86	96.66
044	87.84	96.16	95.88	95.88	91.18	97.47	97.30	97.28
046	83.88	93.84	93.73	93.58	86.87	95.25	95.12	94.99
049	85.18	95.19	95.30	95.16	88.53	96.51	96.63	96.49
053	81.25	93.42	93.31	93.11	83.85	94.50	94.40	94.21
054	70.23	82.83	84.63	82.97	72.63	83.90	85.66	84.04
056	83.93	94.21	93.88	93.74	86.43	95.28	94.94	94.82
059	88.87	96.02	95.72	95.70	93.22	97.03	96.69	96.72
063	82.23	94.38	93.94	93.76	85.53	95.71	95.33	95.16
064	81.56	92.49	92.46	92.33	85.28	93.65	93.66	93.50
069	85.18	93.22	93.16	92.99	88.98	94.64	94.59	94.41
070	83.64	94.81	94.68	94.63	87.02	96.11	95.95	95.91
072	85.93	95.57	94.78	95.00	89.41	96.92	96.26	96.42
073	84.08	93.70	93.11	93.23	87.38	94.90	94.38	94.46
077	83.47	95.60	95.53	95.46	85.53	96.64	96.56	96.48
079	71.95	84.18	85.44	84.23	74.75	85.54	86.58	85.47
083	81.68	92.66	92.92	92.71	85.07	93.88	94.11	93.93
085	82.59	95.32	95.21	95.15	86.42	96.77	96.79	96.71
086	83.45	95.07	95.21	95.06	86.69	96.38	96.53	96.39
089	85.69	96.07	95.81	95.88	89.53	97.32	97.11	97.16
091	85.86	95.39	95.25	95.22	89.66	96.87	96.75	96.72
093	83.56	94.15	93.96	93.90	86.99	95.71	95.69	95.58
097	85.76	95.66	95.48	95.48	89.00	97.04	96.92	96.91
098	87.20	95.77	95.65	95.66	93.01	97.39	97.26	97.26

Table 30: Results of team NCC_NEXT for task3 recognition. (continued)

Sequence	Frame-by-Frame				Application-Dependant			
	Accuracy	Precision	recall	F1	Accuracy	Precision	recall	F1
101	83.06	95.19	95.30	95.18	86.67	96.76	96.90	96.77
104	90.76	95.75	95.78	95.72	94.92	97.32	97.28	97.27
106	85.82	95.69	95.60	95.54	89.62	97.12	96.95	96.95
108	88.60	96.55	96.25	96.34	92.84	97.71	97.50	97.55
112	86.35	96.21	96.03	96.08	90.70	97.62	97.43	97.47
113	85.17	95.30	94.94	94.98	88.54	96.71	96.31	96.37
116	82.35	93.28	93.73	93.38	85.22	94.60	94.97	94.72
117	90.09	96.46	96.10	96.19	94.71	97.92	97.59	97.69
121	80.40	94.78	93.93	93.96	83.18	95.69	94.88	94.93
123	88.65	96.12	95.32	95.58	92.92	97.39	96.59	96.84
126	81.39	94.85	94.48	94.54	85.13	96.36	95.93	96.02
129	88.96	95.03	94.62	94.66	92.99	96.67	96.16	96.28
134	85.29	96.28	96.32	96.27	89.66	97.84	97.85	97.83
135	86.49	96.03	96.03	95.98	91.03	97.61	97.63	97.58
138	83.65	95.02	94.71	94.68	87.51	96.62	96.38	96.39
139	87.88	95.85	95.77	95.69	93.28	97.77	97.72	97.69
142	86.94	96.21	96.15	96.01	91.30	97.84	97.73	97.65
145	83.58	94.23	94.52	94.23	88.36	95.84	96.08	95.88
148	87.96	95.13	94.85	94.88	91.00	96.55	96.22	96.27
150	87.31	94.08	94.15	93.99	91.53	95.62	95.75	95.56
Mean	84.24	94.53	94.35	94.27	87.71	95.85	95.68	95.61

Table 31: Results of team NCC_NEXT for task4 recognition.

Sequence	Frame-by-Frame				Application-Dependant			
	Accuracy	Precision	recall	F1	Accuracy	Precision	recall	F1
003	89.92	95.84	94.36	94.86	91.19	96.69	95.47	95.88
004	93.79	96.96	95.58	96.08	96.12	97.58	96.47	96.86
006	87.17	96.74	95.00	95.64	88.87	97.54	96.07	96.61
009	88.29	95.38	93.95	94.46	89.85	96.32	95.28	95.64
012	85.37	93.67	90.29	91.41	86.64	94.06	90.90	91.92
015	87.20	94.41	90.75	92.02	88.99	94.92	91.58	92.71
019	85.74	94.85	92.22	93.17	86.88	95.36	92.94	93.81
020	90.97	95.78	93.66	94.38	92.60	96.51	94.69	95.28
022	89.44	94.96	92.64	93.42	91.29	95.67	93.67	94.32
023	92.50	96.88	94.69	95.53	94.03	97.62	95.67	96.40
029	93.10	95.82	93.41	94.26	94.95	96.45	94.48	95.14
030	86.42	94.82	91.06	92.42	87.67	95.31	91.83	93.06
031	92.83	95.89	93.62	94.50	93.97	96.39	94.36	95.16
032	88.45	94.76	92.08	92.95	90.91	95.51	93.23	93.95
036	92.72	95.58	92.57	93.59	94.38	96.36	93.64	94.55
040	92.80	95.44	92.76	93.64	94.33	96.05	93.76	94.49
043	92.16	95.60	93.77	94.39	93.92	96.44	94.92	95.42
044	95.09	96.83	95.47	95.97	96.59	97.63	96.62	97.00
046	91.56	94.94	92.58	93.35	93.60	95.85	93.76	94.44
049	91.64	95.32	93.26	93.99	94.36	96.47	94.79	95.36
053	92.14	95.02	92.48	93.22	93.99	96.05	93.94	94.58
054	76.00	83.95	81.26	80.88	78.72	84.91	82.60	82.07
056	93.23	96.41	93.59	94.49	95.15	97.06	94.63	95.38
059	92.71	96.56	94.30	95.13	94.97	97.36	95.39	96.09
063	93.06	95.82	94.19	94.72	95.33	96.80	95.63	95.98
064	90.51	95.15	93.44	93.92	92.17	95.75	94.42	94.75
069	91.05	95.33	92.79	93.58	93.62	96.19	93.98	94.65

Table 31: Results of team NCC_NEXT for task4 recognition. (continued)

Sequence	Frame-by-Frame				Application-Dependant			
	Accuracy	Precision	recall	F1	Accuracy	Precision	recall	F1
070	91.35	96.36	94.81	95.34	93.88	97.16	95.91	96.33
072	92.27	96.68	94.63	95.38	94.23	97.53	96.02	96.57
073	89.03	95.28	93.43	94.02	92.90	96.06	94.61	95.03
077	89.53	97.03	95.41	96.05	92.30	97.99	96.67	97.19
079	84.83	87.59	87.22	86.95	86.79	88.64	88.60	88.22
083	93.00	96.14	94.45	95.06	95.02	97.02	95.69	96.16
085	90.94	96.30	94.51	95.16	94.55	97.30	95.97	96.43
086	91.49	96.41	94.89	95.45	93.76	97.44	96.25	96.66
089	91.48	97.24	95.15	96.02	94.42	98.42	96.55	97.34
091	89.68	95.63	93.57	94.31	92.07	96.88	95.34	95.86
093	90.85	95.42	93.25	93.92	92.61	96.25	94.65	95.13
097	93.07	97.02	95.22	95.85	95.47	97.91	96.51	96.99
098	91.14	97.07	95.85	96.30	93.62	98.02	97.17	97.48
101	91.40	95.81	94.00	94.64	93.11	96.62	95.32	95.77
104	93.44	96.89	95.12	95.80	95.48	97.86	96.39	96.97
106	93.50	96.46	94.30	95.11	95.51	97.34	95.54	96.22
108	94.97	97.55	95.71	96.44	96.57	98.39	97.02	97.56
112	93.41	97.44	95.42	96.23	95.58	98.18	96.58	97.21
113	92.80	96.53	93.95	94.89	94.89	97.37	95.25	96.01
116	88.46	94.93	92.79	93.48	89.97	95.81	93.95	94.54
117	94.02	96.95	95.16	95.77	96.06	98.02	96.50	97.02
121	90.75	96.37	94.28	95.08	94.78	97.22	95.36	96.03
123	92.89	96.50	94.35	95.13	94.58	97.15	95.34	95.99
126	91.30	96.40	94.27	95.05	94.77	97.35	95.41	96.09
129	90.48	96.14	93.44	94.56	93.40	97.26	94.80	95.82
134	87.48	96.08	94.05	94.75	89.74	97.10	95.39	95.98
135	92.59	96.56	94.84	95.47	94.73	97.47	96.17	96.63
138	94.08	95.66	93.25	94.09	96.52	96.72	94.73	95.40
139	94.12	96.78	95.26	95.80	96.67	98.18	97.04	97.45
142	93.62	97.30	94.98	95.89	95.88	98.30	96.28	97.08
145	91.23	96.46	94.90	95.44	93.93	97.66	96.63	96.98
148	91.99	95.96	93.65	94.49	94.22	96.97	95.11	95.81
150	90.16	95.17	93.44	94.05	92.48	96.10	94.95	95.33
Mean	90.95	95.68	93.59	94.30	93.09	96.54	94.81	95.38

Table 32: Results of team NCC_NEXT for task5 recognition.

Sequence	Frame-by-Frame				Application-Dependant			
	Accuracy	Precision	recall	F1	Accuracy	Precision	recall	F1
003	90.16	95.93	94.58	95.05	91.42	96.78	95.70	96.07
004	93.63	96.83	95.46	95.95	95.99	97.48	96.39	96.77
006	86.85	96.39	94.62	95.26	88.51	97.16	95.66	96.20
009	88.50	95.60	94.16	94.67	90.05	96.51	95.47	95.83
012	85.87	94.09	90.75	91.88	87.10	94.44	91.33	92.35
015	87.02	94.10	90.45	91.71	88.79	94.60	91.27	92.39
019	85.79	95.00	92.40	93.35	86.98	95.58	93.18	94.05
020	90.43	95.29	93.04	93.78	92.05	95.99	94.06	94.66
022	89.67	95.05	92.84	93.62	91.47	95.73	93.86	94.50
023	92.20	96.61	94.39	95.23	93.70	97.32	95.35	96.07
029	93.08	95.80	93.38	94.23	94.91	96.42	94.43	95.10
030	86.05	94.31	90.12	91.52	87.22	94.74	90.84	92.11
031	92.95	96.00	93.72	94.60	94.22	96.58	94.54	95.34
032	88.42	94.68	91.94	92.82	90.91	95.45	93.16	93.86

Table 32: Results of team NCC_NEXT for task5 recognition. (continued)

Sequence	Frame-by-Frame				Application-Dependant			
	Accuracy	Precision	recall	F1	Accuracy	Precision	recall	F1
036	92.71	95.62	92.63	93.65	94.46	96.49	93.79	94.70
040	92.57	95.33	92.69	93.58	94.15	95.99	93.73	94.47
043	92.36	95.69	93.97	94.58	94.17	96.54	95.14	95.62
044	94.91	96.78	95.41	95.90	96.44	97.60	96.57	96.95
046	91.59	95.04	92.54	93.34	93.63	95.95	93.73	94.44
049	91.72	95.36	93.29	94.02	94.37	96.45	94.77	95.34
053	92.43	95.39	92.86	93.60	94.33	96.44	94.34	94.97
054	76.83	83.17	82.08	81.52	79.50	84.12	83.39	82.69
056	93.36	96.52	93.69	94.58	95.29	97.17	94.73	95.47
059	92.79	96.60	94.41	95.24	94.99	97.34	95.45	96.15
063	93.09	95.73	93.71	94.28	95.23	96.62	95.09	95.49
064	90.57	95.16	93.45	93.93	92.15	95.70	94.38	94.70
069	91.28	95.43	93.03	93.82	93.77	96.27	94.17	94.84
070	91.09	96.12	94.58	95.10	93.62	96.92	95.69	96.09
072	92.20	96.67	94.59	95.35	94.15	97.48	95.97	96.52
073	88.94	94.99	93.26	93.82	92.79	95.74	94.42	94.81
077	89.48	96.97	95.35	95.99	92.22	97.90	96.58	97.10
079	84.20	87.59	86.61	86.49	86.12	88.65	87.97	87.74
083	92.35	95.42	93.71	94.30	94.41	96.27	94.92	95.38
085	91.07	96.46	94.65	95.30	94.64	97.40	96.07	96.52
086	91.86	96.69	95.23	95.79	93.99	97.58	96.47	96.88
089	91.71	97.51	95.43	96.30	94.56	98.59	96.73	97.52
091	90.16	96.08	94.03	94.77	92.44	97.22	95.69	96.22
093	90.69	95.26	93.14	93.84	92.48	96.15	94.60	95.08
097	93.07	97.03	95.23	95.86	95.41	97.86	96.45	96.93
098	91.25	97.19	96.01	96.46	93.77	98.20	97.39	97.69
101	91.34	95.81	93.99	94.64	93.11	96.67	95.35	95.80
104	93.25	96.68	94.89	95.58	95.22	97.61	96.13	96.71
106	93.64	96.59	94.47	95.29	95.49	97.35	95.59	96.28
108	95.20	97.78	95.94	96.67	96.76	98.58	97.21	97.76
112	93.35	97.41	95.38	96.20	95.61	98.23	96.63	97.26
113	92.68	96.43	93.81	94.77	94.75	97.26	95.10	95.88
116	88.81	95.50	93.79	94.42	90.22	96.32	94.89	95.42
117	94.05	96.93	95.13	95.74	96.01	97.95	96.43	96.95
121	90.70	96.35	94.26	95.06	94.69	97.14	95.28	95.95
123	93.18	96.69	94.53	95.31	94.92	97.34	95.53	96.18
126	91.15	96.36	94.24	95.02	94.54	97.23	95.30	95.98
129	90.64	96.25	93.55	94.68	93.60	97.39	94.92	95.93
134	87.93	96.46	94.45	95.16	90.18	97.47	95.79	96.38
135	92.83	96.76	95.05	95.69	94.89	97.59	96.31	96.77
138	94.14	95.72	93.35	94.20	96.58	96.75	94.83	95.52
139	94.01	96.66	95.13	95.67	96.55	98.07	96.93	97.33
142	93.36	97.11	94.76	95.67	95.52	98.02	95.97	96.77
145	90.73	96.02	94.41	94.96	93.36	97.13	96.05	96.41
148	91.95	95.72	93.34	94.18	94.22	96.75	94.83	95.53
150	90.12	95.07	93.30	93.90	92.50	96.03	94.88	95.25
Mean	90.97	95.66	93.59	94.30	93.09	96.51	94.79	95.36

B.6 SK

Table 33: Results of team SK for task1 recognition.

Sequence	Frame-by-Frame				Application-Dependant			
	Accuracy	Precision	recall	F1	Accuracy	Precision	recall	F1
003	88.23	96.50	96.05	96.15	91.08	97.48	97.03	97.14
004	87.26	96.84	96.50	96.59	88.82	97.63	97.32	97.39
006	86.00	96.50	95.93	96.12	89.57	97.39	96.97	97.10
009	88.79	95.59	94.81	94.98	90.59	96.51	95.81	95.94
012	85.68	95.48	95.12	95.23	88.50	96.40	96.07	96.16
015	83.33	94.83	93.33	93.75	86.11	95.51	94.12	94.49
019	83.06	94.07	93.14	93.23	84.37	94.80	93.97	94.01
020	87.88	96.31	96.08	96.10	90.35	97.05	96.86	96.85
022	90.48	96.46	95.53	95.78	93.12	97.24	96.46	96.65
023	92.92	96.51	95.84	96.04	94.40	97.30	96.75	96.91
029	89.63	96.08	95.06	95.34	91.83	97.03	96.20	96.41
030	86.15	94.17	93.20	93.41	87.79	94.87	94.09	94.22
031	85.89	95.10	94.67	94.76	87.72	95.84	95.50	95.57
032	84.13	95.35	94.45	94.62	86.12	96.26	95.60	95.68
036	95.95	97.24	96.71	96.88	97.55	98.28	97.81	97.95
040	87.44	95.88	94.92	95.15	90.62	96.64	95.77	95.97
043	89.44	96.23	95.88	95.94	91.83	97.40	97.07	97.14
044	95.74	97.71	97.38	97.48	98.04	98.72	98.44	98.53
046	86.24	94.56	93.77	93.86	89.27	95.59	94.80	94.88
049	90.23	96.61	96.32	96.36	92.75	97.67	97.50	97.49
053	84.89	94.58	94.21	94.25	87.26	95.60	95.22	95.23
054	73.46	85.05	84.58	83.95	75.15	85.81	85.38	84.72
056	86.71	95.43	94.76	94.89	90.11	96.55	95.91	96.03
059	91.51	96.80	96.22	96.41	94.53	97.61	97.13	97.27
063	84.86	94.99	93.73	94.02	88.20	96.24	95.12	95.36
064	82.45	92.69	92.25	92.34	85.20	93.47	93.13	93.16
069	87.42	93.88	93.50	93.38	90.92	95.15	94.80	94.64
070	88.13	96.25	95.58	95.83	92.68	97.63	97.06	97.26
072	88.88	96.07	94.81	95.20	91.55	97.20	96.09	96.41
073	87.29	95.30	94.35	94.58	90.05	96.40	95.69	95.82
077	86.56	96.61	95.86	96.09	89.50	97.60	96.93	97.12
079	78.57	86.11	86.17	85.58	83.30	87.30	87.33	86.76
083	86.69	95.01	94.54	94.57	89.81	96.19	95.73	95.76
085	87.70	96.25	96.02	96.07	89.88	97.34	97.20	97.22
086	87.50	96.81	96.40	96.48	89.90	97.88	97.50	97.56
089	88.30	96.64	95.47	95.94	91.98	97.68	96.69	97.08
091	88.53	96.47	96.02	96.16	92.29	98.00	97.69	97.77
093	88.29	95.20	94.50	94.62	92.32	96.50	95.98	96.03
097	88.20	96.54	95.80	96.01	91.43	97.81	97.26	97.39
098	91.31	97.70	97.32	97.47	94.29	98.84	98.57	98.65
101	86.11	96.19	95.58	95.69	88.88	97.11	96.58	96.64
104	94.77	97.11	96.59	96.76	97.20	98.21	97.82	97.94
106	90.67	96.68	96.40	96.45	94.84	97.94	97.73	97.77
108	92.69	97.10	96.29	96.55	96.05	98.05	97.44	97.60
112	89.37	96.71	96.12	96.27	91.92	97.57	97.15	97.23
113	91.37	96.71	96.09	96.30	94.58	97.64	97.19	97.32
116	86.29	94.48	94.41	94.27	88.93	95.89	95.80	95.69
117	91.27	97.04	96.54	96.69	94.56	98.57	98.26	98.31
121	86.57	96.54	94.84	95.41	88.90	97.39	95.88	96.34
123	92.19	96.85	95.44	95.93	93.85	97.60	96.37	96.80
126	84.55	96.19	95.34	95.61	87.99	97.54	96.88	97.08
129	91.36	96.43	95.52	95.86	93.80	97.36	96.53	96.84
134	87.56	96.74	96.04	96.29	90.66	97.93	97.43	97.58

Table 33: Results of team SK for task1 recognition. (continued)

Sequence	Frame-by-Frame				Application-Dependant			
	Accuracy	Precision	recall	F1	Accuracy	Precision	recall	F1
135	89.76	97.10	96.87	96.92	92.51	98.38	98.19	98.21
138	86.13	93.10	92.32	92.46	89.28	94.31	93.64	93.74
139	89.39	95.56	95.13	95.14	92.65	97.20	96.84	96.86
142	92.75	97.23	96.60	96.85	95.75	98.40	97.89	98.09
145	86.44	94.50	94.22	94.14	88.72	95.58	95.44	95.31
148	90.40	96.25	95.66	95.82	92.55	97.21	96.75	96.86
150	88.39	95.09	93.99	94.22	91.67	96.35	95.24	95.46
Mean	88.00	95.60	94.95	95.09	90.77	96.64	96.09	96.19

Table 34: Results of team SK for task2 recognition.

Sequence	Frame-by-Frame				Application-Dependant			
	Accuracy	Precision	recall	F1	Accuracy	Precision	recall	F1
003	87.85	96.24	96.04	96.04	89.37	97.07	97.02	96.95
004	87.69	96.73	96.18	96.25	89.02	97.41	96.97	97.00
006	87.35	97.42	97.06	97.17	89.03	98.31	98.08	98.15
009	89.21	96.38	96.42	96.28	91.05	97.22	97.41	97.21
012	78.89	90.14	89.49	89.27	80.61	90.74	90.22	89.95
015	81.24	92.63	89.98	88.80	82.72	93.05	90.62	89.36
019	79.12	90.98	89.31	89.35	80.50	91.55	90.00	89.97
020	88.56	96.30	96.31	96.24	90.45	97.00	97.18	97.04
022	86.88	95.59	95.28	95.32	88.39	96.40	96.22	96.22
023	92.10	97.17	96.84	96.91	94.07	98.05	97.95	97.95
029	88.65	94.97	93.27	93.52	90.53	95.79	94.53	94.63
030	83.12	91.92	89.90	89.90	84.42	92.52	90.72	90.63
031	86.24	95.61	94.88	95.03	88.26	96.50	95.91	96.01
032	76.25	85.04	84.24	82.60	77.81	85.85	85.32	83.56
036	90.22	94.47	92.79	92.70	91.88	95.50	94.11	93.91
040	87.17	94.84	93.66	93.84	88.92	95.63	94.71	94.80
043	88.56	96.12	95.80	95.78	90.26	97.03	96.90	96.81
044	91.17	96.93	96.61	96.67	92.87	98.00	97.92	97.90
046	86.63	94.62	94.32	94.17	88.85	95.62	95.39	95.20
049	87.55	96.06	96.09	95.97	89.45	97.09	97.34	97.14
053	85.66	95.75	95.61	95.38	87.81	96.64	96.59	96.34
054	69.98	78.68	78.95	78.05	72.19	79.54	80.08	79.08
056	90.83	97.31	96.97	97.04	92.80	98.15	98.00	98.00
059	95.29	98.31	97.96	98.08	97.73	99.24	99.14	99.18
063	86.74	95.35	94.17	94.02	88.92	96.46	95.49	95.27
064	83.24	90.85	88.49	87.33	85.25	91.68	89.47	88.22
069	89.47	96.13	95.98	95.89	91.91	97.18	97.20	97.06
070	88.51	96.00	95.74	95.78	91.12	97.04	96.89	96.87
072	91.09	97.51	97.07	97.23	93.15	98.49	98.24	98.31
073	89.05	96.35	95.34	95.34	91.62	97.30	96.45	96.40
077	88.42	97.46	97.42	97.40	90.72	98.50	98.58	98.52
079	74.50	85.07	85.07	83.74	76.49	86.28	86.30	84.96
083	89.87	95.67	95.48	95.46	91.92	96.62	96.53	96.47
085	86.94	96.75	96.84	96.77	88.94	97.77	98.03	97.89
086	75.02	88.02	89.90	88.59	76.67	89.07	91.12	89.74
089	90.62	97.33	97.13	97.18	92.74	98.16	98.07	98.08
091	90.11	96.77	96.39	96.47	93.78	98.17	98.03	98.02
093	87.93	96.63	96.47	96.43	90.78	97.89	98.02	97.89
097	90.76	97.60	97.43	97.44	93.35	98.64	98.60	98.59
098	92.42	97.87	97.77	97.78	94.71	99.00	99.05	99.01

Table 34: Results of team SK for task2 recognition. (continued)

Sequence	Frame-by-Frame				Application-Dependant			
	Accuracy	Precision	recall	F1	Accuracy	Precision	recall	F1
101	87.13	96.87	96.62	96.66	89.30	97.87	97.88	97.82
104	93.50	96.19	95.80	95.86	95.72	97.23	96.96	96.99
106	90.72	96.73	96.36	96.45	92.20	97.53	97.34	97.37
108	94.73	97.80	97.31	97.47	96.89	98.64	98.35	98.44
112	90.74	97.81	97.45	97.58	94.09	98.86	98.70	98.75
113	86.81	96.61	96.17	96.29	88.82	97.40	97.25	97.25
116	84.65	93.73	92.27	92.41	86.43	94.62	93.33	93.42
117	90.81	96.92	96.47	96.57	93.46	98.00	97.76	97.78
121	84.55	96.07	95.45	95.66	87.48	97.00	96.51	96.64
123	93.94	96.28	95.38	95.60	95.88	97.06	96.38	96.52
126	84.75	95.92	95.19	95.42	88.39	97.12	96.54	96.69
129	92.28	96.73	95.97	96.24	95.76	97.92	97.35	97.52
134	85.56	96.03	95.52	95.63	87.56	96.94	96.70	96.71
135	91.46	97.19	96.77	96.89	93.48	98.17	98.01	98.02
138	87.45	96.44	95.94	96.06	89.48	97.50	97.27	97.30
139	90.91	96.84	96.59	96.66	93.03	98.07	97.97	97.99
142	90.94	96.53	95.86	95.97	93.70	97.60	97.12	97.15
145	86.69	95.93	96.00	95.89	89.67	97.14	97.37	97.19
148	91.53	96.85	96.55	96.59	93.47	98.02	97.95	97.92
150	91.14	96.44	96.48	96.35	93.70	97.39	97.62	97.43
Mean	87.52	95.19	94.68	94.59	89.66	96.14	95.81	95.65

Table 35: Results of team SK for task3 recognition.

Sequence	Frame-by-Frame				Application-Dependant			
	Accuracy	Precision	recall	F1	Accuracy	Precision	recall	F1
003	86.19	95.29	94.73	94.92	88.85	96.33	95.95	96.06
004	85.50	95.64	95.20	95.34	87.61	96.52	96.17	96.28
006	87.45	95.99	94.92	95.24	89.77	96.96	96.05	96.32
009	85.56	94.96	94.14	94.29	87.55	95.97	95.25	95.37
012	82.77	94.46	93.00	93.52	85.43	95.23	93.88	94.35
015	81.81	93.98	91.42	92.29	84.35	94.63	92.27	93.04
019	85.39	94.23	92.65	92.95	87.67	95.06	93.58	93.84
020	88.13	95.26	94.77	94.90	91.33	96.46	96.16	96.20
022	87.39	94.63	93.39	93.77	89.42	95.58	94.49	94.81
023	88.82	95.23	93.90	94.35	90.96	96.20	94.94	95.34
029	87.98	95.25	93.78	94.30	91.03	96.39	95.20	95.60
030	85.30	93.45	91.34	91.85	87.49	94.30	92.31	92.78
031	85.00	94.56	93.90	94.11	87.01	95.52	94.92	95.11
032	82.69	93.37	92.57	92.71	84.78	94.33	93.69	93.76
036	91.04	96.31	95.34	95.64	92.70	97.35	96.58	96.82
040	86.02	94.61	92.70	93.23	88.19	95.52	93.73	94.22
043	87.86	95.44	95.02	95.06	90.09	96.59	96.38	96.36
044	88.40	95.83	95.00	95.25	90.60	97.00	96.31	96.50
046	84.39	93.25	92.43	92.48	87.10	94.53	93.84	93.87
049	85.87	94.99	94.27	94.37	87.90	95.84	95.30	95.34
053	82.90	93.27	92.48	92.62	84.96	94.25	93.54	93.65
054	68.62	82.45	81.41	80.90	70.64	83.48	82.52	81.98
056	86.08	94.53	93.97	93.94	89.27	95.45	94.97	94.92
059	88.67	95.06	93.79	94.14	91.25	95.95	94.83	95.12
063	84.22	93.30	92.07	92.31	86.24	94.33	93.26	93.42
064	83.55	92.88	92.75	92.67	86.34	93.75	93.74	93.60
069	85.86	92.91	91.01	91.54	88.72	93.92	92.28	92.68

Table 35: Results of team SK for task3 recognition. (continued)

Sequence	Frame-by-Frame				Application-Dependant			
	Accuracy	Precision	recall	F1	Accuracy	Precision	recall	F1
070	87.66	95.50	94.89	95.07	90.35	96.65	96.23	96.34
072	86.17	95.34	93.81	94.38	88.43	96.30	94.98	95.44
073	85.51	93.33	91.69	92.05	88.63	94.45	93.11	93.34
077	86.16	95.64	95.03	95.21	88.55	96.75	96.33	96.43
079	71.46	82.83	82.53	81.93	73.33	84.03	83.71	83.11
083	84.56	94.23	93.73	93.88	87.02	95.16	94.73	94.84
085	85.24	95.55	94.96	95.14	88.71	96.88	96.43	96.57
086	85.29	94.88	94.03	94.24	87.13	95.75	95.14	95.25
089	86.39	95.66	94.36	94.88	90.34	96.63	95.57	95.97
091	85.73	95.08	94.10	94.45	89.58	96.39	95.58	95.84
093	84.39	94.05	93.06	93.37	87.62	95.56	95.03	95.15
097	86.76	95.87	94.56	95.03	89.75	97.17	96.14	96.51
098	90.00	96.41	95.61	95.91	94.96	98.12	97.55	97.75
101	85.86	95.28	94.80	94.90	88.75	96.42	96.16	96.19
104	89.61	94.71	92.67	93.32	92.74	96.18	94.22	94.80
106	89.28	95.60	94.97	95.14	92.35	96.84	96.41	96.50
108	93.06	97.12	96.54	96.75	96.04	98.30	97.91	98.05
112	87.69	95.80	94.95	95.25	91.37	97.00	96.42	96.60
113	87.66	95.44	93.52	94.23	90.41	96.48	94.81	95.42
116	84.99	94.36	93.91	93.93	88.32	95.75	95.37	95.39
117	89.31	95.74	95.00	95.21	92.57	97.14	96.69	96.77
121	83.93	94.94	93.08	93.69	85.42	95.66	93.92	94.47
123	89.34	95.90	93.94	94.60	90.89	96.60	94.90	95.47
126	84.25	95.72	94.33	94.77	87.74	96.85	95.80	96.12
129	89.85	95.19	93.92	94.27	93.43	96.69	95.66	95.94
134	89.71	96.20	95.47	95.71	92.33	97.60	97.04	97.22
135	88.73	95.73	95.15	95.31	92.13	97.18	96.69	96.79
138	74.64	91.69	90.05	89.81	77.53	92.84	91.37	91.06
139	79.36	89.53	90.37	89.74	83.12	91.31	92.29	91.64
142	90.38	94.84	93.69	93.93	94.12	96.34	95.38	95.56
145	84.82	93.98	93.73	93.62	88.28	95.61	95.38	95.28
148	88.82	95.33	94.44	94.73	91.44	96.52	95.72	95.97
150	86.89	93.72	92.66	92.95	89.72	94.78	93.83	94.06
Mean	85.78	94.37	93.36	93.60	88.51	95.49	94.64	94.82

Table 36: Results of team SK for task4 recognition.

Sequence	Frame-by-Frame				Application-Dependant			
	Accuracy	Precision	recall	F1	Accuracy	Precision	recall	F1
003	89.94	97.50	97.44	97.42	92.04	98.32	98.28	98.24
004	88.41	97.88	97.93	97.88	90.29	98.67	98.75	98.70
006	86.98	97.58	97.52	97.52	88.61	98.39	98.38	98.35
009	90.25	96.76	96.64	96.56	92.09	97.72	97.56	97.49
012	86.17	95.75	95.83	95.72	87.51	96.34	96.46	96.34
015	83.86	94.87	94.19	94.14	85.32	95.40	94.91	94.79
019	83.42	95.05	94.18	94.22	84.53	95.78	94.95	94.95
020	88.26	96.73	96.74	96.66	91.33	97.59	97.64	97.55
022	89.88	97.21	96.99	97.01	91.94	98.01	97.86	97.87
023	94.16	97.41	97.19	97.25	95.71	98.20	98.08	98.11
029	91.37	96.84	96.51	96.57	93.53	97.85	97.69	97.69
030	86.45	94.31	93.35	93.40	87.55	94.85	93.96	93.96
031	87.83	96.37	96.18	96.17	89.87	97.23	97.10	97.08
032	84.54	95.36	95.15	95.07	86.17	96.20	96.16	96.02

Table 36: Results of team SK for task4 recognition. (continued)

Sequence	Frame-by-Frame				Application-Dependant			
	Accuracy	Precision	recall	F1	Accuracy	Precision	recall	F1
036	93.20	97.51	97.23	97.32	94.42	98.36	98.16	98.22
040	88.52	96.15	95.62	95.71	89.66	96.75	96.32	96.37
043	90.31	97.08	96.95	96.92	91.97	97.92	97.85	97.81
044	92.77	97.66	97.50	97.53	96.28	98.78	98.66	98.69
046	87.48	95.75	95.08	95.04	89.60	96.66	96.03	95.99
049	91.25	97.23	97.14	97.12	92.85	98.17	98.12	98.08
053	87.45	96.69	96.70	96.56	89.23	97.55	97.49	97.36
054	73.79	85.76	84.96	84.00	75.59	86.56	85.84	84.86
056	89.11	96.84	96.63	96.61	91.98	97.86	97.67	97.65
059	93.91	98.32	98.15	98.20	96.41	99.12	99.05	99.06
063	87.12	96.11	95.68	95.61	89.70	97.23	96.91	96.84
064	85.75	94.78	94.97	94.77	88.39	95.71	96.00	95.75
069	88.68	95.06	95.05	94.84	92.22	96.20	96.19	95.99
070	88.75	96.76	96.78	96.70	92.04	98.02	98.08	98.00
072	91.38	97.69	97.10	97.30	93.96	98.65	98.24	98.35
073	89.67	96.95	96.77	96.74	92.03	97.98	97.84	97.80
077	88.11	97.74	97.67	97.67	90.41	98.68	98.67	98.65
079	81.01	89.75	89.13	88.60	85.19	90.81	90.08	89.61
083	90.04	96.76	96.84	96.75	92.06	97.78	97.89	97.79
085	88.75	97.08	97.03	97.02	90.49	97.94	97.95	97.92
086	87.95	97.25	97.32	97.22	89.80	98.14	98.26	98.15
089	90.50	97.55	97.25	97.36	93.01	98.53	98.28	98.37
091	91.27	97.79	97.80	97.78	94.54	99.26	99.30	99.28
093	88.30	96.73	96.59	96.48	91.24	98.02	98.01	97.88
097	90.90	97.83	97.81	97.75	93.98	98.97	99.02	98.97
098	92.84	98.28	98.31	98.29	95.11	99.26	99.32	99.28
101	87.39	96.87	96.59	96.55	89.78	97.81	97.62	97.56
104	95.86	97.86	97.75	97.78	98.23	98.95	98.91	98.92
106	90.84	97.15	97.03	97.03	93.03	98.22	98.15	98.14
108	94.79	98.00	97.69	97.78	97.92	99.00	98.88	98.90
112	91.02	97.79	97.61	97.65	93.94	98.84	98.75	98.75
113	92.21	97.60	97.32	97.39	95.28	98.49	98.37	98.39
116	86.46	95.21	95.71	95.38	88.22	96.34	96.77	96.46
117	92.74	97.93	97.64	97.67	95.34	99.09	98.92	98.91
121	86.51	96.93	96.47	96.59	89.66	97.93	97.60	97.67
123	95.32	98.00	97.63	97.75	97.46	98.87	98.62	98.69
126	85.88	96.86	96.67	96.72	88.71	98.10	98.01	98.01
129	92.75	97.09	96.65	96.82	95.32	98.12	97.75	97.89
134	87.82	97.26	96.91	97.02	90.74	98.34	98.19	98.23
135	90.71	97.69	97.66	97.64	92.92	98.68	98.75	98.69
138	87.39	95.81	95.45	95.50	90.32	96.87	96.58	96.61
139	91.66	97.39	97.40	97.36	94.45	98.88	98.91	98.89
142	94.45	97.98	97.71	97.81	97.44	99.11	98.89	98.97
145	88.33	96.22	96.49	96.28	91.31	97.37	97.73	97.51
148	92.55	97.57	97.50	97.51	94.72	98.63	98.61	98.61
150	90.72	96.21	96.06	95.94	93.31	97.20	97.15	97.01
Mean	89.26	96.60	96.40	96.36	91.61	97.57	97.44	97.38

Table 37: Results of team SK for task5 recognition.

Sequence	Frame-by-Frame				Application-Dependant			
	Accuracy	Precision	recall	F1	Accuracy	Precision	recall	F1
003	89.78	97.61	97.61	97.56	92.14	98.62	98.67	98.61
004	88.65	97.68	97.65	97.63	90.39	98.51	98.52	98.49
006	86.69	97.16	96.90	96.94	88.74	98.16	98.00	98.01
009	88.84	96.50	96.32	96.25	90.34	97.44	97.30	97.19
012	85.75	96.08	96.14	96.04	87.54	96.78	96.91	96.78
015	84.69	95.61	94.81	94.95	86.48	96.12	95.47	95.56
019	84.41	95.39	94.40	94.45	85.82	96.18	95.23	95.25
020	89.76	96.97	96.94	96.89	91.95	97.74	97.81	97.72
022	91.44	97.24	96.96	97.02	93.43	98.05	97.89	97.90
023	94.92	97.28	96.90	97.01	96.35	97.95	97.71	97.78
029	91.62	96.87	96.25	96.42	93.82	97.87	97.50	97.59
030	86.55	94.80	94.05	94.10	87.58	95.42	94.81	94.81
031	87.78	96.68	96.50	96.51	89.59	97.60	97.48	97.47
032	85.94	95.95	95.55	95.57	87.68	96.80	96.61	96.55
036	93.34	97.57	97.28	97.37	94.51	98.64	98.50	98.54
040	87.91	96.06	95.21	95.41	89.09	96.77	96.04	96.18
043	90.27	96.92	96.79	96.73	91.79	97.74	97.71	97.63
044	92.13	97.44	97.33	97.33	93.79	98.49	98.47	98.45
046	87.39	95.15	95.12	94.91	89.39	96.08	96.13	95.92
049	88.69	96.86	96.71	96.60	90.54	97.85	97.69	97.53
053	86.01	95.79	95.79	95.65	88.13	96.78	96.74	96.58
054	73.31	85.58	84.83	83.99	75.69	86.62	85.95	85.04
056	88.19	96.10	95.85	95.77	91.31	97.08	96.83	96.74
059	94.33	98.07	97.81	97.88	96.84	98.92	98.77	98.81
063	86.61	95.72	95.57	95.44	88.95	96.95	96.90	96.73
064	86.28	94.97	95.35	95.08	88.04	95.69	96.14	95.85
069	89.01	94.98	94.86	94.74	92.27	96.08	96.03	95.87
070	89.24	96.72	96.57	96.58	92.44	97.98	97.89	97.89
072	90.42	97.22	96.47	96.73	92.52	98.09	97.53	97.69
073	89.66	96.21	95.71	95.79	92.00	97.20	96.88	96.90
077	88.40	97.28	97.19	97.18	90.54	98.23	98.23	98.19
079	77.76	87.19	87.50	86.54	79.28	88.13	88.40	87.45
083	88.63	96.13	96.14	96.07	91.51	97.22	97.28	97.19
085	87.48	96.76	96.73	96.68	90.14	97.95	97.97	97.88
086	87.98	97.21	97.06	97.01	90.45	98.24	98.11	98.07
089	89.44	97.28	96.67	96.91	92.70	98.34	97.83	98.02
091	90.60	97.28	97.17	97.19	93.83	98.84	98.82	98.81
093	87.86	96.02	95.91	95.88	90.41	97.25	97.38	97.26
097	90.95	97.53	97.35	97.38	93.88	98.69	98.65	98.64
098	92.13	98.06	97.96	97.99	94.77	99.22	99.23	99.22
101	87.74	96.91	96.73	96.69	89.88	97.84	97.78	97.70
104	95.68	97.58	97.34	97.41	97.67	98.53	98.39	98.43
106	91.41	97.28	97.14	97.15	93.58	98.28	98.22	98.21
108	95.71	98.31	98.02	98.12	98.46	99.20	99.07	99.10
112	90.34	97.48	97.21	97.29	93.56	98.53	98.41	98.42
113	90.41	97.22	96.80	96.93	92.43	98.09	97.89	97.93
116	86.86	95.42	95.88	95.59	88.93	96.58	97.03	96.76
117	91.68	97.35	97.37	97.31	94.36	98.61	98.75	98.65
121	86.89	96.72	95.88	96.15	89.44	97.64	96.98	97.16
123	94.32	97.69	96.75	97.03	95.64	98.37	97.58	97.81
126	86.80	97.13	96.78	96.86	89.96	98.28	98.09	98.12
129	92.78	96.95	96.30	96.54	95.65	98.06	97.55	97.73
134	88.48	97.48	97.32	97.35	91.64	98.72	98.72	98.68

Table 37: Results of team SK for task5 recognition. (continued)

Sequence	Frame-by-Frame				Application-Dependant			
	Accuracy	Precision	recall	F1	Accuracy	Precision	recall	F1
135	91.23	97.53	97.50	97.49	94.07	98.73	98.77	98.72
138	87.05	96.36	96.15	96.14	89.83	97.51	97.41	97.38
139	91.53	97.34	97.25	97.23	94.69	98.89	98.90	98.89
142	94.67	97.89	97.52	97.65	97.34	99.04	98.78	98.87
145	87.49	96.15	96.25	96.05	90.59	97.27	97.47	97.28
148	92.47	97.36	97.09	97.17	94.59	98.38	98.23	98.27
150	90.49	96.07	95.79	95.76	93.26	97.24	97.06	97.00
Mean	89.08	96.44	96.18	96.17	91.37	97.43	97.28	97.23

B.6 MediCIS

Table 38: Results of team MediCIS for task1 recognition.

Sequence	Frame-by-Frame				Application-Dependant			
	Accuracy	Precision	recall	F1	Accuracy	Precision	recall	F1
003	85.61	96.36	96.54	96.41	88.70	97.51	97.70	97.57
004	86.52	96.93	96.93	96.84	88.88	97.81	97.79	97.72
006	84.20	96.57	96.47	96.47	86.25	97.51	97.39	97.40
009	86.84	95.98	96.09	95.92	89.00	96.98	97.13	96.94
012	84.08	95.23	95.33	95.21	86.69	95.95	96.06	95.94
015	83.74	95.62	95.12	95.14	86.20	96.24	95.86	95.83
019	78.48	88.99	87.36	87.19	80.06	89.77	88.16	87.98
020	87.04	97.06	96.98	96.95	90.21	98.05	97.97	97.93
022	84.70	94.54	93.86	93.80	86.17	95.23	94.61	94.53
023	90.44	97.09	96.86	96.89	94.26	98.00	97.82	97.84
029	87.72	96.49	96.02	96.13	90.93	97.49	97.12	97.20
030	83.82	94.61	94.53	94.40	85.67	95.33	95.37	95.21
031	84.62	94.31	93.32	93.30	86.13	94.96	93.99	93.97
032	83.67	94.95	94.66	94.61	85.61	95.85	95.65	95.55
036	88.58	95.39	94.20	94.17	90.74	96.46	95.31	95.27
040	86.86	96.38	96.23	96.19	89.18	97.23	97.11	97.04
043	86.73	96.18	96.16	95.85	88.92	97.04	97.02	96.72
044	91.76	97.20	97.14	97.13	95.25	98.43	98.36	98.35
046	86.03	95.57	95.80	95.48	88.60	96.60	96.83	96.53
049	87.30	96.79	96.78	96.63	90.67	97.98	97.92	97.80
053	82.14	94.40	94.63	94.33	84.17	95.21	95.45	95.17
054	77.56	88.96	88.37	87.15	81.62	90.12	89.34	88.15
056	89.07	96.51	96.47	96.39	91.67	97.35	97.28	97.24
059	91.62	97.73	97.52	97.58	95.38	98.74	98.62	98.65
063	85.08	95.11	95.37	95.15	87.31	96.06	96.30	96.10
064	78.05	88.50	84.83	84.42	80.66	89.36	85.64	85.25
069	86.33	95.03	95.39	95.15	89.18	96.18	96.48	96.28
070	86.81	96.34	96.17	96.06	90.35	97.52	97.32	97.28
072	89.83	97.47	97.37	97.39	92.62	98.39	98.36	98.35
073	89.49	97.24	97.18	97.15	92.41	98.36	98.32	98.31
077	85.84	97.02	97.19	97.02	87.75	98.11	98.20	98.02
079	74.07	85.72	86.88	85.73	76.40	86.73	87.74	86.65
083	84.66	93.93	93.71	93.43	86.99	95.15	94.84	94.61
085	84.06	96.09	96.30	96.11	87.86	97.38	97.56	97.41
086	85.10	96.35	96.45	96.25	87.55	97.41	97.48	97.32
089	89.43	97.67	97.66	97.65	92.08	98.70	98.72	98.70
091	88.22	96.51	96.42	96.43	92.14	97.91	97.84	97.83
093	86.84	96.23	96.37	96.23	89.58	97.34	97.52	97.37

Table 38: Results of team MediCIS for task1 recognition. (continued)

Sequence	Frame-by-Frame				Application-Dependant			
	Accuracy	Precision	recall	F1	Accuracy	Precision	recall	F1
097	87.38	96.62	96.84	96.69	90.27	97.81	97.94	97.82
098	88.86	97.20	97.43	97.23	92.08	98.35	98.45	98.34
101	84.13	96.20	96.52	96.31	86.83	97.15	97.43	97.24
104	93.60	97.12	96.98	96.99	96.10	98.20	98.08	98.09
106	89.56	97.13	97.02	97.02	92.40	98.16	98.06	98.06
108	91.89	97.30	97.04	97.12	95.17	98.39	98.22	98.26
112	89.80	97.42	97.31	97.33	92.18	98.34	98.29	98.28
113	86.14	96.52	96.46	96.36	90.91	97.63	97.47	97.43
116	84.17	93.49	92.98	92.72	86.75	94.84	94.19	94.00
117	90.23	97.01	96.97	96.90	92.92	98.26	98.18	98.09
121	82.61	95.73	95.58	95.52	85.06	96.45	96.39	96.30
123	90.87	96.61	96.41	96.44	93.90	97.63	97.45	97.48
126	82.65	95.66	95.06	95.21	86.44	96.72	96.15	96.28
129	90.80	96.26	96.10	96.11	93.62	97.38	97.21	97.24
134	84.04	96.02	96.32	96.03	87.12	97.27	97.41	97.18
135	88.15	96.57	96.60	96.55	90.60	97.59	97.64	97.57
138	85.68	96.46	96.48	96.36	89.47	97.75	97.74	97.68
139	88.21	95.96	96.07	95.83	91.81	97.62	97.64	97.52
142	87.92	96.79	97.02	96.85	91.08	98.08	98.26	98.14
145	84.97	95.53	96.06	95.73	87.92	96.65	97.14	96.84
148	89.94	96.06	95.96	95.91	92.37	97.26	97.19	97.15
150	87.60	95.06	95.29	95.03	89.92	96.09	96.30	96.08
Mean	86.37	95.63	95.49	95.34	89.15	96.67	96.52	96.39

Table 39: Results of team MediCIS for task2 recognition.

Sequence	Frame-by-Frame				Application-Dependant			
	Accuracy	Precision	recall	F1	Accuracy	Precision	recall	F1
003	85.54	96.05	96.12	96.04	87.60	96.93	96.96	96.90
004	88.48	96.34	95.86	95.94	91.73	97.00	96.45	96.54
006	88.24	96.80	96.44	96.56	93.43	97.89	97.54	97.65
009	86.65	95.47	95.41	95.32	88.52	96.29	96.30	96.17
012	82.99	94.40	93.57	93.83	84.84	95.06	94.32	94.53
015	78.54	89.23	87.77	87.52	81.42	89.87	88.49	88.20
019	77.73	87.63	86.82	86.92	79.43	88.34	87.62	87.67
020	87.50	96.64	96.44	96.51	89.97	97.51	97.33	97.39
022	85.70	95.18	95.09	95.06	88.74	96.30	96.17	96.15
023	90.55	96.29	95.93	96.05	92.77	97.15	96.83	96.92
029	89.01	96.25	95.94	96.04	91.41	97.04	96.80	96.86
030	80.90	91.93	91.73	91.57	82.58	92.58	92.38	92.21
031	85.30	94.15	92.85	93.14	86.77	94.84	93.70	93.93
032	86.59	95.38	94.82	94.74	89.01	96.36	95.82	95.73
036	87.35	93.35	91.14	91.31	89.71	94.56	92.47	92.58
040	92.05	95.58	94.53	94.82	94.55	96.45	95.58	95.79
043	86.23	95.10	94.33	94.07	88.44	96.12	95.47	95.16
044	90.52	96.63	96.19	96.32	92.05	97.65	97.31	97.41
046	85.04	93.91	93.67	93.63	87.87	95.15	94.94	94.87
049	87.32	95.89	95.73	95.66	89.70	97.10	96.78	96.71
053	84.29	94.98	94.78	94.67	88.61	95.77	95.62	95.51
054	75.41	86.23	84.91	83.91	79.43	87.45	86.12	85.14
056	89.98	96.41	95.88	96.08	93.48	97.47	97.02	97.18
059	94.55	97.83	97.40	97.56	96.84	98.88	98.62	98.72
063	87.54	95.42	95.33	95.32	90.06	96.38	96.34	96.30

Table 39: Results of team MediCIS for task2 recognition. (continued)

Sequence	Frame-by-Frame				Application-Dependant			
	Accuracy	Precision	recall	F1	Accuracy	Precision	recall	F1
064	80.78	90.29	88.24	88.56	83.67	91.29	89.26	89.57
069	84.72	94.54	94.75	94.59	87.98	95.79	95.98	95.84
070	85.87	94.58	94.08	94.19	88.20	95.65	95.21	95.28
072	91.28	97.15	96.74	96.89	94.13	98.28	97.99	98.08
073	88.45	96.67	96.29	96.43	91.26	97.59	97.23	97.36
077	86.83	96.93	96.74	96.78	89.41	98.14	97.96	98.00
079	79.20	90.20	90.53	89.96	82.75	91.74	91.81	91.34
083	82.67	90.75	90.25	90.29	85.83	91.81	91.26	91.33
085	84.98	96.44	96.44	96.38	87.44	97.47	97.50	97.44
086	84.28	96.22	96.39	96.21	86.70	97.28	97.44	97.28
089	89.67	96.92	96.44	96.59	92.74	97.87	97.50	97.61
091	88.89	97.44	97.19	97.27	93.91	99.10	98.77	98.92
093	86.34	96.31	96.31	96.26	89.51	97.53	97.54	97.49
097	90.50	97.22	96.86	96.90	93.44	98.39	98.10	98.14
098	91.79	97.39	97.37	97.32	95.45	98.53	98.48	98.47
101	86.97	96.60	96.42	96.45	92.08	97.72	97.62	97.63
104	93.48	97.06	96.95	96.97	96.39	98.17	98.06	98.10
106	88.35	96.27	96.02	96.01	91.05	97.37	97.09	97.11
108	92.43	97.37	96.78	97.00	95.17	98.34	97.86	98.04
112	88.55	97.07	96.73	96.87	91.91	98.03	97.77	97.87
113	87.19	96.47	96.09	96.20	90.66	97.54	97.23	97.31
116	79.45	90.01	87.95	87.99	81.80	91.14	89.01	89.09
117	91.17	96.85	96.51	96.59	94.28	98.05	97.72	97.80
121	84.42	95.99	95.61	95.72	87.93	97.07	96.75	96.84
123	90.84	95.87	95.45	95.57	94.00	96.86	96.42	96.53
126	83.74	95.78	95.19	95.36	87.19	96.85	96.40	96.52
129	90.32	96.11	95.60	95.80	93.27	97.30	96.87	97.04
134	83.97	95.55	95.38	95.44	87.59	96.85	96.66	96.72
135	88.58	96.78	96.60	96.64	92.49	98.02	97.86	97.88
138	85.23	96.21	95.98	96.03	88.53	97.49	97.32	97.35
139	88.50	96.45	96.37	96.31	93.19	97.79	97.67	97.67
142	87.59	96.48	96.38	96.38	90.83	97.70	97.65	97.65
145	85.42	95.98	96.19	96.01	89.30	97.19	97.35	97.19
148	89.57	96.01	95.76	95.81	91.59	97.05	96.81	96.86
150	89.01	95.34	95.33	95.18	92.14	96.69	96.72	96.57
Mean	86.75	95.21	94.78	94.79	89.71	96.26	95.86	95.87

Table 40: Results of team MediCIS for task3 recognition.

Sequence	Frame-by-Frame				Application-Dependant			
	Accuracy	Precision	recall	F1	Accuracy	Precision	recall	F1
003	86.78	95.85	95.75	95.75	89.59	96.89	96.75	96.75
004	82.49	95.00	94.84	94.84	83.94	95.63	95.49	95.48
006	84.63	95.81	95.52	95.60	87.92	96.84	96.59	96.64
009	85.60	95.13	95.13	94.99	87.67	96.02	96.06	95.92
012	82.65	95.00	94.46	94.49	84.97	95.73	95.26	95.27
015	81.43	93.90	93.08	93.01	83.03	94.48	93.75	93.63
019	77.07	89.05	87.37	87.43	78.84	89.78	88.16	88.19
020	84.68	95.95	96.01	95.91	87.31	97.04	97.11	97.01
022	83.33	94.44	93.83	93.86	85.23	95.26	94.70	94.70
023	84.65	94.93	94.74	94.64	88.25	95.88	95.73	95.64
029	87.40	94.92	94.42	94.57	91.14	96.06	95.63	95.74
030	81.86	93.82	93.16	93.23	83.96	94.69	93.90	93.96

Table 40: Results of team MediCIS for task3 recognition. (continued)

Sequence	Frame-by-Frame				Application-Dependant			
	Accuracy	Precision	recall	F1	Accuracy	Precision	recall	F1
031	80.28	93.76	93.07	93.02	82.15	94.53	93.85	93.81
032	79.96	93.10	92.40	92.28	82.19	94.30	93.67	93.51
036	84.75	93.00	90.91	91.00	86.96	94.14	92.12	92.18
040	83.27	94.58	93.68	93.88	86.94	95.75	94.93	95.09
043	84.25	95.10	94.90	94.71	87.08	96.07	96.00	95.82
044	87.42	95.82	95.62	95.66	91.23	97.35	97.22	97.22
046	85.03	95.45	94.83	94.68	87.83	96.53	95.89	95.84
049	84.66	95.46	95.66	95.46	87.08	96.60	96.88	96.66
053	80.44	93.12	93.25	92.98	82.08	93.97	94.10	93.82
054	74.84	89.48	87.21	85.98	76.79	90.68	88.35	87.11
056	86.48	95.53	95.70	95.56	90.18	96.56	96.73	96.59
059	90.41	96.84	96.67	96.72	93.99	97.90	97.81	97.83
063	82.41	93.11	92.23	92.12	85.11	94.28	93.44	93.34
064	76.83	87.66	84.63	83.83	79.54	88.42	85.47	84.69
069	85.73	94.30	94.25	94.11	89.05	95.41	95.37	95.22
070	84.77	94.92	94.79	94.69	88.01	96.05	95.84	95.80
072	87.72	96.66	96.44	96.51	90.87	97.66	97.53	97.55
073	88.11	96.12	95.51	95.68	90.80	97.10	96.60	96.71
077	83.78	96.08	96.21	96.06	85.70	97.19	97.24	97.09
079	70.48	86.43	85.41	83.80	72.81	87.45	86.26	84.75
083	84.92	94.67	94.90	94.71	88.51	95.94	96.11	95.96
085	83.46	95.87	96.04	95.88	87.30	97.06	97.23	97.08
086	83.04	95.14	95.38	95.20	86.05	96.53	96.67	96.53
089	86.11	96.24	96.30	96.24	89.39	97.45	97.48	97.44
091	87.10	95.57	95.51	95.49	91.00	97.01	96.98	96.96
093	85.63	95.05	94.99	94.92	88.56	96.32	96.40	96.28
097	85.27	95.54	95.31	95.35	88.94	96.98	96.82	96.82
098	86.82	94.97	94.77	94.72	90.92	96.54	96.36	96.35
101	84.71	96.14	96.24	96.14	87.49	97.17	97.28	97.17
104	88.01	94.89	94.83	94.82	91.43	96.35	96.22	96.25
106	86.04	95.97	95.93	95.86	89.88	97.24	97.13	97.10
108	91.10	96.84	96.49	96.55	94.53	97.81	97.56	97.60
112	86.76	95.95	95.69	95.76	89.79	97.14	97.04	97.03
113	82.12	94.92	94.50	94.62	85.20	95.81	95.52	95.58
116	79.16	90.79	90.28	89.85	82.81	92.22	91.39	91.14
117	88.17	96.28	96.27	96.16	91.24	97.41	97.43	97.33
121	81.16	95.17	94.64	94.74	82.80	95.75	95.28	95.36
123	89.30	95.02	93.94	94.14	91.44	95.81	94.86	95.03
126	85.20	95.66	94.97	95.14	88.58	96.65	96.09	96.22
129	87.88	95.04	94.80	94.85	91.05	96.27	96.03	96.06
134	82.87	95.33	95.38	95.25	86.79	96.69	96.72	96.60
135	85.43	95.69	95.86	95.70	88.51	96.85	96.93	96.81
138	83.59	95.19	94.64	94.64	86.67	96.45	95.94	95.96
139	85.13	95.06	95.28	94.96	88.68	96.78	96.81	96.59
142	87.12	96.17	96.28	96.17	90.99	97.44	97.47	97.41
145	84.16	94.71	95.05	94.81	88.17	95.99	96.28	96.09
148	86.62	95.00	94.82	94.78	88.86	96.21	95.96	95.94
150	86.47	95.21	95.53	95.21	89.45	96.45	96.76	96.49
Mean	84.29	94.64	94.27	94.16	87.22	95.74	95.39	95.28

Table 41: Results of team MediCIS for task4 recognition.

Sequence	Frame-by-Frame				Application-Dependant			
	Accuracy	Precision	recall	F1	Accuracy	Precision	recall	F1
003	86.70	96.77	96.76	96.66	88.69	97.57	97.58	97.50
004	87.96	97.33	97.29	97.24	89.89	98.06	98.04	97.99
006	85.25	96.88	96.78	96.78	87.19	97.91	97.79	97.81
009	88.30	96.48	96.61	96.45	89.89	97.30	97.49	97.30
012	84.69	94.33	94.17	94.07	87.03	95.41	94.96	94.88
015	83.18	95.03	93.03	92.81	85.05	95.53	93.58	93.32
019	78.62	88.43	87.80	87.39	80.25	89.07	88.50	88.08
020	87.00	96.80	96.90	96.80	89.27	97.69	97.78	97.67
022	86.50	95.61	95.60	95.53	87.98	96.38	96.37	96.28
023	92.80	97.51	97.44	97.45	95.95	98.42	98.38	98.37
029	89.08	96.46	96.24	96.28	91.86	97.47	97.28	97.31
030	80.00	93.34	92.57	92.55	81.58	94.02	93.34	93.30
031	86.86	96.06	95.19	95.20	88.34	96.78	95.91	95.92
032	86.77	95.88	95.69	95.64	88.47	96.73	96.66	96.57
036	90.76	96.15	94.71	94.66	92.74	97.17	95.75	95.69
040	87.36	96.08	95.75	95.74	89.06	96.89	96.58	96.54
043	87.19	96.31	96.12	95.68	89.04	97.02	96.80	96.37
044	92.89	97.58	97.51	97.49	95.52	98.54	98.49	98.48
046	86.68	95.65	95.77	95.52	89.08	96.58	96.70	96.46
049	89.17	97.03	97.04	96.86	91.31	98.09	98.09	97.91
053	83.10	94.65	94.76	94.49	84.94	95.44	95.56	95.31
054	79.94	90.93	91.62	90.95	82.18	91.87	92.55	91.90
056	90.83	97.21	97.14	97.11	94.21	98.22	98.17	98.17
059	92.89	97.81	97.67	97.70	95.75	98.77	98.67	98.69
063	85.77	94.85	95.12	94.86	88.42	96.02	96.29	96.06
064	82.43	91.56	89.80	89.50	85.08	92.44	90.69	90.42
069	88.18	95.73	96.05	95.81	91.38	96.91	97.22	97.01
070	88.33	96.67	96.67	96.57	91.09	97.77	97.80	97.72
072	90.96	97.58	97.45	97.47	93.49	98.45	98.39	98.38
073	90.39	97.66	97.61	97.59	92.97	98.48	98.42	98.41
077	87.72	97.79	97.92	97.82	89.84	98.62	98.73	98.66
079	76.07	86.22	88.08	86.62	78.61	87.23	88.95	87.55
083	87.52	95.41	95.53	95.34	90.10	96.54	96.63	96.47
085	85.88	96.70	96.90	96.74	88.38	97.65	97.88	97.72
086	86.21	96.92	97.14	96.89	88.70	97.85	98.02	97.82
089	89.63	97.63	97.64	97.61	92.90	98.61	98.61	98.59
091	89.32	96.87	96.82	96.81	92.58	98.16	98.14	98.12
093	87.84	96.59	96.73	96.60	92.22	97.91	98.08	97.96
097	90.00	97.19	97.30	97.22	92.64	98.11	98.19	98.12
098	90.11	97.74	97.89	97.75	93.23	98.79	98.89	98.83
101	86.07	96.81	97.08	96.91	88.53	97.83	98.08	97.91
104	94.87	97.79	97.79	97.77	97.53	98.82	98.80	98.80
106	90.22	97.25	97.19	97.19	92.67	98.22	98.16	98.16
108	93.88	97.97	97.79	97.84	97.17	99.07	98.94	98.98
112	90.88	97.83	97.74	97.75	93.76	98.86	98.87	98.84
113	87.67	96.66	96.50	96.48	92.80	97.70	97.57	97.56
116	83.89	93.32	92.03	91.75	86.73	94.75	93.36	93.18
117	90.81	97.01	97.23	97.09	93.43	98.19	98.41	98.27
121	83.86	96.06	95.94	95.90	85.82	96.85	96.78	96.72
123	91.09	96.27	96.08	96.05	93.90	97.27	97.08	97.06
126	84.42	96.00	95.66	95.75	87.98	96.97	96.68	96.74
129	91.09	96.73	96.71	96.67	94.39	97.90	97.84	97.82
134	84.59	95.77	96.02	95.80	88.40	97.13	97.30	97.12

Table 41: Results of team MediCIS for task4 recognition. (continued)

Sequence	Frame-by-Frame				Application-Dependant			
	Accuracy	Precision	recall	F1	Accuracy	Precision	recall	F1
135	90.28	97.35	97.44	97.36	92.92	98.33	98.40	98.33
138	86.42	96.41	96.09	96.00	88.89	97.33	97.06	96.99
139	89.58	96.62	96.72	96.56	92.64	98.12	98.21	98.12
142	88.77	97.03	97.27	97.12	91.74	98.08	98.26	98.15
145	86.11	95.89	96.38	96.06	88.87	97.05	97.55	97.24
148	90.83	96.56	96.53	96.48	93.12	97.66	97.64	97.60
150	89.31	95.76	95.88	95.66	92.51	96.89	97.02	96.83
Mean	87.59	96.01	95.91	95.78	90.18	96.99	96.90	96.77

Table 42: Results of team MediCIS for task5 recognition.

Sequence	Frame-by-Frame				Application-Dependant			
	Accuracy	Precision	recall	F1	Accuracy	Precision	recall	F1
003	86.27	96.85	96.70	96.63	88.56	97.72	97.55	97.50
004	87.75	97.30	97.20	97.13	89.50	97.97	97.88	97.83
006	85.08	97.10	97.12	97.09	86.76	97.88	97.93	97.89
009	87.84	96.41	96.55	96.36	89.60	97.23	97.44	97.23
012	85.49	95.99	96.23	96.06	88.12	96.95	97.20	97.04
015	82.71	94.94	93.43	93.38	85.10	95.62	94.10	94.03
019	80.90	91.08	89.96	89.71	82.45	91.79	90.68	90.42
020	87.93	97.50	97.52	97.40	90.42	98.33	98.42	98.28
022	85.91	95.69	95.65	95.56	87.44	96.39	96.38	96.27
023	89.81	96.96	96.81	96.78	93.44	97.87	97.72	97.72
029	89.90	97.15	97.00	97.04	92.86	98.27	98.20	98.20
030	83.69	94.52	94.12	93.99	85.45	95.25	94.91	94.76
031	86.16	95.88	95.22	95.19	87.92	96.67	96.00	95.98
032	86.04	96.41	96.54	96.41	88.28	97.45	97.63	97.48
036	90.88	96.52	96.09	96.08	92.70	97.50	97.10	97.09
040	87.56	95.94	95.38	95.42	89.24	96.81	96.30	96.32
043	86.79	96.24	96.11	95.75	89.17	97.18	97.07	96.72
044	92.00	97.54	97.55	97.51	94.60	98.86	98.90	98.85
046	85.91	95.53	95.59	95.32	88.59	96.50	96.60	96.35
049	87.60	96.82	97.23	96.99	89.88	97.78	98.19	97.95
053	82.95	94.16	94.34	94.04	84.47	94.84	95.02	94.74
054	76.96	88.70	87.92	87.25	79.72	89.72	88.91	88.26
056	88.69	96.60	96.64	96.52	92.01	97.63	97.64	97.56
059	92.05	98.09	98.10	98.08	95.08	99.05	99.05	99.03
063	86.86	95.55	95.83	95.61	89.01	96.50	96.81	96.60
064	81.93	91.49	88.91	88.98	84.59	92.42	89.83	89.91
069	87.77	95.53	95.80	95.61	91.05	96.63	96.90	96.72
070	87.12	96.14	96.30	96.16	90.22	97.36	97.48	97.39
072	90.83	97.74	97.64	97.66	92.95	98.50	98.45	98.45
073	89.28	97.21	97.18	97.16	91.96	98.17	98.13	98.11
077	86.93	97.39	97.46	97.38	89.09	98.33	98.44	98.35
079	76.51	88.53	88.49	87.73	78.81	89.73	89.61	88.88
083	86.80	94.58	94.25	94.04	89.53	95.62	95.18	95.02
085	86.34	96.54	96.71	96.54	88.98	97.57	97.76	97.58
086	84.88	96.04	96.20	95.93	87.28	96.95	97.03	96.83
089	90.35	97.49	97.45	97.44	92.65	98.33	98.33	98.30
091	89.90	97.13	97.12	97.09	93.36	98.54	98.54	98.53
093	87.29	96.62	96.83	96.65	90.28	97.70	97.92	97.76
097	88.95	97.13	97.26	97.16	91.67	98.06	98.14	98.07
098	89.96	97.74	97.89	97.74	93.30	98.95	99.05	98.97

Table 42: Results of team MediCIS for task5 recognition. (continued)

Sequence	Frame-by-Frame				Application-Dependant			
	Accuracy	Precision	recall	F1	Accuracy	Precision	recall	F1
101	86.26	97.05	97.30	97.14	89.28	98.03	98.27	98.12
104	93.52	97.31	97.25	97.23	95.69	98.21	98.13	98.13
106	88.84	97.02	96.97	96.95	91.84	98.03	97.96	97.95
108	93.53	97.95	97.71	97.78	96.95	98.92	98.73	98.78
112	90.41	97.62	97.51	97.53	93.19	98.69	98.70	98.68
113	84.09	96.27	96.39	96.28	87.36	97.23	97.29	97.20
116	82.00	92.56	91.71	91.37	84.31	93.67	92.73	92.51
117	91.12	97.28	97.49	97.34	93.58	98.31	98.53	98.39
121	83.27	95.90	95.78	95.70	85.71	96.69	96.56	96.50
123	91.45	97.10	96.96	96.96	93.70	97.97	97.86	97.84
126	85.77	96.19	95.97	96.01	89.06	97.35	97.13	97.15
129	91.23	96.34	96.18	96.19	93.78	97.39	97.21	97.22
134	84.92	95.71	95.84	95.66	88.13	96.81	96.89	96.73
135	89.63	97.32	97.40	97.30	91.87	98.16	98.22	98.14
138	87.07	97.02	96.95	96.86	90.07	98.08	98.02	97.96
139	90.15	96.91	96.92	96.83	93.38	98.23	98.27	98.21
142	88.18	97.01	97.26	97.10	91.36	98.17	98.36	98.25
145	86.50	96.09	96.61	96.28	88.78	97.03	97.54	97.23
148	89.95	96.23	96.08	96.03	92.38	97.28	97.15	97.12
150	88.91	95.72	95.90	95.67	92.33	97.07	97.26	97.06
Mean	87.26	96.06	95.94	95.81	89.81	97.03	96.92	96.80